NASA
Technical
Paper
3228

October 1992

Deployable Reflector Antenna Performance Optimization Using Automated Surface Correction and Array-Feed Compensation

Lyle C. Schroeder,
M. C. Bailey,
and John L. Mitchell

NASA

NASA Technical Paper 3228

1992

Deployable Reflector Antenna Performance Optimization Using Automated Surface Correction and Array-Feed Compensation

Lyle C. Schroeder
and M. C. Bailey
Langley Research Center
Hampton, Virginia

John L. Mitchell
Lockheed Engineering & Sciences Company
Hampton, Virginia

National Aeronautics and Space Administration
Office of Management
Scientific and Technical Information Program

Acknowledgments

The authors acknowledge the initiation of the computer-controlled adjustment study by William L. Grantham; the antenna deployment and systems engineering support by David H. Butler, Richard L. Kurtz, and Roger N. Messier; and metric camera measurements by Richard A. Adams, all of the Langley Research Center.

Contents

1. Summary

The ability to minimize the reflector surface roughness of a large mesh antenna with a computer-controlled actuator system has been tested. In this test program, one quadrant of the 15-meter hoop-column antenna was retrofitted with a computer-driven, control-actuator motor to allow automated adjustment of the reflector surface. The control cord adjustments necessary to optimally reduce the surface errors were calculated with a code based on a finite element model of the antenna-control cord structure. The surface errors relative to a best-fit paraboloid were measured with metric photogrammetry.

With this system, a very rough antenna surface (rms of $\approx$0.180 inch) was corrected to approximately the limit in surface smoothness of 0.060 inch. The correction was accomplished in one to three iterations. These results show that the limiting surface smoothness could be reached very rapidly in space if a suitable optical sensor and computer were available.

The electromagnetic performance improvement resulting from surface adjustments was evaluated with a computer program for distorted reflector antennas. This computer code had been previously verified with experimental data. Calculations with this code showed that after two corrections, the antenna pattern and gain performance improved significantly.

In additional computer simulations, the effects of the surface distortions were compensated for by superimposing excitation from an array feed to maximize antenna performance relative to an undistorted reflector. Results showed that a 61-element array could produce essentially the same electromagnetic performance improvements as the maximum achieved with surface adjustments. Additional improvement in gain and radiation pattern was achieved by applying both mechanical surface adjustment and feed compensation techniques, which essentially increases the operating frequency range from approximately 6 to 18 GHz with a reasonable size feed array.

2. Introduction

In 1986, after completion of the performance evaluation of the 15-meter hoop-column antenna, the accomplishments and lessons learned were assessed (ref. 1). Among the most notable accomplishments was the development within structural tolerances of a lightweight, deployable large antenna to a predicted surface precision. Also, the measurement of high-quality antenna radiation patterns in the largest near-field facility in the United States showed that the antenna performance was better than expected. Although the deployment of the antenna was far from "hands off," the deployment system was shown to be workable, and the 531-lb mass of the antenna yielded a very low areal density (1.36 kg/m^2) for a 0.060-inch (1.5 millimeter) rms surface roughness. The demonstration of the ability to make manual postdeployment corrections to the antenna surface, which improved its performance, was the most dramatic accomplishment and also the most significant lesson learned. The need for a system to allow for postdeployment surface improvement adjustments was further demonstrated in a follow-on study of a 5-meter antenna (ref. 2).

Based on these results, a test program was developed for the 15-meter hoop-column antenna to demonstrate a system suitable for remotely correcting a deployable antenna for space application. This interdisciplinary program included plans for measurement of the surface geometry, active shape control, and adaptive electromagnetic feed compensation for surface distortions.

This report describes computer-controlled corrections to the reflector surface, analytical predictions of the resulting electromagnetic performance improvements, and analytical simulations of the electromagnetic performance improvements due to optimization of excitation of an array feed to compensate for residual reflector distortion. The analytical models used for electromagnetic performance studies were previously verified with data from the 1985 near-field tests at Martin Marietta Denver Aerospace Division (MMA) (ref. 1).

3. Objectives

This test program was conducted in order to study techniques for optimization of the 15-meter hoop-column antenna with a distorted reflector surface. With the use of a computer-controlled, motor-driven actuator system, metric camera measurements, and a surface adjustment model, this set of experiments adjusted surface control cords by using an automated system until no further reduction in antenna reflector surface roughness could be achieved. The resulting improved reflector surfaces are the basis for estimating electromagnetic performance improvements, which are calculated with radiation models previously verified with test data. Finally, additional improvements in electromagnetic performance that can be obtained by using array-feed compensation to correct for remaining surface distortions are assessed.

4. Surface Correction Tests

4.1. System Description

4.1.1. 15-meter hoop-column antenna. The 15-meter-diameter hoop-column antenna is described in detail in references 1 and 3 and is only briefly described here. The primary structural elements of this antenna design are a telescoping column, which deploys from a central hub, and a hoop consisting of 24 articulating segments. Both the hoop and the column are composed primarily of laminated graphite-epoxy material. Figure 1 shows the antenna in the 16-meter thermal-vacuum cylinder at the Langley Structural Dynamics Research Laboratory in its deployed and stowed configuration (both views are approximately the same scale). In the stowed configuration (inset in fig. 1), the antenna fits into a package 2.7 meters long by 0.9 meter in diameter.

Deployment is driven by electric motors on the column and at hinge joints on the hoop. As these motors extend the column and open the hoop, cords emanating from each hoop joint to the upper and lower masts are drawn from spools into position. The lower cords are graphite, and the upper cords are quartz because of the need for low conductivity and high RF transparency. The length of the cords in conjunction with the manufacturing precision and thermal stability of the materials of the hoop and column structures provides a stable, reproducible, cable-stiffened structure upon which the mesh reflector and feed are attached.

The reflector surface is a gold-plated molybdenum mesh material which has been shaped and stitched to a network of cord elements. (See fig. 2 and ref. 3 for details.) This reflector surface is attached radially at the hoop joints and at the lower part of the center hub and is shaped by 24 cord trusses and a network of front cord elements which support and contour the reflective mesh surface. Each cord truss has four rear control cords, which can be adjusted in length to allow limited surface adjustment capability (figs. 2 and 3). The "effective surface" shown in figure 3 excludes approximately the outermost 10 percent of the reflector, which is not adjustable with the control cords. The surface and control cords are made of multifiber unidirectional graphite material, which has a high stiffness and a low coefficient of thermal expansion to provide a stable foundation for the mesh surface.

The antenna mesh and control cord lengths have been designed so that each quadrant of the antenna surface comprises a portion of a separate offset-fed paraboloid in the "cup-up" attitude in a $1g$ environment, as shown in the lower portion of figure 3. The plan view of figure 3 shows the antenna from the top. The four design paraboloids have vertices at $x = y = \pm a$ and $z = 0$. The antenna vertical axis is along the z-axis, with $z = 0$ at the vertex location.

4.1.2. Surface figure measurement technique. Measurement of the reflector surface was accomplished with convergent close range photography (often called metric camera measurements). The application of this technique to the 15-meter antenna is described in reference 1. Photographs of the antenna were taken from above at 8 to 15 different camera azimuth positions. Photographic images of targets on the reflector surfaces were read by an autocomparator, and the results iteratively triangulated to produce the Cartesian coordinates of each target to within 0.003 to 0.007 inch. The rms surface accuracy of all targets in one quadrant was predicted to be within about 0.001 inch. These results were subsequently transformed to the antenna design coordinate system to allow direct comparison with design surface coordinates. A best-fit paraboloid through these results was used to compare the deviation from design at each target and to assess the rms surface roughness of the antenna. Most of the reflector measurements and analyses used a set of targets at the junctions of surface cords (defined in ref. 1 as Tie Points I). The final measurement included analysis of targets located at centers of stretched mesh (defined in ref. 1 as Pillows I).

The deployed 15-meter-diameter antenna in the 16-meter cylinder (fig. 4) precluded taking metric camera photographs of the antenna upper surface from a lift as was done in reference 1. For this reason, a removable walkway was installed above the antenna and counterbalancing system. This walkway allowed the metric camera to be positioned at any azimuth angle.

This technique is suitable for these quasi-static tests, where negligible movement occurs during the 2- to 4-hour photography period. For dynamic systems measurements, sensors such as the SHAPES system (ref. 4) or the remote attitude measurement system could be used. An in-house-developed system (ref. 5) using photogrammetry with 16 charge-coupled device (CCD) cameras photographing light-emitting diode (LED) targets, with resolution of better than 0.001 inch and an output frequency of 20 measurements per second, appears promising for future dynamic measurements.

4.1.3. Surface adjustment model. A computer model was developed (refs. 1 and 6) to calculate the control cords length adjustments necessary

to obtain a corrected reflector surface with the smallest rms deviation relative to the design paraboloid. The model is based on finite element structural analyses to calculate sensitivities of surface target displacements to control cord length adjustments. A least-squares analysis using the finite element model sensitivities provides a method of determining the control cord adjustments required to correct the distorted surface. This model proved very satisfactory for application to these 15-meter antenna tests.

A more comprehensive surface adjustment model that removes assumptions about linearity and constrained target movement is described in reference 7. This model was not used for the present study because the linearity assumptions of the model in references 1 and 6 were not violated in these tests. The model would show very little improvement for the current tests.

4.1.4. Antenna modifications. Tests with this antenna at the near-field facility at MMA (ref. 1) demonstrated that the reflector surface can be significantly improved by making small adjustments to the length of the surface control cords (G01–G04 in figs. 2 and 3). In those tests, adjustments required the removal of the surface preload tension; adjustment, using measurements by a hand-held micrometer, of the cord end position with a set screw (fig. 5); and reapplication of surface tensioning. This procedure took 4 to 8 hours. If precision adjustment of such an antenna were required in a space environment, such a procedure would be extremely difficult in low Earth orbit and nearly impossible in geostationary Earth orbit.

To allow for automatic adjustment of the reflector surface, a system was designed to use small motor actuators to adjust the surface control cords. One quadrant of the antenna was modified so that the control cords were attached directly to a motor drive whose position was computer controlled to within 0.001 inch. These changes required replacement of the lower hoop and surface control cords and mounting hardware for this quadrant. Figure 6 shows photographs of the system in its new configuration. The details of these changes are given in the appendix.

Since the actuator system and the control cords of quadrant 4 were completely changed, alignment of the antenna was required before any testing could be done. Tests were conducted to verify acceptable tolerances for column verticality, hoop leveling, hoop planarity, control and hoop cord tension, and initial surface smoothness. Details of these tests are given in the appendix.

4.2. Test Program

The timeline of figure 7 gives a summary of the significant activities (left-hand side) and measurements (right-hand side) leading to and during the test program. The test program began after installation and checkout of the surface control system (3/31/89), leveling of the hoop (4/19/89), and crude manual adjustment of the control cord lengths to be within the adjustment limits of 0.231 inch for the G04 cords and 0.375 inch for all other control cords (6/6/89). The first attempt at computer-controlled adjustment on 7/27/89 resulted in a broken G04 cord at station 22 (22 G04) and a slipping brake on 19 G04. Analysis showed that drive motor torque was being applied too rapidly to the control cords, and the motor speed was reduced. Subsequently, on 8/14/89, the first successful computer-controlled adjustment was completed. A second computer-controlled adjustment on 8/29/89 indicated that little further improvement was achievable without eliminating error sources not corrected by the control cords.

Because the hoop planarity, one such source of error, was somewhat worse than in previous tests, the hoop joints were rotated and hoop cords adjusted (10/13/89 to 11/6/89) to improve the hoop planarity. In addition, a wiring error was corrected (11/29/89) in the motor tachometer circuit of the 19 G03 cord which caused variable erroneous starting points for corrections to this cord. Computer-controlled adjustments were performed 11/30/89 and 12/14/89 to determine the effect of improved planarity on surface smoothness.

After reviewing results from the adjustments of 12/14/89, a final computer adjustment was conducted on 4/17/90 to correct areas of roughness on the reflector. The test program concluded after these tests.

4.3. Results and Discussion

In general, metric camera measurements of the position of surface targets were used as discussed in section 4.1.2 to determine the smoothness of the reflector surface relative to a best-fit paraboloid. The surface roughness and other best-fit paraboloid characteristics most relevant for smoothness optimization are for the effective surface (which excludes the outermost 10 percent of the reflector), but values are also given for the complete reflector surface. (See table 1.) For logistical reasons, metric camera measurements follow the test date by one or more days. The metric camera measurements were also input to the surface correction model (ref. 1) to calculate the adjustments required in the control cords and the predicted smoothness resulting therefrom. Since

the computer-controlled actuators affect only quadrant 4, only those results are of direct interest.

4.3.1. First series. The measured surface for quadrant 4 prior to computer-controlled testing is shown in figure 8. This is a false color plot which shows increasing deviations in darker hues. The reflector shows large regions with deviations in excess of 0.375 inch for the lower two and upper two gores and −0.375 inch for the center gores, with an rms deviation of 0.147 inch (effective surface values are used throughout this discussion). This surface is clearly very distorted and, based on the experience of reference 1 and as shown in section 5, would be a poorly performing microwave antenna. Table 2 gives adjustments required as calculated from the surface correction model for all quadrants, but adjustments are made only for quadrant 4. The surface rms deviations for quadrants 1, 2, and 3 were nearly unchanged from those obtained during the 1985 tests at MMA (ref. 1). Tests with the surface adjustment model show that the influence of the other quadrants on the test quadrant can be neglected for these conditions.

For the first computer-controlled adjustment on 8/14/89, figure 9 shows the control cord adjustments for quadrant 4 only and the false color plot of the predicted surface after adjustment, based on metric camera data of 6/8/89; the plot of the actual (measured) surface after adjustment is also shown for comparison. It can be seen that in the upper half of the antenna quadrant, substantial improvement is realized, which is in fair agreement with the predicted performance. However, the lower half still has sizable distortions up to 0.375 inch, which is not in agreement with predictions. These distortions were partially caused by improper manual adjustment of the G04 control cord at station 22, which was broken and replaced during the test attempt on 7/27/89.

This surface was corrected during the second computer-controlled adjustment test of 8/29/89. As before, the control cord adjustments required, the predicted surface, and the actual surface after adjustment are shown in figure 10. The adjusted surface for this case compares qualitatively with the predicted surface, except in gores 22 and 23 and near the antenna top (gore 19). The rms surface deviations predicted and measured were 0.060 and 0.064 inch, respectively. The problem with gore 19 was found to be caused by an improperly wired tachometer, which made the start point for the 19 G03 cord adjustment to be in error.

4.3.2. Hoop planarity adjustment. Upon completion of the test on 8/29/89, it was apparent that the reflector surface was approaching a limit at an rms deviation of about 0.060 inch. Application of the surface correction model to the metric camera data on 8/31/89 yielded only small corrections to the control cords in quadrant 4. (See table 3.) Because one purpose of this test program was to determine experimentally the optimum smoothness, the impact of other variables on smoothness was considered. Lengths of cords in the trusses affected by control cords could not be changed because this would violate the design of the reflector. To check the influence of other quadrants on quadrant 4 smoothness, the surface correction model was used to calculate the smoothness of quadrant 4 with and without correction to the other three quadrants. The results showed that optimal correction of errors in all other quadrants decreases the rms surface deviation for quadrant 4 from 0.061 to 0.060 inch. The improvement of 0.001 inch is considered insignificant.

Hoop planarity was examined and found to have greater deviation than on previous tests. Since errors in hoop planarity could affect achievable surface smoothness, the hoop joint angles and hoop cord lengths were adjusted to improve the planarity. Figure 11 shows that these adjustments reduced the standard deviation of the seven hoop joints in quadrant 4 from 0.133 to 0.045 inch, which is lower than it was during the MMA 1985 tests for quadrant 4 (0.093 inch) and the whole hoop (0.074 inch).

4.3.3. Second series. After completion of the hoop planarity adjustments, the analysis of the metric camera data for 11/7/89 (fig. 12) shows that the surface had become somewhat rougher (rms deviation of 0.124 inch) due to adjustment of the hoop joints and cords. The false color plot shows systematic rises and falls in the radial direction with gore 19 high, 20 and 21 low, 22 high, 23 low, and 24 high. The deviation at gore 24 is in excess of 0.525 inch.

Before attempting any further computer-controlled adjustments a wiring problem for control cord 19 G03 that caused the motor to lose its reference starting point for adjustments was corrected on 11/29/89. The effect of this problem is evident on some of the prior surface roughness plots. The correction of this wiring problem was completed without loss of the current position reference; therefore the metric camera data taken 11/7/89 remained valid for the following experiments.

Computer-controlled surface adjustments were completed 11/30/89. As before, figure 13 shows the control cord adjustments, the predicted surface based on the metric camera data before adjustment, and the actual surface after adjustment, based on the

metric camera data of 12/1/89. Although the surface was predicted to be smooth with an rms deviation of 0.059 inch, results in the vicinity of gore 24 showed a surface with a deviation in excess of 0.187 inch. The overall actual rms deviation of the surface was 0.070 inch. It is hypothesized that the large difference in the vicinity of gore 24 is caused by the influence of the large hoop adjustments made prior to this test, since the hoop cords and the G04 cords share the tension load from the hoop.

A computer-controlled adjustment was conducted 12/14/89 to correct the latent surface aberrations. Figure 14 shows the adjustments calculated, the surface predicted after the application of the adjustments, and the actual measured surface after adjustment. The measured surface agrees well with that predicted with an rms deviation of 0.063 and 0.059 inch, respectively. The false color plots show that actual deviations compare well with predictions except for larger areas with deviations in gore 24 and the outer part of gore 23. At this point, the reflector is as smooth as the reflector that was shown to have good performance as an antenna in the test of reference 1.

The metric camera data of 12/18/89 were used with the correction model to determine the need for further adjustments. Figure 15 shows that only four control cords require adjustments greater than 0.012 inch. Clearly, the surface has approached the limits imposed by system fabrication tolerances.

On 4/4/90, new metric camera data were taken to see if the antenna had changed noticeably during this 3-month period and to help decide whether further testing was warranted. The results of these tests show a slight improvement in gores 23 and 24 (fig. 16). The surface rms deviation is lower by 0.001 inch, and the hoop planarity is decreased. Possible reasons for the marginal improvement are mechanical relaxation, thermal differences, and a difference in measurement precision.

A final computer-controlled adjustment was completed 4/17/90 with the corrections computed from the metric camera data of 4/4/90 and shown in figure 17 along with false color plots of predicted and postadjustment surfaces. The false color plot shows surface smoothness in good agreement with predictions. The rms deviation of the reflector surface was unchanged at 0.063 inch.

At this time, the effect of an additional surface correction was calculated. The resulting adjustments were small (fig. 18), and the rms deviation for the predicted surface was 0.058 inch, unchanged from the prior prediction. The predicted corrected surface, also on figure 18, shows very little improvement. Thus, the test program was considered complete.

*4.3.4. **Surface measurement including pillow targets.*** All the surface measurements and analyses used measured data taken at the targets located at junctions of surface cords (Tie Points I), which are the surface points used in the surface adjustment model correction program. The metric camera data of April 19 were expanded to include approximately an equal number of targets in the center of mesh segments (Pillows I targets, ref. 1). The plot of figure 19 shows that the effect of the pillow targets is to raise the surface (the blue areas are lower and the red areas are higher). Because previous studies showed that the pillows were raised at the center, this effect was expected. Since the effect of the pillows is to bias the surface upward and the correction model was designed to minimize the surface error at the tie points targets only, this limitation is inherent in this mesh correction application. The location of the pillow targets in the center of a mesh segment would have required the development of a model to assess the sensitivity of the pillow targets to the control cords. The effect of pillows for this configuration does not significantly alter the rms surface error results.

5. Electromagnetic Performance

Although surface roughness is an important indicator, the performance of the antenna is more appropriately evaluated with respect to the electromagnetic properties (i.e., radiation characteristics). These properties or characteristics could be measured in an antenna facility (e.g., the near-field facility at MMA); however, the cost versus benefit for the present experiments was not justifiable. Previous measurements of this same antenna in the near-field facility were used to verify an analytical computer code, which was developed to calculate the radiation characteristics of reflector antennas (such as the hoop column) whose surface distortion can be described by the Cartesian coordinates of discrete points. The analytical method, with verification data, is described in reference 8.

The reflector antenna radiation characteristics in this present report were calculated for an array feed illuminating the measured surface of quadrant 4 of the hoop-column antenna. The complete surface including the outermost section, which was not adjustable, was included in the calculations. In all calculations, the presence of the other three quadrants was neglected. Although the presence of the other quadrants could have been included, previous results have shown that the presence of the other quadrants

results in additional far-out side lobes in specific directions due to feed radiation pattern spillover onto the adjacent quadrants and insignificant elsewhere. (See ref. 9.) For purposes of evaluating the radiation characteristics due to adjusting the surface of quadrant 4, the feed spillover illumination of the other three quadrants can be neglected. The nomenclature used for identification of specific surfaces used in calculating radiation characteristics is the date on which the metric camera data were obtained (e.g., 8/15/89 would indicate the surface which was measured on August 15, 1989).

The feed used in the calculations was a hexagonal planar array of seven elements with center-to-center spacings of 1.5 wavelengths at the frequency of interest. Feed geometry is illustrated later. The radiation pattern of the electric field intensity used for each element of the array was $(\cos^{12}\ \theta)$, where $\theta = 0$ is normal to the feed array and pointing at an angle of 21.5° with respect to the reflector paraboloidal axis. (See fig. 3.) The radiation pattern for each array element was also assumed to be rotationally symmetrical about the axis at $\theta = 0$. This element radiation pattern closely approximates that obtainable from a 1.5-wavelength-diameter, conical dual-mode horn, which is a practical feed element for many applications. The elements of the feed array were assumed to be excited with uniform phase and rotationally symmetrical amplitude, in which the outer element amplitudes were −11.5-dB power relative to the center element. (See table 4.) This feed array was selected for use in performance calculations so that all side lobes for the "ideal" perfect paraboloidal reflector would be below −30 dB, which is representative of high-beam-efficiency antennas for radiometry.

The radiation characteristics for a perfect paraboloidal reflector were calculated in order to provide a basis for evaluation. Figure 20 shows the amplitude of the aperture field (in 5-dB increments), and figure 21 shows the corresponding radiation pattern contour plots (in 10-dB increments over an angular region of ±3° at 6 GHz) for the perfect reflector (referred to as "ideal"). The circular aperture in figure 20 is for a 6.09-meter-diameter "circular equivalent" of the "scalloped pie" aperture for one quadrant of the hoop-column antenna, as indicated by the circles in the sketch of figure 3. The apertures are equivalent in the sense that the gains and beamwidths are very close; however, as seen in figure 21, the side lobes below −30 dB are significantly different. Therefore, the scalloped pie aperture was used for all subsequent calculations.

A comparison of the radiation characteristics for the five cases described in the previous sections was made in order to illustrate the improvement in antenna performance to be achieved by computer-controlled surface adjustment. The radiation pattern contour plots are presented in figure 22 (in 10-dB increments over an angular region of ±3° at 6 GHz). The contours of $-10, -20$, and -30 dB for the perfect (i.e., ideal) paraboloid scalloped pie aperture are also included in figure 22 for comparison. One can readily observe that significant improvement was achieved with one adjustment of the surface (i.e., 6/8/89 to 8/15/89). A small additional improvement in side lobes was achieved by the second adjustment (i.e., 8/15/89 to 8/31/89); however, further surface adjustment appears to only affect the distribution of the side lobes with only an insignificant overall reduction in side lobe level. One should note that the redistribution of side lobes may be due to other intermediate effects (i.e., hoop planarity adjustments, cord replacements, and drive motor failures) which could change the distribution of the surface errors. Observation of the data in figure 22 indicates that, after two surface adjustments, the reduction in side lobe level appears to have reached a limit. Calculations at other frequencies resulted in similar observations.

Figure 23 shows the antenna gain for these same surface distortions. The same observations can be made for improvement due to surface adjustment. A significant improvement in gain was achieved by one surface adjustment. A second surface adjustment produced an additional gain improvement. After two surface adjustments, the improvement in gain appears to have reached a limit. This antenna performance limit appears to be related to the surface smoothness limit (approximately 0.06 inch rms) imposed by the inaccuracies in manufacture and assembly of the interconnecting tie cords and to the small number of control cords (28 per quadrant) available for surface adjustment.

6. Surface Distortion Compensation Using Array Feeds

Computer simulations were performed in order to determine what additional improvement in antenna performance could be realized by utilization of a larger feed array in which the amplitude and phase excitations depend upon the reflector distortion. The feed-array configurations used in the simulations were obtained by the addition of more elements around the original 7-element configuration, as illustrated in figure 24 for arrays of 7, 19, and 37 elements. Figure 25 shows the array configuration for 217 elements (the largest used in the present simulations). For all array configurations, the center-

to-center spacings of array elements were maintained at 1.5 wavelengths and the individual element radiation patterns were ($\cos^{12}\theta$). The amplitude and phase excitations were determined for each feed array such that the superposition of the distorted reflector aperture fields from each array element approximates the ideal aperture field in a least-squares sense. This method is described in more detail in reference 10 with further modifications discussed in reference 11. The change in reflector spillover from the feed side lobes was initially neglected in establishing the least-squares fit to the ideal aperture field as described in reference 10. Neglecting this change in spillover can sometimes result in a decrease in antenna gain, although the aperture field (and corresponding reflector radiation pattern) is improved. An improved procedure (ref. 11) was developed which utilizes a constrained function minimization algorithm (ref. 12) adapted to the present problem. This improved procedure allows the feed spillover to be constrained so as to remain within acceptable limits during the process of determining the excitation coefficients. The calculations in this paper are based upon the improved procedure. The feed-array excitation coefficients for distortion compensation of the 4/19/90 measured surface are listed in tables 4 through 21.

Figures 26 and 27 show the improved performance realized by increasing the number of elements in the feed array, when compared with the uncompensated (i.e., original 7-element feed array) results. The radiation pattern contour plots in figure 26 for 6 GHz are presented in 10-dB increments over an angular region of $\pm 3°$. The plots in figure 27 for 12 GHz are presented in 10-dB increments over an angular region of $\pm 1.5°$, which corresponds approximately to the radiation pattern frequency scaling factor for a perfect antenna. The data in figures 26 and 27 show that increasing the array size, with an appropriate change in array excitation, can provide a significant improvement in side lobe reduction near the main beam. This angular region of side lobe suppression grows larger as the size of the feed array increases.

The additional improvement in antenna gain is illustrated in figure 28 for the 4/19/90 surface. The data of figure 28 indicate that a significant increase in usable frequency range is potentially achievable with a reasonable number of feed-array elements. The uncompensated gain at 6 GHz is -0.52 dB relative to the ideal, the 127-element compensated gain at 12 GHz is -0.54 dB relative to the ideal, and the 217-element compensated gain at 18 GHz is -0.81 dB relative to the ideal.

The data in figures 22, 23, 26, 27, and 28 were calculated for surface distortions based upon optical measurements of target coordinates located on the mesh surface near the interconnecting tie points of the surface shaping tension cords. In between these tie points, the deviation of the surface from a paraboloid is convex ("pillows"). The effect of these pillows is to produce quasi-grating lobes in the radiation pattern. The position and level of these additional lobes can be calculated for a specific frequency (refs. 8 and 9) from the height of the pillows and the spacing between tie points. Figure 29 shows the radiation pattern contours (in 10-dB increments over an angular range of $\pm 4°$ at 12 GHz) calculated for the measured pillowed surface of 4/19/90. The primary effect of the pillows is to produce a ring of side lobes approximately 3° from the main beam. An attempt to utilize a feed array of 217 elements to compensate for the distortion of the pillowed surface resulted in the radiation pattern contours in figure 30. Observation of these data shows that although significant improvements occur near the main beam, the size of the 217-element array is insufficient to suppress the far-out quasi-grating lobes. A synthesis procedure has been developed (ref. 13) which has the capability to suppress side lobes in specific directions. In order to suppress the close-in side lobes around the main beam as well as the far-out quasi-grating lobes, the procedure of reference 11 could be combined with the procedure of reference 13. This combined approach would establish the configuration and excitation of a feed array to place cancellation beams in the direction of the quasi-grating lobes while maintaining suppression of the close-in side lobes.

Additional calculations were performed in order to evaluate the potential for using an array feed to produce acceptable performance from a reflector which is severely distorted such that it would not normally be usable. This evaluation was performed by utilizing the measured surface of 6/8/89. The excitations of the previously described feed arrays were recalculated to compensate for the 6/8/89 surface distortion. The resulting radiation patterns are presented in figures 31 and 32 at 6 GHz and 12 GHz. The corresponding gain calculations are plotted in figure 33 for a range of frequencies. The data in figure 31 indicate that a 6-GHz array feed could be designed to produce "near-ideal" performance from the severely distorted reflector antenna. Even at 12 GHz, the data of figure 32 show possibilities. Upon examination of the gain calculations in figure 33, one can readily note that utilization of a 61-element array feed for distortion compensation alone could produce the same gain performance as the best obtainable with surface adjustments alone. Obviously combining surface adjustments with feed-array

compensation would yield the maximum improvement in performance.

7. Concluding Remarks

Testing has been completed to demonstrate a computer-controlled actuator system to minimize the reflector surface roughness of a large-scale mesh antenna. This program used the 15-meter hoop-column antenna developed for Langley by the Harris Corporation. Prior testing at the near-field facility at the Martin Marietta Denver Aerospace Division had shown that large-scale deployable antennas will require post deployment adjustment to obtain the surface figure required for most microwave applications.

In the current test program, one quadrant of the test antenna was retrofitted with control-actuator motors to allow automated adjustment of the set of 28 rear control cords, which, in turn, provided adjustment of the reflector surface. A computer was used to implement the required adjustment commands to the control-actuator motors, accurate to within 0.001 inch. The system was employed by using an optical sensor (in this case, metric photogrammetry) to determine the surface errors at retroreflecting targets relative to a best-fit paraboloid. A code was then employed which calculates the control cord adjustments necessary to optimally reduce the surface roughness and implements commands to the actuator motors to adjust the surface to the new position. The cycle was repeated if necessary.

After installation of the control-actuator system and debugging of the computer-control system, a preliminary set of tests indicated that a very rough surface (rms of $\approx$0.180 inch) was corrected to approximately the limit in surface roughness of 0.060 inch for this antenna. The correction was accomplished in one to three iterations. A second set of tests to see if planarity was limiting the smoothness achievable showed essentially the same results. These results show that the limiting surface smoothness could be reached very rapidly in space if a suitable optical sensor and computer were available.

The electromagnetic performance improvement resulting from surface adjustments was evaluated with a computer program validated in previous tests with the hoop-column antenna. These calculations showed that after two corrections, the antenna performance improved significantly in pattern and gain performance.

The effects of the remaining surface distortions were compensated for by superimposing excitation from an array feed to maximize antenna performance relative to an undistorted reflector. Results from this computer simulation showed that additional improvement in gain and radiation pattern could be achieved which essentially increased the operating frequency range from approximately 6 to 18 GHz with a reasonable size feed array.

Additional calculations were made to assess the improvement in antenna performance due to array-feed compensation alone. The calculations indicated that distortion compensation with a 61-element feed array alone could produce essentially the same performance improvement as that achieved by surface adjustments alone.

NASA Langley Research Center
Hampton, VA 23681-0001
August 5, 1992

Appendix

Automated Control Cord Actuation System

The 15-meter hoop-column antenna described in reference 3 was modified to allow for rapid, computer-controlled adjustment of the reflector surface. Details of the redesigned control cord actuation system are described in this appendix. Additional sections describe the tests conducted subsequent to installation of this system to verify the antenna alignment prior to the computer-controlled surface adjustment tests.

A1. Computer-Controlled Surface Adjustment System

The surface control system of one quadrant of the antenna was modified to add computer-controlled motors to allow precision step adjustment of each control cord length. A computer-based control and driver software system was implemented to initiate control cord changes derived from optical measurements of the surface and the surface adjustment model described in the previous section.

The installation of the computer-controlled actuator system required replacing the lower hoop and control cords and hardware in quadrant 4. The new control cords were refabricated with templates and specifications developed for NASA by the Harris Corporation but modified for the new geometry and with bead-bonding procedures developed at Langley during the original antenna fabrication. Figure 6 shows photographs of the modified antenna system.

The surface contour control system is described in detail in reference 14 and is only briefly described here. As shown in figure A1, the lower end of each control cord is bonded to a bead, which is retained in a spring-loaded piston which can be translated by up to 0.75 inch in a retaining block. For test purposes, however, the adjustment travel distance was kept to 0.375 inch or less by using limit switches. A cable from the piston to a reversible torque motor allows direct actuation of the position of the end of the control cord. After actuation, the position of the cord is held by a brake assembly. The precise location of the position of the cable is monitored by optical emitters-detectors. Position commands from an external source (the optical figure sensor and surface adjustment model) are provided to the computer to drive motors, which adjust the position of the 28 control cords to the desired new position.

A block diagram of the control computer-driver system is shown in figure A2. The system consists of a host personal computer; seven cord stations, each containing four cord controllers to drive the cord actuators and a station controller; and 28 cord load cells and a load interface unit (LIU). Communications with the host computer, the control stations, and the LIU are via a parallel communications bus. The station controller employs a locally developed protocol operating with a multiprocessor serial communications configuration to communicate with the four cord controllers. The host computer software provides an interactive user interface to the system to control access; transmit commands; and acquire, display, and log system data and status. This software also creates a historical record of all commands entered and the status of the system in the form of hard disk files. When the system is powered down, each actuator is stowed. The position data from each control station and the position offset values are then stored in a file to be retrieved when the system is activated.

A2. Initial Adjustments to Modified 15-Meter Antenna

Since the actuator system and control cords of quadrant 4 were completely changed for this test program, alignment of the antenna had to be measured and adjusted to be within acceptable tolerances. The following steps give the details of these activities:

1. Column verticality: The pedestal was adjusted to align the column to within specification (approximately 0.3 inch from top to bottom). The procedures developed in reference 1 were used for this measurement. Table A1 gives the metric camera measurements of the position of targets on the upper column hub, the central hub, and the lower hub to provide the means of checking vertical alignment of the column. Each target set is analyzed to determine its centroid, best-fit plane, and the residual of targets relative to the best-fit plane. Centroids at these locations are used to determine off-axis deviation and tilt. Since the data after the first set are quite consistent, mean values for the 10 sets starting 4/29/89 and ending 4/19/90 are used to assess verticality. From the upper hub to the center hub, the offset is about 0.2 inch, which results in a tilt angle of about 0.06°. These results are approximately the same as determined in references 1 and 3. Targets for the lower hub were obscured by the antenna reflector and could not be measured for these tests. However, table top targets are shown to indicate stability of the antenna-metric camera reference system.

2. Leveling of the hoop: This was initially accomplished by the methods of reference 1. The modified pedestal allowed more systematic adjustment of the hoop. The tilt of the hoop was monitored by scale height at the end of precision cables hanging from hoop joints at several azimuth locations. Metric camera data of the hoop targets were used to monitor tilt angle during the test period. Table A2 shows that the hoop was within 0.03° of the horizontal throughout the test period.

3. Adjustment of hoop planarity: Metric camera data of the location of targets at the hoop joints were used with computer programs to determine a best-fit plane and the residuals of the targets from the best-fit plane. The centroid of the targets and the tilt of the plane from horizontal were also computed. These data show (table A2) maximum standard deviation of target residuals of 0.1 inch and maximum tilt angles of 0.03°. These data are consistent with earlier test results.

4. Control and hoop cord tension adjustment: The tensions on the cords were initially adjusted to approximately the mean value for the previous measurements (table A3) by manually adjusting the cord lengths. After these adjustments, adjusting screws at the piston retainers in the newly installed drive brackets were used for this purpose. Table A3 also includes a sequence of cord tension measurements throughout the test program.

5. Manual surface smoothness adjustment: After completing the prior adjustments, the control cords were adjusted manually to within the adjustment range of the computer-controlled actuators (about 0.2 inch of the best-fit paraboloid location). This adjustment was made by measuring the surface roughness with the metric camera, calculating the cord length changes necessary by using the surface adjustment model, and implementing the changes for all cords with >0.020-inch error. A second metric camera measurement showed that further changes were within the adjustment range of the computer-controlled drive motors. The metric camera data indicated that the surface roughness was approximately the same as previous tests at MMA for the three other quadrants so as not to degrade the surface of quadrant 4.

After completion of these steps, the automated antenna surface adjustment tests began.

Table A1. Column Verticality Measurements

(a) Upper column targets

Event	Centroid, in.			Unit normal, deg		Std. dev. residuals	No. of targets
	x	y	z	Azimuth	Elevation		
05/24/88	0.0470	0.0037	211.3269	26.2046	0.4040	0.0171	23
04/24/89	0.0899	−0.0142	211.4481	21.4606	0.3850	0.0160	21
06/08/89	0.0465	−0.0149	211.4408	23.2582	0.3807	0.0125	22
08/15/89	0.0715	−0.0247	211.4387	21.2862	0.3864	0.0119	22
08/31/89	0.0803	−0.0572	211.4419	20.7271	0.3813	0.0157	21
10/24/89	0.0720	−0.0494	211.4620	18.3732	0.3850	0.0152	18
11/07/89	0.0787	−0.0695	211.4392	21.8489	0.3879	0.0171	20
12/01/89	0.0871	−0.0640	211.4422	17.0966	0.3811	0.0146	22
12/18/89	0.0689	−0.0672	211.4311	20.1330	0.3936	0.0151	21
04/04/90	0.0837	−0.0828	211.4507	16.1756	0.3862	0.0137	18
04/19/90	0.0878	−0.0902	211.4593	15.9675	0.4042	0.0122	19
Mean. . . .	0.07664	−0.05341	211.4454				

(b) Central hub targets

Event	Centroid, in.			Unit normal, deg		Std. dev. residuals	No. of targets
	x	y	z	Azimuth	Elevation		
05/24/88	−0.0905	−0.1280	30.9584	−48.0075	0.1511	0.0172	22
04/24/89	−0.0896	−0.0640	31.0358	−48.2867	0.1550	0.0143	21
06/08/89	−0.1173	−0.0560	31.0249	−53.5940	0.1675	0.0119	21
08/15/89	−0.1003	−0.0553	31.0270	−56.1148	0.1690	0.0156	21
08/31/89	−0.0920	−0.0621	31.0344	−46.8352	0.1623	0.0144	21
10/24/89	−0.0933	−0.0657	31.0339	−43.9795	0.2476	0.0231	10
11/07/89	−0.1032	−0.0703	31.0345	−44.7306	0.1574	0.0116	21
12/01/89	−0.0972	−0.0787	31.0247	−47.3912	0.1947	0.0176	21
12/18/89	−0.1027	−0.0770	31.0283	−46.5338	0.1659	0.0114	21
04/04/90	−0.1075	−0.0808	31.0357	−51.5343	0.1494	0.0107	20
04/19/90	−0.1036	−0.0825	31.0417	−49.7768	0.1566	0.0115	21
Mean. . . .	−0.10067	−0.06924	31.03209				

(c) Table targets

Event	Centroid, in.			Unit normal, deg		Std. dev. residuals	No. of targets
	x	y	z	Azimuth	Elevation		
05/24/88	0.1478	0.5615	−179.3942	32.1503	0.1029	0.0520	16
04/24/89	0.3389	0.7390	−179.2461	81.9194	0.0271	0.0557	16
06/08/89	0.2737	0.7430	−179.2804	67.0360	0.0301	0.0546	16
08/15/89	0.2531	0.7579	−179.2775	46.4712	0.0370	0.0533	16
08/31/89	0.2479	0.7757	−179.2608	38.8478	0.0329	0.0547	16
10/24/89	0.1930	0.7779	−179.2477	27.1909	0.0439	0.0547	16
11/07/89	0.2020	0.7534	−179.2431	36.0842	0.0368	0.0524	16
12/01/89	0.3185	0.7851	−179.2484	61.6734	0.0124	0.0547	16
12/18/89	0.2995	0.7780	−179.2200	−66.7743	0.0140	0.0513	16
04/04/90	0.3138	0.7944	−179.2455	62.1169	0.0128	0.0552	16
04/19/90	0.3141	0.8060	−179.2331	22.8885	0.0084	0.0537	16
Mean. . . .	0.27545	0.77104	−179.2502				

Table A2. Hoop Planarity Measurements

[Planarity equation: $H = H_o + Ax + By$; H is height above reference; H_o, A, and B are coefficients of equation of derived best-fit plane]

Event	Coefficients			Std. dev. residuals	Normal vector		No. of targets
	H_o	$A \times 10^4$	$B \times 10^4$		Azimuth, deg	Elevation, deg	
05/24/88	48.1744	0.4166	−0.0330	0.0906	−4.5221	0.0024	45
04/24/89	48.2129	2.2915	−1.3348	0.1042	−30.2214	0.0152	43
06/08/89	48.1902	0.4196	−0.9721	0.1041	−66.6548	0.0061	42
08/15/89	48.1901	1.5300	−1.7661	0.1008	−49.0960	0.0134	43
08/31/89	48.2055	1.8379	−2.8545	0.1045	−57.2245	0.0194	43
10/24/89	48.1842	2.1981	−2.4010	0.0962	−47.5262	0.0186	40
11/07/89	48.2125	1.8383	−3.8045	0.0724	−64.2102	0.0242	43
12/01/89	48.1934	2.5301	−4.0402	0.0722	−57.9439	0.0273	40
12/18/89	48.2070	2.1453	−3.4627	0.0767	−58.2200	0.0233	42
04/04/90	48.2085	2.2031	−4.6334	0.0719	−64.5702	0.0294	38
04/19/90	48.2224	2.5618	−4.1618	0.0867	−58.3856	0.0280	43

Event	Hoop centroid, in.		
	x	y	z
05/24/89	−0.0008	0.0168	48.1749
04/24/89	0.0130	0.0013	48.2171
06/08/89	−0.0039	0.0045	48.1909
08/15/89	0.0066	0.0037	48.1935
08/31/89	0.0068	−0.0087	48.2102
10/24/89	0.0093	−0.0100	48.1897
11/07/89	0.0108	−0.0094	48.2180
12/01/89	0.0091	−0.0112	48.2033
12/18/89	0.0095	−0.0112	48.2154
04/04/90	0.0042	−0.0176	48.2228
04/19/90	0.0141	−0.0186	48.2243

Table A3. Cord Tension Data

Gore	Cord	Measured cord tension, lb, on—													
		04/19/88	09/09/89	10/13/89	10/24/89	03/31/89	04/04/89	04/11/89	04/20/89	06/09/89	08/15/89	10/12/89	10/18/89	10/23/89	11/06/89
19	G01				1.62	1.88	2.20		2.19	1.46	1.56			1.50	1.67
	G02				1.59	1.67	1.64		1.52	1.22	1.20			1.29	1.14
	G03				1.93	1.13	1.57		1.64	1.23	1.66			1.34	1.48
	G04	11.61	10.64	10.33	9.75	12.33	11.24	11.38	11.14	9.82	11.32		11.90	10.44	11.29
	Hoop	5.27	7.10	6.27	6.60		7.06	6.42	5.94	5.40	5.41		4.59	4.49	7.29
	Right quartz								25.70			26.00			
	Left quartz								26.60			26.60			
20	G01				2.00	0.00	0.00		0.00	1.63	1.56			1.47	1.53
	G02				1.70	1.43	1.53		1.42	1.41	1.36			1.33	1.51
	G03				2.06	1.16	1.51		1.37	1.52	1.49			1.47	1.61
	G04	7.90	9.57	9.32	8.98	10.02	10.49	10.69	10.41	10.65	10.40		12.96	10.55	9.79
	Hoop	2.37	7.34	8.20	8.03		8.31	8.12	7.60	9.42	10.83		11.33	9.87	7.10
	Right quartz								25.30			24.00			
	Left quartz								30.20			28.90			
21	G01				2.29	2.10	2.47		2.41	1.59	1.63			1.58	1.56
	G02				1.93	1.81	1.65		1.72	1.16	1.53			1.20	1.35
	G03				2.40	1.47	1.55		1.88	1.25	1.72			1.58	1.66
	G04	13.06	6.08	9.98	9.45	14.79	15.23	15.24	14.70	9.95	12.46		10.69	8.97	11.26
	Hoop	6.92	11.67	5.68	5.73		4.94	3.70	4.39	5.11	4.56		9.03	9.24	5.09
	Right quartz								24.90			26.00			
	Left quartz								23.20			24.50			
22	G01				1.97	1.84	1.99		1.95	1.53	1.49			1.60	1.43
	G02				1.48	1.22	1.16		1.23	1.47	1.45			1.71	1.24
	G03				1.41	1.18	0.00		0.00	1.69	1.81			2.02	1.43
	G04	8.89	4.41	8.60	8.21	10.16	9.55	9.03	8.86	12.10	10.42		15.70	13.30	8.71
	Hoop	3.81	10.77	6.54	6.67		6.61	5.65	4.80	10.10	12.70		5.32	4.80	10.50
	Right quartz								27.90			23.40			
	Left quartz								30.40			25.30			
23	G01				1.92	1.76	2.14		1.88	1.44	1.44			1.50	1.45
	G02				1.74	1.89	1.69		1.84	1.21	1.42			1.34	1.34
	G03				2.30	1.67	2.07		2.09	1.15	1.61			1.43	1.81
	G04	10.27	12.39	12.19	11.66	15.20	14.64	14.56	13.25	8.77	11.35		12.36	10.20	11.46
	Hoop	5.22	6.34	5.95	6.19		6.44	5.94	5.85	2.77	3.42		2.60	2.53	2.96
	Right quartz								23.40			25.70			
	Left quartz								27.90			30.20			
24	G01				1.88	1.62	1.77		1.54	1.66	1.69			1.86	1.72
	G02				1.67	1.36	1.38		1.99	1.41	1.61			1.93	1.65
	G03				1.66	0.00	1.22		0.00	1.64	1.72			2.13	2.03
	G04	8.76	9.55	8.98	8.78	10.67	9.21	8.84	7.13	10.57	12.71		19.15	15.50	11.74
	Hoop	5.36	2.02	1.08	1.28		3.29	1.97	7.06	5.52	5.58		7.07	6.68	4.27
	Right quartz								27.00			26.20			
	Left quartz								29.60			28.90			
1	G01				2.44	2.21	2.89		2.77	1.57	1.62			1.27	1.58
	G02				1.89	1.86	1.64		1.69	1.31	1.43			0.00	1.37
	G03				2.14	1.50	1.91		1.86	1.37	1.44			0.00	1.63
	G04	10.09	12.15	11.96	11.70	15.79	13.22	13.07	13.23	9.61	10.82		5.95	4.94	10.20
	Hoop	3.22	7.76	7.69	7.30		8.90	10.01	6.87	8.66	8.33		9.91	9.36	5.03
	Right quartz								21.50			21.10			
	Left quartz								27.40			26.80			

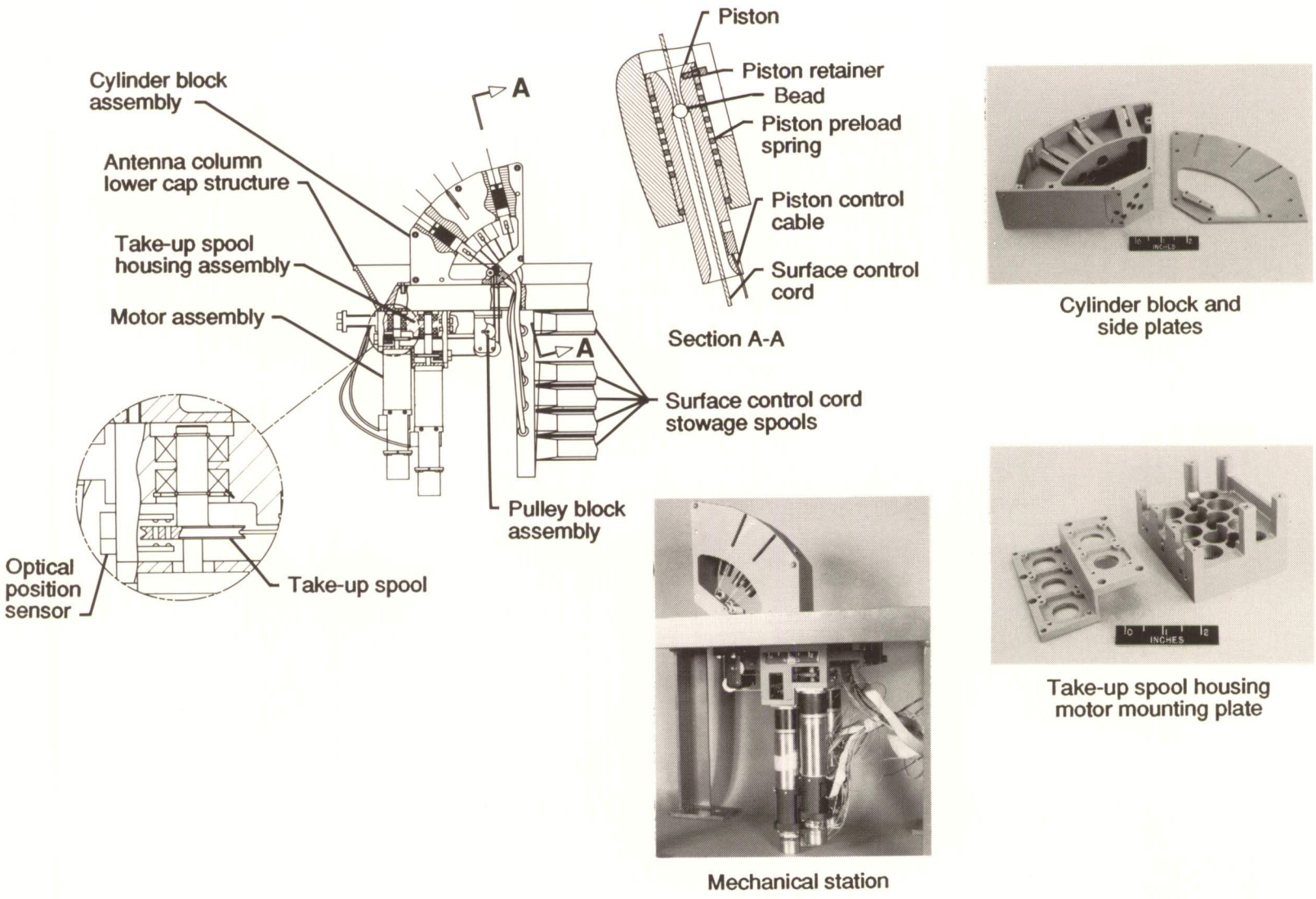

Figure A1. Control system motor-driver assembly.

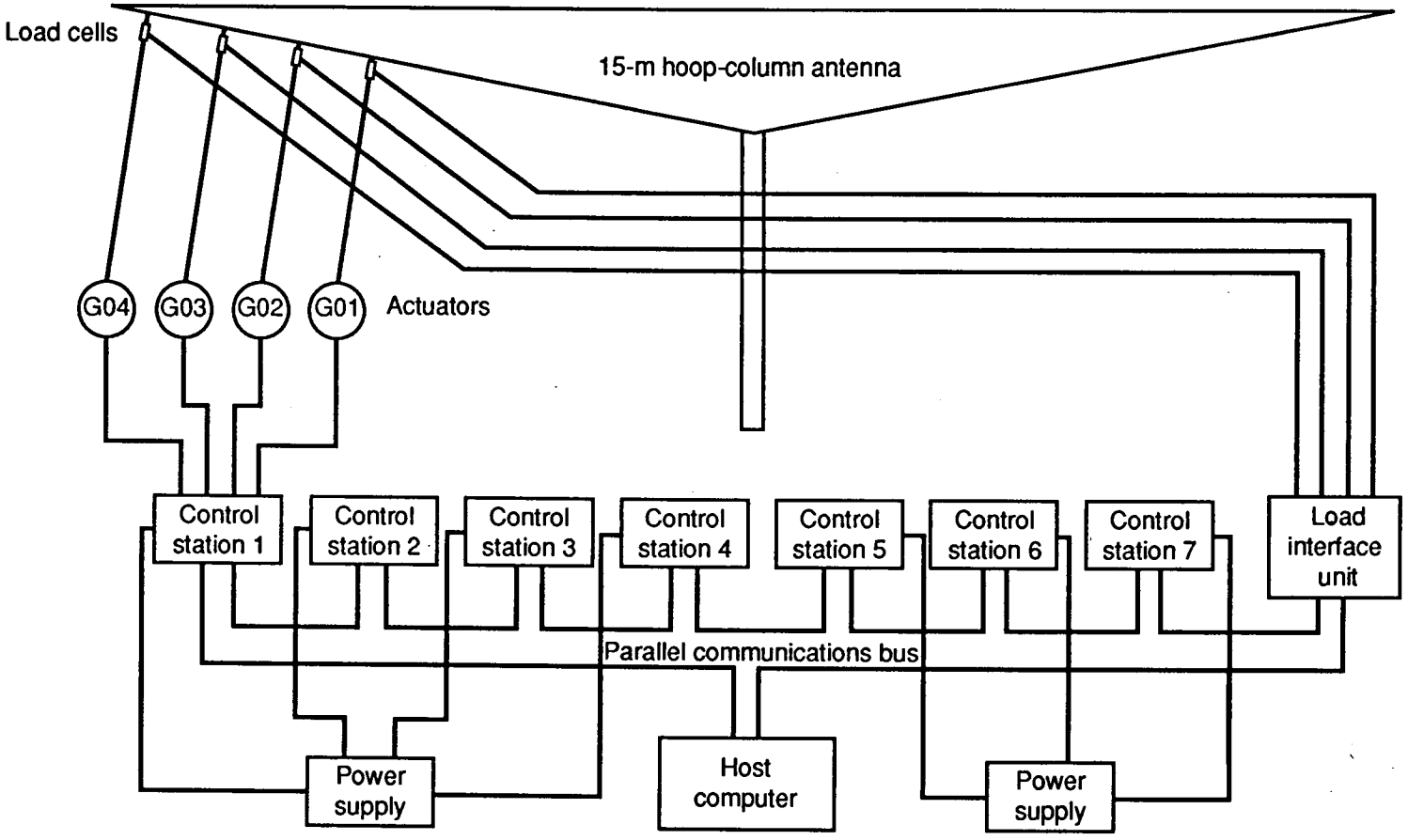

Figure A2. Block diagram of computer-driver system.

References

1. Schroeder, Lyle C.; Adams, Richard C.; Bailey, M. C.; Belvin, W. Keith; Butler, David H.; and Campbell, Thomas G.: *Near-Field Testing of the 15-Meter Hoop-Column Antenna.* NASA TM-4073, 1989.

2. Kefauver, Neill; Cencich, Tom; Osborn, Jim; and Osmanski, J. T.: *Near-Field Testing of the 5-Meter Model of the Tetrahedral Truss Antenna.* NASA CR-178147, 1986.

3. *Development of the 15 Meter Diameter Hoop Column Antenna—A Final Report.* NASA CR-4038, 1986.

4. McLauchlan, J. M.: Spatial, High-Accuracy, Positioning-Encoding Sensor (Shapes) for Large Space System Control Applications. *Large Space Systems Technology—1981,* William J. Boyer, compiler, NASA CP-2215, Part 1, 1982, pp. 282–296.

5. Welch, Sharon S.; and Clemmons, James I., Jr.: The Optical Position Measurement System for a Large-Gap Magnetic Suspension System (LGMSS). *Aerospace Applications of Magnetic Suspension Technology,* Nelson J. Groom and Colin P. Britcher, eds., NASA CP-10066, Part 2, 1991, pp. 731–765.

6. Belvin, W. Keith; Edighoffer, Harold H.; and Herstrom, Catherine L.: Quasistatic Shape Adjustment of a 15-Meter-Diameter Space Antenna. *J. Spacecr. & Rockets,* vol. 26, no. 3, May–June 1989, pp. 129–136.

7. Lim, Kyong Been; Juang, Jer-Nan; and Maghami, Peiman: *A Study on the Sensitivity and Simultaneous Adjustment of a Hoop-Column Antenna Surface.* NASA TM-101538, 1988.

8. Lee, Teh-Hong; Rudduck, Roger C.; and Bailey, Marion C.: A Surface Distortion Analysis Applied to the Hoop/Column Deployable Mesh Reflector Antenna. *IEEE Trans. Antennas & Propag.*, vol. 37, no. 4, Apr. 1989, pp. 452–458.

9. Bailey, M. C.: Multiple-Aperture Mesh Reflector Antenna Radiation Pattern Characteristics. *Antennas and Propagation—AP-S International Symposium 1986, Symposium Digest,* Volume I, IEEE Catalog No. 86CH2325-9, Inst. of Electrical and Electronics Engineers, Inc., 1986, pp. 405–408.

10. Bailey, M. C.: Cockrell, C. R.; and Staton, L. D.: *Electronic Compensation for Reflector Surface Distortion To Improve Radiation Pattern Characteristics of Antennas.* NASA TM-100652, 1989.

11. Bailey, M. C.: Determination of Array Feed Excitation To Improve Performance of Distorted or Scanned Reflector Antennas. *Antennas and Propagation Society Symposium, 1991 Digest,* Volume 1, IEEE Catalog No. 91CH3036-1, Inst. of Electrical and Electronics Engineers, Inc., 1991, pp. 175–178.

12. Vanderplaats, Garret N.: *CONMIN—A FORTRAN Program for Constrained Function Minimization, User's Manual.* NASA TM X-62282, 1973.

13. Smith, William Travis: A Synthesis Procedure for Array Feeds To Improve Radiation Performance of Large Distorted Reflector Antennas. Ph.D. Diss., Virginia Polytechnic Inst. and State Univ., June 1990.

14. Ahl, Elvin L.; and Miller, James B.: Antenna Surface Contour Control System. U.S. Patent No. 4,811,033, Mar. 7, 1989.

Table 1. Best-Fit Paraboloid History

(a) Effective surface

Date	Focal length, in.	Vertex offset			(Δz) rms, in.	No. of targets
		x, in.	y, in.	z, in.		
Quadrant 1						
04/24/89	373.445	12.479	12.456	−0.1907	0.121	211
06/08/89	366.459	14.771	14.638	−0.0211	0.076	211
08/15/89	367.871	14.435	13.965	−0.0792	0.077	211
08/31/89	367.227	14.556	14.383	−0.0334	0.076	211
10/24/89	366.863	14.545	14.594	−0.0179	0.076	211
11/07/89	366.741	14.569	14.584	−0.0159	0.074	211
12/01/89	367.574	14.345	14.247	−0.0454	0.072	211
12/18/89	368.008	14.262	14.153	−0.0476	0.072	211
04/04/90	367.789	14.313	14.280	−0.0374	0.073	211
04/19/90	367.810	14.274	14.284	−0.0368	0.072	211
04/19/90	367.977	14.239	14.231	−0.0061	0.071	[a]435
Quadrant 2						
04/24/89	369.978	−13.876	13.730	−0.0596	0.148	211
06/08/89	364.740	−15.438	15.110	0.0761	0.090	211
08/15/89	364.901	−15.419	15.049	0.0728	0.092	211
08/31/89	364.884	−15.462	15.159	0.0861	0.091	211
10/24/89	364.771	−15.499	15.207	0.0838	0.093	211
11/07/89	364.801	−15.476	15.179	0.0903	0.094	211
12/01/89	364.784	−15.485	15.204	0.0864	0.095	211
12/18/89	364.857	−15.435	15.293	0.0939	0.095	211
04/04/90	364.561	−15.536	15.390	0.1023	0.095	211
04/19/90	364.665	−15.540	15.377	0.1048	0.094	211
04/19/90	364.487	−15.641	15.517	0.1626	0.096	[a]439
Quadrant 3						
04/24/89	368.767	−14.183	−13.951	−0.0879	0.145	213
06/08/89	366.530	−14.677	−14.833	−0.0208	0.098	213
08/15/89	367.381	−14.391	−14.508	−0.0470	0.097	213
08/31/89	368.216	−14.078	−14.266	−0.0614	0.098	213
10/24/89	364.471	−15.558	−15.092	0.0724	0.132	213
11/07/89	368.132	−13.952	−14.460	−0.0740	0.105	213
12/01/89	368.943	−13.647	−14.195	−0.0962	0.104	213
12/18/89	368.352	−13.850	−14.385	−0.0729	0.102	213
04/04/90	368.512	−13.790	−14.342	−0.0735	0.103	213
04/19/90	368.659	−13.753	−14.282	−0.0748	0.103	213
04/19/90	369.020	−13.611	−14.116	−0.0628	0.094	[a]439
Quadrant 4						
05/24/88	368.580	14.127	−13.879	−0.0605	0.088	213
04/24/89	367.100	15.549	−13.464	−0.0358	0.283	213
06/08/89	366.800	14.896	−14.356	0.0370	0.147	213
08/15/89	367.735	14.506	−13.930	−0.0356	0.077	213
08/31/89	367.889	14.328	−14.368	−0.0114	0.064	213
10/24/89	362.854	16.084	−16.130	0.1788	0.166	213
11/07/89	364.834	15.227	−14.634	−0.0242	0.124	213
12/01/89	367.200	14.717	−14.257	−0.0117	0.070	213
12/18/89	367.442	14.582	−14.332	−0.0079	0.063	213
04/04/90	367.637	14.406	−14.419	−0.0165	0.062	213
04/19/90	366.758	14.673	−14.649	−0.0057	0.063	213
04/19/90	366.558	14.728	−14.721	0.0366	0.065	[a]440

[a]Includes pillow targets.

Table 1. Concluded

(b) Complete surface

Date	Focal length, in.	Vertex offset			(Δz) rms, in.	No. of targets
		x, in.	y, in.	z, in.		
Quadrant 1						
04/24/89	373.373	12.700	12.700	−0.1426	0.136	235
06/08/89	368.202	14.560	14.425	−0.0005	0.106	235
08/15/89	369.278	14.273	13.882	−0.0520	0.107	235
08/31/89	368.801	14.367	14.240	−0.0093	0.106	235
10/24/89	368.643	14.335	14.388	0.0050	0.108	235
11/07/89	368.579	14.342	14.373	0.0067	0.108	235
12/01/89	369.427	14.120	14.052	−0.0203	0.108	235
12/18/89	369.676	14.068	13.992	−0.0225	0.106	235
04/04/90	369.485	14.115	14.111	−0.0126	0.106	235
04/19/90	369.476	14.081	14.121	−0.0120	0.105	235
04/19/90	369.412	14.069	14.097	0.0148	0.100	[a]471
Quadrant 2						
04/24/89	370.890	−13.877	13.667	−0.0315	0.160	236
06/08/89	366.983	−15.126	14.783	0.0929	0.129	236
08/15/89	367.316	−15.086	14.700	0.0913	0.133	236
08/31/89	367.246	−15.138	14.820	0.1047	0.132	236
10/24/89	367.152	−15.169	14.857	0.1013	0.133	236
11/07/89	367.225	−15.143	14.827	0.1088	0.135	236
12/01/89	367.392	−15.122	14.820	0.1052	0.138	236
12/18/89	367.393	−15.090	14.906	0.1117	0.137	236
04/04/90	366.889	−15.243	15.022	0.1197	0.134	234
04/19/90	366.950	−15.256	15.020	0.1225	0.132	235
04/19/90	366.586	−15.357	15.177	0.1737	0.127	[a]475
Quadrant 3						
04/24/89	370.172	−13.919	−13.694	−0.0906	0.153	239
06/08/89	368.325	−14.335	−14.483	−0.0269	0.117	239
08/15/89	369.158	−14.078	−14.176	−0.0489	0.117	239
08/31/89	369.645	−13.852	−13.986	−0.0615	0.115	239
10/24/89	367.443	−14.909	−14.532	0.0556	0.154	239
11/07/89	369.437	−13.779	−14.164	−0.0747	0.120	239
12/01/89	370.322	−13.485	−13.897	−0.0933	0.122	239
12/18/89	369.854	−13.653	−14.053	−0.0728	0.121	239
04/04/90	369.811	−13.637	−14.036	−0.0734	0.120	239
04/19/90	369.924	−13.607	−13.985	−0.0744	0.119	239
04/19/90	370.130	−13.490	−13.881	−0.0598	0.108	[a]477
Quadrant 4						
05/24/88	370.679	13.855	−13.595	−0.0412	0.188	239
04/24/89	368.569	15.156	−13.449	−0.0237	0.283	239
06/08/89	369.236	14.451	−14.047	0.0477	0.164	239
08/15/89	369.716	14.144	−13.710	−0.0235	0.105	239
08/31/89	369.365	14.091	−14.151	−0.0044	0.085	239
10/24/89	365.931	15.446	−15.499	0.1595	0.176	239
11/07/89	367.065	14.834	−14.270	−0.0209	0.138	239
12/01/89	368.910	14.415	−14.006	−0.0066	0.091	239
12/18/89	369.053	14.307	−14.083	−0.0034	0.084	239
04/04/90	368.959	14.207	−14.184	−0.0131	0.079	239
04/19/90	368.172	14.438	−14.386	−0.0057	0.080	239
04/19/90	367.864	14.514	−14.484	0.0366	0.079	[a]478

[a]Includes pillow targets.

Table 2. Control Cord Adjustments Required for First Computer-Controlled Adjustment Based on Metric Camera Data for 6/8/89

Quadrant	Hoop joint	Radial	Adjustment required, in., for—			
			G01	G02	G03	G04
3	19	1	0.026	−0.019	−0.014	−0.022
	18	2	−0.022	−0.030	−0.003	0.047
	17	3	0.030	−0.008	−0.025	−0.013
	16	4	0.001	0.043	0.038	0.037
	15	5	0.024	0.000	−0.013	−0.041
	14	6	0.000	0.057	0.057	0.027
2	13	7	0.028	−0.036	0.010	−0.032
	12	8	0.016	−0.043	−0.032	−0.007
	11	9	−0.007	0.000	0.021	−0.018
	10	10	0.004	0.006	0.018	0.016
	9	11	0.020	−0.026	−0.014	0.008
	8	12	0.029	−0.013	0.024	−0.068
1	7	13	0.019	−0.015	−0.013	−0.032
	6	14	−0.007	0.057	0.003	0.016
	5	15	0.006	−0.002	−0.010	−0.038
	4	16	−0.009	0.060	0.035	0.022
	3	17	0.015	0.000	−0.026	−0.033
	2	18	−0.010	0.047	0.026	0.046
4	1	19	0.013	−0.003	−0.048	−0.027
	24	20	0.107	0.024	0.000	0.005
	23	21	0.088	0.015	−0.050	−0.050
	22	22	−0.010	−0.001	0.059	0.095
	21	23	0.060	−0.031	−0.086	−0.094
	20	24	0.050	−0.122	−0.127	−0.030
	19	1	0.026	−0.019	−0.014	−0.022

Table 3. Control Cord Adjustments Required After Second Computer-Controlled Adjustment Based on Metric Camera Data for 8/31/89

[Quadrant 4 only]

Hoop joint	Radial	Adjustment required, in., for—			
		G01	G02	G03	G04
1	19	−0.006	−0.002	−0.080	−0.001
24	20	−0.014	−0.016	−0.012	−0.001
23	21	−0.008	−0.017	−0.005	−0.011
22	22	−0.016	−0.010	−0.007	−0.014
21	23	−0.015	−0.007	−0.007	−0.015
20	24	−0.016	−0.022	0.000	−0.001
19	1	−0.016	−0.004	−0.001	−0.004

Table 4. Array-Feed Element Excitation Coefficients for Ideal Paraboloidal Reflector Illumination

Element	Complex amplitude	Amplitude, dB	Phase, deg
1	(1.0000, 0.0000)	0.0000	0.0
2	(0.2661, 0.0000)	−11.4991	0.0
3	(0.2661, 0.0000)	−11.4991	0.0
4	(0.2661, 0.0000)	−11.4991	0.0
5	(0.2661, 0.0000)	−11.4991	0.0
6	(0.2661, 0.0000)	−11.4991	0.0
7	(0.2661, 0.0000)	−11.4991	0.0

Table 5. Excitation Coefficients at 6 GHz for 7-Element Array Feed for 4/19/90 Surface Compensation

Element	Complex amplitude	Amplitude, dB	Phase, deg
1	(1.0000, 0.0000)	0.0	0.0
2	(0.3457, 0.0854)	−9.0	13.9
3	(0.2779, 0.0957)	−10.6	19.0
4	(0.3207, 0.0561)	−9.7	9.9
5	(0.2621, 0.0620)	−11.4	13.3
6	(0.2669, 0.0609)	−11.2	12.9
7	(0.2650, 0.0977)	−11.0	20.2

Table 6. Excitation Coefficients at 6 GHz for 19-Element Array Feed for 4/19/90 Surface Compensation

Element	Amplitude, dB	Phase, deg	Element	Amplitude, dB	Phase, deg
1	0.0	0	11	−24.4	−141
2	−10.2	18	12	−23.7	−4
3	−10.4	16	13	−38.2	−113
4	−9.8	15	14	−23.2	−172
5	−10.2	12	15	−26.2	−124
6	−11.0	13	16	−26.4	123
7	−11.0	22	17	−23.3	−35
8	−19.4	4	18	−24.4	−164
9	−23.1	−54	19	−31.8	−34
10	−24.7	62			

Table 7. Excitation Coefficients at 6 GHz for 37-Element Array Feed for 4/19/90 Surface Compensation

Element	Amplitude, dB	Phase, deg	Element	Amplitude, dB	Phase, deg	Element	Amplitude, dB	Phase, deg
1	0.0	0	13	−30.2	95	25	−25.7	−117
2	−10.2	7	14	−25.6	117	26	−24.9	−80
3	−10.8	13	15	−29.4	−176	27	−25.4	−6
4	−10.4	1	16	−31.5	75	28	−31.4	−122
5	−11.7	−1	17	−31.3	−38	29	−19.6	−118
6	−11.3	11	18	−26.9	−167	30	−26.0	−109
7	−11.5	9	19	−35.2	76	31	−26.4	−88
8	−24.6	34	20	−19.0	−31	32	−36.0	−111
9	−27.0	−36	21	−24.9	−28	33	−36.4	166
10	−28.7	52	22	−31.2	−36	34	−27.3	−21
11	−31.1	156	23	−30.5	−119	35	−23.3	−59
12	−27.7	−22	24	−34.5	−126	36	−30.3	−156
						37	−36.8	−69

Table 8. Excitation Coefficients at 6 GHz for 61-Element Array Feed for 4/19/90 Surface Compensation

Element	Amplitude, dB	Phase, deg	Element	Amplitude, dB	Phase, deg	Element	Amplitude, dB	Phase, deg
1	0.0	0	21	−23.8	−24	41	−25.1	30
2	−10.4	5	22	−27.3	−90	42	−29.3	82
3	−10.7	13	23	−28.9	−99	43	−37.9	−30
4	−10.3	−1	24	−38.6	−174	44	−31.5	136
5	−11.4	2	25	−24.9	−103	45	−34.2	114
6	−11.5	7	26	−36.5	−83	46	−26.0	−52
7	−11.1	10	27	−23.3	−24	47	−42.6	−25
8	−25.6	22	28	−29.7	−57	48	−24.8	126
9	−26.7	−16	29	−21.0	−131	49	−26.1	164
10	−25.5	59	30	−26.3	−122	50	−30.4	−77
11	−29.5	−138	31	−25.7	−66	51	−30.4	−33
12	−27.7	4	32	−41.2	−142	52	−36.5	139
13	−28.3	114	33	−31.5	−58	53	−28.9	−155
14	−28.9	122	34	−31.8	−12	54	−41.9	−136
15	−31.0	−173	35	−24.6	−53	55	−29.9	165
16	−28.0	98	36	−27.5	−144	56	−30.3	112
17	−31.1	−26	37	−31.1	−65	57	−33.8	48
18	−27.9	−180	38	−33.4	−67	58	−24.7	−67
19	−32.5	79	39	−34.0	−101	59	−37.0	61
20	−19.9	−21	40	−29.6	77	60	−30.1	53
						61	−26.4	111

Table 9. Excitation Coefficients at 6 GHz for 91-Element Array Feed for 4/19/90 Surface Compensation

Element	Amplitude, dB	Phase, deg	Element	Amplitude, dB	Phase, deg	Element	Amplitude, dB	Phase, deg
1	0.0	0	31	−25.5	−88	61	−34.1	80
2	−10.3	7	32	−34.3	−85	62	−27.2	122
3	−10.6	11	33	−36.4	18	63	−26.2	166
4	−10.6	3	34	−28.9	−28	64	−25.1	138
5	−11.5	1	35	−26.4	−74	65	−26.4	95
6	−11.5	9	36	−27.2	−142	66	−32.7	103
7	−11.4	10	37	−36.8	−85	67	−30.1	−37
8	−25.7	3	38	−30.2	−65	68	−33.2	90
9	−28.2	−17	39	−27.6	−47	69	−29.8	−170
10	−28.5	54	40	−37.8	−15	70	−24.9	−170
11	−32.1	166	41	−28.0	31	71	−27.5	−25
12	−30.6	−20	42	−30.7	73	72	−26.6	51
13	−31.9	79	43	−42.5	−139	73	−29.0	38
14	−36.9	143	44	−31.3	45	74	−29.3	128
15	−29.9	138	45	−36.1	153	75	−32.3	−176
16	−34.3	122	46	−25.4	−81	76	−40.4	−156
17	−32.8	−18	47	−46.2	26	77	−27.2	133
18	−31.0	−159	48	−29.2	123	78	−26.9	109
19	−32.2	71	49	−28.6	164	79	−23.6	131
20	−21.0	−21	50	−23.8	−61	80	−24.1	−174
21	−26.2	−13	51	−25.8	−57	81	−33.2	−148
22	−29.5	−84	52	−29.8	−8	82	−28.9	−10
23	−30.3	−84	53	−33.0	−163	83	−35.3	168
24	−31.4	−143	54	−35.7	−169	84	−28.3	67
25	−27.0	−119	55	−31.3	165	85	−26.2	75
26	−28.3	−71	56	−31.8	−171	86	−26.5	−32
27	−24.8	−13	57	−35.2	84	87	−27.9	−113
28	−33.6	−105	58	−26.0	−33	88	−25.3	−153
29	−21.6	−149	59	−31.9	−12	89	−26.9	127
30	−25.4	−136	60	−30.2	69	90	−43.3	42
						91	−29.9	155

Table 10. Excitation Coefficients at 6 GHz for 127-Element Array Feed for 4/19/90 Surface Compensation

Element	Amplitude, dB	Phase, deg	Element	Amplitude, dB	Phase, deg	Element	Amplitude, dB	Phase, deg
1	0.0	0	43	−38.8	−83	85	−35.4	68
2	−10.4	8	44	−43.8	76	86	−37.5	−49
3	−10.9	9	45	−39.9	135	87	−33.7	−100
4	−10.8	3	46	−28.0	−80	88	−26.9	−138
5	−11.4	0	47	−37.6	108	89	−30.2	118
6	−11.9	9	48	−29.0	143	90	−34.9	131
7	−11.7	10	49	−30.2	147	91	−34.4	163
8	−25.4	12	50	−26.1	−82	92	−41.1	165
9	−26.9	−20	51	−29.2	−65	93	−43.2	114
10	−27.9	54	52	−33.9	−18	94	−43.2	142
11	−31.6	171	53	−28.9	−151	95	−34.6	175
12	−29.8	7	54	−42.5	−157	96	−40.9	159
13	−35.9	97	55	−31.4	−176	97	−31.4	124
14	−31.3	132	56	−35.0	137	98	−34.3	−108
15	−27.3	161	57	−36.3	54	99	−29.7	−41
16	−30.7	80	58	−28.0	−44	100	−29.9	−135
17	−32.2	−47	59	−34.4	20	101	−25.2	−126
18	−31.8	−173	60	−31.2	51	102	−26.3	−101
19	−34.6	46	61	−32.7	75	103	−27.9	−7
20	−20.6	−21	62	−27.0	125	104	−25.2	43
21	−26.0	−21	63	−27.4	179	105	−25.6	101
22	−29.1	−88	64	−27.5	134	106	−32.0	162
23	−32.1	−104	65	−26.4	90	107	−37.7	−125
24	−34.4	−141	66	−41.2	42	108	−43.5	−41
25	−27.8	−126	67	−35.7	12	109	−42.1	16
26	−24.6	−71	68	−33.0	93	110	−34.4	79
27	−25.6	−11	69	−30.4	157	111	−31.7	146
28	−34.0	−70	70	−30.8	157	112	−31.5	173
29	−22.0	−140	71	−36.7	−67	113	−36.7	165
30	−26.2	−120	72	−31.6	10	114	−43.2	−162
31	−27.4	−66	73	−28.2	16	115	−33.1	−134
32	−31.7	−116	74	−32.5	113	116	−32.5	22
33	−37.1	7	75	−32.9	164	117	−30.4	−21
34	−31.6	−31	76	−31.8	−148	118	−31.0	79
35	−24.6	−61	77	−30.3	138	119	−25.6	73
36	−27.3	−151	78	−28.5	68	120	−27.7	43
37	−35.3	−123	79	−25.4	127	121	−28.5	−26
38	−29.8	−57	80	−25.7	−177	122	−26.4	−65
39	−32.3	−50	81	−39.0	−128	123	−28.9	−143
40	−37.6	11	82	−36.8	12	124	−25.9	158
41	−28.6	34	83	−35.7	−168	125	−36.2	26
42	−32.7	72	84	−31.8	84	126	−34.3	−120
						127	−35.3	41

Table 11. Excitation Coefficients at 6 GHz for 169-Element Array Feed for 4/19/90 Surface Compensation

Element	Amplitude, dB	Phase, deg	Element	Amplitude, dB	Phase, deg	Element	Amplitude, dB	Phase, deg	Element	Amplitude, dB	Phase, deg
1	0.0	0	43	−58.3	−168	85	−32.3	63	127	−44.1	78
2	−10.5	9	44	−43.7	98	86	−32.2	−30	128	−46.1	−169
3	−10.8	11	45	−35.0	152	87	−32.8	−95	129	−33.8	−117
4	−10.5	3	46	−28.3	−68	88	−27.7	−147	130	−35.0	−40
5	−11.5	3	47	−43.1	−14	89	−28.3	125	131	−32.2	−58
6	−11.8	9	48	−28.0	134	90	−42.8	109	132	−36.6	−83
7	−11.4	11	49	−28.8	175	91	−34.3	146	133	−38.1	−66
8	−24.4	12	50	−25.6	−76	92	−42.9	85	134	−39.8	59
9	−26.3	−29	51	−29.7	−52	93	−36.6	104	135	−38.6	105
10	−26.8	57	52	−49.9	−4	94	−34.1	140	136	−36.0	−11
11	−30.7	−168	53	−33.3	−140	95	−32.2	134	137	−33.9	−90
12	−29.1	3	54	−37.5	−159	96	−36.2	124	138	−30.4	−68
13	−36.0	108	55	−33.0	163	97	−31.6	139	139	−31.2	−25
14	−31.3	134	56	−34.5	134	98	−32.6	−87	140	−45.5	43
15	−30.1	166	57	−39.5	82	99	−34.2	−39	141	−37.7	157
16	−31.2	96	58	−27.0	−42	100	−33.0	−142	142	−30.2	20
17	−29.1	−32	59	−33.1	−8	101	−25.0	−143	143	−35.6	37
18	−30.1	178	60	−30.9	60	102	−26.9	−107	144	−34.5	−174
19	−37.7	60	61	−32.5	102	103	−28.3	−28	145	−30.1	−136
20	−21.3	−20	62	−27.8	128	104	−26.4	62	146	−45.6	−163
21	−26.6	−24	63	−27.6	179	105	−28.1	98	147	−35.9	71
22	−30.3	−73	64	−28.1	140	106	−31.8	114	148	−41.6	165
23	−30.6	−110	65	−29.2	92	107	−37.4	−53	149	−43.8	65
24	−36.4	−126	66	−36.7	49	108	−40.8	−113	150	−34.4	134
25	−27.6	−117	67	−35.5	16	109	−37.5	−24	151	−39.5	−31
26	−27.7	−77	68	−35.7	83	110	−40.6	109	152	−35.4	17
27	−25.3	−11	69	−33.4	172	111	−37.2	138	153	−31.1	57
28	−34.4	−45	70	−31.2	165	112	−28.4	159	154	−38.0	−158
29	−21.4	−141	71	−32.2	−23	113	−28.9	173	155	−35.7	−107
30	−26.4	−115	72	−31.5	8	114	−38.4	−86	156	−40.2	−70
31	−26.8	−80	73	−29.7	26	115	−40.9	146	157	−36.2	−31
32	−36.0	−107	74	−30.6	140	116	−33.3	16	158	−33.3	37
33	−43.5	−66	75	−32.6	145	117	−33.2	−10	159	−35.2	17
34	−30.1	−22	76	−36.9	−165	118	−32.3	87	160	−41.0	105
35	−26.0	−67	77	−29.2	126	119	−26.6	76	161	−39.6	−12
36	−27.2	−143	78	−28.8	88	120	−28.9	46	162	−44.8	−42
37	−37.7	−70	79	−30.4	118	121	−29.9	−32	163	−34.6	−8
38	−29.5	−58	80	−27.0	170	122	−28.7	−80	164	−30.4	−27
39	−30.2	−42	81	−31.6	−136	123	−29.8	−147	165	−33.7	169
40	−36.3	36	82	−35.1	24	124	−29.1	176	166	−31.1	123
41	−28.8	41	83	−35.7	−141	125	−35.9	50	167	−40.7	−65
42	−34.4	56	84	−31.9	81	126	−35.7	−116	168	−43.6	54
									169	−35.3	5

Table 12. Excitation Coefficients at 6 GHz for 217-Element Array Feed for 4/19/90 Surface Compensation

Element	Amplitude, dB	Phase, deg	Element	Amplitude, dB	Phase, deg	Element	Amplitude, dB	Phase, deg	Element	Amplitude, dB.	Phase, deg
1	0.0	0	43	−43.4	−116	85	−29.4	72	127	−40.3	46
2	−10.4	9	44	−37.1	86	86	−34.5	−53	128	−40.2	−60
3	−10.7	11	45	−35.8	149	87	−34.1	−96	129	−32.9	−70
4	−10.4	3	46	−26.0	−68	88	−27.2	−137	130	−31.2	−30
5	−11.2	3	47	−43.1	55	89	−27.0	134	131	−32.2	−57
6	−11.8	9	48	−28.7	136	90	−46.2	60	132	−32.7	−95
7	−11.3	12	49	−29.1	172	91	−31.3	162	133	−35.9	−41
8	−24.6	5	50	−26.6	−79	92	−35.3	107	134	−32.8	98
9	−26.4	−28	51	−28.6	−62	93	−32.4	121	135	−39.2	112
10	−27.0	57	52	−37.2	−54	94	−32.5	157	136	−37.7	−19
11	−32.9	−164	53	−32.7	−156	95	−31.4	120	137	−36.8	−63
12	−30.0	5	54	−36.2	−149	96	−36.1	134	138	−30.3	−76
13	−34.4	119	55	−31.4	−171	97	−32.2	166	139	−32.2	−45
14	−30.4	124	56	−32.6	131	98	−36.1	−103	140	−38.2	66
15	−26.7	172	57	−43.0	71	99	−32.7	−42	141	−38.7	−78
16	−32.7	77	58	−27.6	−39	100	−30.9	−149	142	−32.9	56
17	−34.0	−40	59	−33.3	12	101	−25.5	−141	143	−34.1	107
18	−32.8	−174	60	−30.4	60	102	−28.0	−105	144	−30.6	−154
19	−35.7	65	61	−30.9	101	103	−28.8	−32	145	−35.9	−123
20	−21.1	−22	62	−30.1	126	104	−26.9	37	146	−32.9	−133
21	−26.8	−15	63	−27.9	173	105	−27.2	87	147	−43.7	31
22	−29.3	−75	64	−28.5	138	106	−32.6	132	148	−52.6	−157
23	−31.6	−104	65	−29.0	93	107	−45.5	−33	149	−36.1	84
24	−34.1	−136	66	−34.2	66	108	−40.5	30	150	−34.8	108
25	−28.0	−118	67	−33.6	−10	109	−39.9	−55	151	−37.5	−30
26	−28.1	−81	68	−33.2	95	110	−43.1	146	152	−50.7	94
27	−24.4	−14	69	−35.9	152	111	−32.4	153	153	−30.2	81
28	−36.0	−44	70	−28.8	−175	112	−31.2	159	154	−39.2	155
29	−20.7	−139	71	−33.8	−5	113	−32.0	−161	155	−31.3	−98
30	−27.7	−106	72	−32.9	27	114	−32.8	−70	156	−35.8	−55
31	−27.3	−74	73	−30.0	35	115	−35.7	167	157	−43.9	−27
32	−38.2	−114	74	−34.3	128	116	−31.4	33	158	−33.8	11
33	−37.3	−2	75	−28.8	172	117	−33.7	−19	159	−41.6	91
34	−29.9	−30	76	−38.9	−172	118	−33.2	80	160	−37.9	148
35	−25.6	−61	77	−31.0	127	119	−25.2	68	161	−40.7	43
36	−25.3	−139	78	−29.1	75	120	−28.9	27	162	−44.9	−37
37	−40.1	−73	79	−25.5	123	121	−31.6	−22	163	−31.6	−23
38	−29.4	−61	80	−26.3	167	122	−29.0	−63	164	−33.7	−53
39	−30.9	−37	81	−32.6	−157	123	−27.4	−140	165	−33.8	158
40	−39.1	30	82	−33.8	−25	124	−29.2	161	166	−32.7	105
41	−28.6	41	83	−38.3	161	125	−40.4	52	167	−37.4	−35
42	−32.1	66	84	−35.7	118	126	−35.9	−128	168	−34.6	97

Table 12. Concluded

Element	Amplitude, dB	Phase, deg	Element	Amplitude, dB	Phase, deg	Element	Amplitude, dB	Phase, deg	Element	Amplitude, dB	Phase, deg
169	−33.0	5	181	−37.2	−47	193	−38.1	30	205	−31.8	46
170	−35.7	139	182	−34.7	41	194	−38.5	−114	206	−34.5	−24
171	−32.3	170	183	−45.4	−53	195	−39.0	−100	207	−46.1	−34
172	−31.9	−176	184	−34.9	152	196	−50.7	−133	208	−41.1	−109
173	−39.8	108	185	−33.1	151	197	−38.9	36	209	−30.8	1
174	−46.4	77	186	−40.2	26	198	−36.2	42	210	−34.1	168
175	−36.3	113	187	−29.4	−31	199	−37.4	−76	211	−32.2	80
176	−40.2	−81	188	−30.0	5	200	−39.7	66	212	−32.8	25
177	−34.4	−64	189	−36.2	156	201	−31.7	156	213	−31.8	−121
178	−49.3	−99	190	−39.9	−133	202	−43.2	38	214	−34.3	172
179	−43.2	35	191	−31.3	59	203	−44.4	67	215	−49.1	93
180	−38.4	180	192	−30.3	132	204	−37.9	110	216	−32.0	−46
									217	−36.8	−127

Table 13. Excitation Coefficients at 12 GHz for 7-Element Array Feed for 4/19/90 Surface Compensation

Element	Complex amplitude	Amplitude, dB	Phase, deg
1	(1.0000, 0.0000)	0.0	0.0
2	(0.5162, 0.2277)	−5.0	23.8
3	(0.3232, 0.2424)	−7.9	36.9
4	(0.4330, 0.0908)	−7.1	11.8
5	(0.3287, 0.1340)	−9.0	22.2
6	(0.3001, 0.0955)	−10.0	17.7
7	(0.3288, 0.2966)	−7.1	42.0

Table 14. Excitation Coefficients at 12 GHz for 19-Element Array Feed for 4/19/90 Surface Compensation

Element	Amplitude, dB	Phase, deg	Element	Amplitude, dB	Phase, deg
1	0.0	0	11	−22.7	−134
2	−7.8	27	12	−20.0	3
3	−8.2	23	13	−26.8	−86
4	−8.5	10	14	−20.7	163
5	−9.2	6	15	−20.7	−157
6	−9.9	19	16	−24.9	106
7	−9.1	36	17	−18.5	−56
8	−11.8	0	18	−21.1	−179
9	−16.8	−39	19	−23.4	−38
10	−20.8	52			

Table 15. Excitation Coefficients at 12 GHz for 37-Element Array Feed for 4/19/90 Surface Compensation

Element	Amplitude, dB	Phase, deg	Element	Amplitude, dB	Phase, deg	Element	Amplitude, dB	Phase, deg
1	0.0	0	13	−23.5	53	25	−17.6	−115
2	−7.6	19	14	−20.9	102	26	−19.4	−63
3	−8.9	22	15	−21.2	146	27	−20.1	−4
4	−9.0	0	16	−24.5	36	28	−25.4	−83
5	−10.6	−2	17	−22.9	−70	29	−14.3	−130
6	−10.6	15	18	−21.4	152	30	−21.9	−97
7	−9.4	24	19	−27.8	36	31	−19.1	−99
8	−16.4	13	20	−13.2	−32	32	−23.6	−143
9	−20.4	−36	21	−16.7	−18	33	−30.2	128
10	−20.8	24	22	−22.8	10	34	−19.1	−35
11	−22.4	119	23	−22.9	−126	35	−17.6	−59
12	−24.3	−5	24	−23.9	−120	36	−31.5	−79
						37	−30.3	−118

Table 16. Excitation Coefficients at 12 GHz for 61-Element Array Feed for 4/19/90 Surface Compensation

Element	Amplitude, dB	Phase, deg	Element	Amplitude, dB	Phase, deg	Element	Amplitude, dB	Phase, deg
1	0.0	0	21	−17.0	−19	41	−19.0	32
2	−8.4	14	22	−21.7	−110	42	−24.7	44
3	−9.2	17	23	−25.2	−108	43	−32.6	152
4	−9.6	−5	24	−21.8	−117	44	−24.8	−177
5	−10.5	−3	25	−21.4	−115	45	−29.1	109
6	−11.1	10	26	−22.3	−109	46	−19.1	−64
7	−9.9	23	27	−18.0	−32	47	−23.4	55
8	−16.7	7	28	−21.2	−63	48	−19.2	114
9	−18.2	−19	29	−17.5	−149	49	−18.3	155
10	−21.4	53	30	−21.2	−122	50	−21.6	−108
11	−31.0	136	31	−18.6	−79	51	−23.4	−66
12	−21.4	13	32	−23.9	−165	52	−30.5	147
13	−26.2	96	33	−24.5	−58	53	−22.3	179
14	−25.7	92	34	−23.2	−48	54	−29.2	−106
15	−21.0	149	35	−19.0	−50	55	−19.6	158
16	−26.0	58	36	−24.1	−158	56	−21.9	96
17	−27.4	−73	37	−23.5	−103	57	−23.9	7
18	−24.1	173	38	−33.5	−157	58	−20.3	−91
19	−23.6	42	39	−29.5	−62	59	−25.8	9
20	−14.0	−35	40	−21.9	60	60	−26.8	22
						61	−21.0	105

Table 17. Excitation Coefficients at 12 GHz for 91-Element Array Feed for 4/19/90 Surface Compensation

Element	Amplitude, dB	Phase, deg	Element	Amplitude, dB	Phase, deg	Element	Amplitude, dB	Phase, deg
1	0.0	0	31	−19.1	−106	61	−27.7	110
2	−8.0	18	32	−26.9	−131	62	−20.7	100
3	−9.0	20	33	−39.8	−51	63	−20.2	154
4	−9.1	0	34	−20.7	−36	64	−20.8	139
5	−10.7	−1	35	−20.5	−79	65	−20.2	87
6	−11.1	13	36	−25.1	−134	66	−26.1	82
7	−9.5	25	37	−33.3	−128	67	−26.0	−4
8	−15.9	2	38	−23.7	−79	68	−31.8	58
9	−19.3	−31	39	−22.8	−35	69	−25.5	165
10	−21.4	41	40	−24.6	6	70	−18.4	169
11	−28.7	143	41	−22.6	16	71	−22.6	−49
12	−24.2	0	42	−26.3	56	72	−19.5	39
13	−29.6	84	43	−30.0	−172	73	−23.8	29
14	−32.2	100	44	−39.7	−18	74	−23.6	114
15	−24.1	135	45	−32.3	133	75	−23.4	162
16	−29.7	64	46	−19.3	−85	76	−26.4	−163
17	−24.6	−58	47	−29.9	50	77	−22.6	96
18	−26.3	153	48	−21.3	102	78	−22.6	100
19	−29.7	37	49	−21.6	163	79	−17.0	112
20	−15.0	−30	50	−18.3	−101	80	−17.8	168
21	−18.0	−11	51	−18.1	−73	81	−26.6	−180
22	−30.4	−112	52	−23.7	−41	82	−21.7	−13
23	−23.8	−85	53	−31.0	−166	83	−32.5	128
24	−21.8	−136	54	−26.9	−153	84	−23.7	70
25	−19.6	−115	55	−21.5	167	85	−18.4	54
26	−25.6	−64	56	−28.4	138	86	−19.0	−38
27	−18.6	−31	57	−37.1	81	87	−21.0	−110
28	−27.2	−67	58	−20.1	−46	88	−17.7	−177
29	−18.4	−155	59	−22.0	2	89	−21.1	118
30	−21.9	−158	60	−27.4	14	90	−38.0	39
						91	−24.0	136

Table 18. Excitation Coefficients at 12 GHz for 127-Element Array Feed for 4/19/90 Surface Compensation

Element	Amplitude, dB	Phase, deg	Element	Amplitude, dB	Phase, deg	Element	Amplitude, dB	Phase, deg
1	0.0	0	43	−30.9	−128	85	−24.7	24
2	−8.4	16	44	−28.3	−146	86	−27.6	8
3	−8.9	18	45	−39.6	−127	87	−23.7	−94
4	−9.4	1	46	−25.0	−63	88	−21.0	−171
5	−10.2	−5	47	−31.1	100	89	−23.1	112
6	−10.8	12	48	−23.7	99	90	−37.6	62
7	−9.8	26	49	−20.6	151	91	−25.5	141
8	−15.5	4	50	−20.2	−119	92	−31.3	124
9	−19.4	−16	51	−22.1	−79	93	−36.7	32
10	−21.4	34	52	−24.8	−56	94	−29.5	−155
11	−27.8	140	53	−24.2	−161	95	−27.0	149
12	−25.4	7	54	−26.4	−138	96	−30.1	143
13	−29.3	61	55	−21.3	170	97	−26.4	106
14	−27.2	111	56	−26.6	86	98	−33.6	−118
15	−21.7	148	57	−33.3	12	99	−25.3	−65
16	−27.2	75	58	−21.4	−61	100	−21.4	−154
17	−23.1	−66	59	−23.8	6	101	−17.8	−140
18	−24.4	152	60	−26.8	2	102	−20.4	−122
19	−27.8	21	61	−25.0	104	103	−22.7	−46
20	−14.9	−31	62	−22.1	97	104	−16.7	25
21	−18.0	−19	63	−20.6	151	105	−18.0	90
22	−24.2	−80	64	−24.6	126	106	−28.6	126
23	−24.0	−116	65	−21.4	71	107	−28.3	−137
24	−25.2	−132	66	−32.5	26	108	−31.2	−81
25	−19.5	−127	67	−27.2	26	109	−34.5	−26
26	−19.7	−62	68	−27.4	63	110	−25.6	60
27	−21.1	−19	69	−25.9	130	111	−22.8	115
28	−22.5	−63	70	−21.5	120	112	−22.3	146
29	−17.9	−146	71	−31.0	−90	113	−26.9	129
30	−22.8	−141	72	−24.9	1	114	−30.5	−141
31	−20.9	−87	73	−23.3	−11	115	−25.7	−166
32	−26.5	−140	74	−24.2	96	116	−22.1	−31
33	−33.0	−49	75	−22.2	142	117	−28.8	−16
34	−23.5	−40	76	−23.4	−151	118	−27.3	33
35	−19.5	−64	77	−28.8	82	119	−18.7	51
36	−24.9	−143	78	−27.2	39	120	−24.0	14
37	−31.6	−129	79	−19.7	104	121	−21.1	−64
38	−24.0	−87	80	−18.5	163	122	−19.1	−74
39	−24.8	−32	81	−38.4	62	123	−21.0	−157
40	−27.4	36	82	−29.5	27	124	−19.6	138
41	−22.4	38	83	−39.2	30	125	−39.1	−156
42	−26.4	47	84	−22.9	114	126	−35.2	−159
						127	−29.6	−17

Table 19. Excitation Coefficients at 12 GHz for 169-Element Array Feed for 4/19/90 Surface Compensation

Element	Amplitude, dB	Phase, deg	Element	Amplitude, dB	Phase, deg	Element	Amplitude, dB	Phase, deg	Element	Amplitude, dB	Phase, deg
1	0.0	0	43	−31.3	−159	85	−25.1	38	127	−32.4	20
2	−8.5	18	44	−28.7	−153	86	−23.9	−29	128	−31.3	131
3	−8.8	21	45	−31.0	145	87	−22.5	−89	129	−27.9	−169
4	−9.6	1	46	−21.7	−68	88	−19.6	−174	130	−38.3	10
5	−10.7	−1	47	−28.2	53	89	−21.3	115	131	−28.3	−66
6	−11.0	16	48	−23.6	114	90	−37.2	67	132	−31.1	−62
7	−10.1	26	49	−22.3	147	91	−25.7	134	133	−39.4	45
8	−15.3	8	50	−20.5	−112	92	−35.9	43	134	−31.2	3
9	−19.8	−23	51	−21.8	−82	93	−39.9	29	135	−38.8	67
10	−22.4	40	52	−26.8	−100	94	−28.0	−171	136	−27.7	−57
11	−27.4	144	53	−24.0	−167	95	−23.9	138	137	−29.1	−153
12	−24.0	−1	54	−31.3	−99	96	−28.4	128	138	−20.6	−106
13	−31.8	60	55	−19.6	169	97	−27.9	139	139	−21.3	−60
14	−26.7	115	56	−29.9	73	98	−37.3	−150	140	−35.3	−34
15	−23.6	149	57	−29.3	80	99	−28.4	−68	141	−28.5	140
16	−29.7	76	58	−21.6	−53	100	−23.7	−152	142	−23.7	−17
17	−22.6	−59	59	−21.7	−15	101	−19.6	−167	143	−25.6	39
18	−25.3	167	60	−27.2	22	102	−20.4	−132	144	−27.9	155
19	−28.0	29	61	−27.0	118	103	−23.1	−55	145	−23.6	−164
20	−15.1	−31	62	−20.9	103	104	−19.7	35	146	−34.8	−87
21	−17.7	−19	63	−22.1	154	105	−19.8	79	147	−27.0	88
22	−24.9	−80	64	−25.9	124	106	−32.0	58	148	−38.0	82
23	−25.5	−92	65	−23.5	71	107	−37.7	151	149	−29.5	110
24	−23.6	−125	66	−29.5	30	108	−26.9	−93	150	−29.0	104
25	−21.4	−118	67	−26.4	15	109	−30.2	−61	151	−32.2	−131
26	−20.4	−79	68	−29.4	58	110	−28.6	35	152	−32.5	16
27	−20.6	−4	69	−28.7	123	111	−23.2	106	153	−24.1	11
28	−22.0	−68	70	−24.0	153	112	−22.3	146	154	−29.7	−170
29	−18.2	−151	71	−29.0	−25	113	−22.0	155	155	−28.4	167
30	−24.1	−124	72	−24.6	−2	114	−26.5	−149	156	−26.0	−58
31	−21.6	−88	73	−26.3	36	115	−38.5	176	157	−30.5	−65
32	−23.9	−142	74	−27.6	118	116	−28.5	6	158	−26.1	6
33	−33.2	3	75	−22.1	145	117	−26.8	−18	159	−28.9	2
34	−22.2	−56	76	−25.5	−172	118	−29.8	70	160	−37.4	46
35	−21.4	−59	77	−27.8	125	119	−20.8	55	161	−27.8	−51
36	−24.5	−154	78	−26.4	48	120	−23.1	33	162	−34.3	−102
37	−31.9	−87	79	−20.7	96	121	−23.0	−67	163	−29.7	6
38	−24.9	−85	80	−22.0	149	122	−21.7	−87	164	−21.8	−60
39	−26.7	−35	81	−33.8	−157	123	−23.0	−169	165	−29.4	156
40	−25.6	39	82	−28.3	−16	124	−22.5	152	166	−25.8	134
41	−22.5	43	83	−36.2	134	125	−37.3	8	167	−44.8	−74
42	−27.9	56	84	−23.9	91	126	−27.6	−151	168	−33.2	25
									169	−27.2	−46

Table 20. Excitation Coefficients at 12 GHz for 217-Element Array Feed for 4/19/90 Surface Compensation

Element	Amplitude, dB	Phase, deg	Element	Amplitude, dB	Phase, deg	Element	Amplitude, dB	Phase, deg	Element	Amplitude, dB	Phase, deg
1	0.0	0	43	−38.0	151	85	−22.9	52	127	−32.1	85
2	−8.7	18	44	−28.6	−168	86	−23.7	−25	128	−31.2	−66
3	−9.2	21	45	−33.4	−177	87	−25.6	−109	129	−33.3	−117
4	−9.7	−1	46	−22.4	−70	88	−21.0	−168	130	−26.2	−58
5	−10.8	−1	47	−29.9	42	89	−21.2	108	131	−26.3	−80
6	−11.5	14	48	−21.7	113	90	−34.7	134	132	−32.2	−76
7	−9.9	28	49	−24.0	155	91	−27.1	130	133	−34.6	−126
8	−15.6	7	50	−19.8	−105	92	−28.6	112	134	−25.4	14
9	−18.4	−28	51	−22.3	−85	93	−32.5	98	135	−31.0	78
10	−20.5	40	52	−27.6	−67	94	−27.7	180	136	−30.8	−69
11	−29.8	148	53	−28.3	−151	95	−23.2	122	137	−29.6	−134
12	−23.3	3	54	−29.2	−109	96	−35.6	114	138	−21.6	−107
13	−29.8	75	55	−20.7	162	97	−26.4	133	139	−22.7	−63
14	−26.0	104	56	−27.0	105	98	−28.0	−115	140	−32.0	−60
15	−23.6	152	57	−32.5	−13	99	−28.5	−41	141	−34.1	−169
16	−25.6	52	58	−22.8	−56	100	−24.6	−157	142	−26.9	39
17	−24.8	−67	59	−22.5	−12	101	−18.6	−161	143	−25.1	70
18	−27.3	167	60	−26.4	8	102	−22.7	−120	144	−25.5	150
19	−28.9	30	61	−25.1	109	103	−23.5	−57	145	−28.9	−164
20	−14.7	−32	62	−24.2	92	104	−19.0	15	146	−27.5	−148
21	−18.9	−15	63	−21.8	157	105	−20.5	86	147	−31.6	42
22	−28.7	−69	64	−25.4	126	106	−31.2	63	148	−31.5	−129
23	−23.4	−113	65	−23.8	77	107	−32.9	−131	149	−26.1	97
24	−23.3	−136	66	−27.9	63	108	−33.3	−56	150	−28.3	106
25	−20.6	−108	67	−24.0	19	109	−33.0	−56	151	−30.0	−157
26	−23.8	−87	68	−28.9	121	110	−27.3	21	152	−37.3	−149
27	−18.9	−21	69	−37.4	55	111	−25.7	104	153	−28.6	−19
28	−25.0	−71	70	−21.2	145	112	−23.6	135	154	−33.0	159
29	−18.2	−147	71	−30.6	−56	113	−25.6	136	155	−30.0	−131
30	−23.0	−125	72	−22.1	23	114	−32.1	−156	156	−31.8	−107
31	−21.7	−100	73	−28.1	6	115	−30.0	148	157	−29.3	−80
32	−24.2	−151	74	−24.7	108	116	−21.9	−19	158	−28.6	−25
33	−29.5	−53	75	−23.0	148	117	−28.0	7	159	−29.7	53
34	−22.7	−41	76	−23.5	−166	118	−26.9	61	160	−31.9	60
35	−20.6	−60	77	−24.2	116	119	−22.4	42	161	−29.1	−34
36	−24.1	−158	78	−27.6	54	120	−23.9	25	162	−38.9	−49
37	−31.2	−80	79	−20.3	102	121	−23.8	−71	163	−28.0	−46
38	−26.6	−86	80	−19.4	162	122	−21.5	−78	164	−24.5	−55
39	−24.7	−32	81	−30.0	−153	123	−22.0	−156	165	−28.2	140
40	−26.4	27	82	−30.8	36	124	−21.6	155	166	−28.9	85
41	−23.9	40	83	−35.1	−121	125	−35.5	124	167	−34.7	−84
42	−27.6	26	84	−23.9	90	126	−30.4	−83	168	−34.6	59

Table 20. Concluded

Element	Amplitude, dB	Phase, deg	Element	Amplitude, dB	Phase, deg	Element	Amplitude, dB	Phase, deg	Element	Amplitude, dB	Phase, deg
169	−24.6	−25	181	−33.3	−148	193	−30.5	42	205	−26.8	−12
170	−27.6	120	182	−28.6	−36	194	−34.1	−132	206	−27.1	−58
171	−24.4	133	183	−37.9	15	195	−34.2	−127	207	−27.9	−155
172	−25.1	157	184	−29.8	135	196	−42.1	39	208	−34.4	−35
173	−30.9	101	185	−24.8	102	197	−27.2	1	209	−26.4	−58
174	−33.2	78	186	−28.8	−55	198	−26.0	35	210	−26.6	126
175	−31.1	46	187	−20.6	−48	199	−35.6	−138	211	−29.4	50
176	−32.1	−88	188	−23.7	−37	200	−40.4	137	212	−30.9	−63
177	−32.0	−142	189	−34.8	−172	201	−24.8	109	213	−26.7	−157
178	−36.0	−156	190	−37.2	−147	202	−34.4	−89	214	−26.5	139
179	−35.3	−98	191	−25.1	56	203	−34.1	29	215	−35.6	105
180	−37.3	112	192	−28.3	94	204	−27.4	43	216	−32.2	−72
									217	−27.8	−157

Table 21. Excitation Coefficients at 12 GHz for 217-Element Array Feed for 4/19/90 Pillowed Surface Compensation

Element	Amplitude, dB	Phase, deg	Element	Amplitude, dB	Phase, deg	Element	Amplitude, dB	Phase, deg	Element	Amplitude, dB	Phase, deg
1	0.0	0	43	−36.5	−154	85	−24.3	26	127	−31.0	55
2	−7.5	18	44	−22.2	169	86	−22.0	−27	128	−35.7	−26
3	−8.2	16	45	−24.4	−150	87	−28.3	−85	129	−37.8	−88
4	−9.7	−2	46	−23.3	−53	88	−20.8	−161	130	−24.9	−50
5	−12.2	7	47	−31.0	66	89	−22.3	112	131	−24.8	−88
6	−12.4	22	48	−22.1	108	90	−28.6	82	132	−33.3	−67
7	−10.2	27	49	−22.7	155	91	−25.9	159	133	−31.3	−100
8	−15.0	10	50	−18.9	−108	92	−31.2	125	134	−26.2	21
9	−21.5	−22	51	−21.3	−86	93	−29.7	92	135	−36.2	76
10	−18.1	51	52	−38.1	−52	94	−27.0	135	136	−29.5	−76
11	−25.3	114	53	−33.8	−137	95	−24.0	129	137	−28.6	−115
12	−21.8	−5	54	−26.7	143	96	−32.8	130	138	−21.1	−106
13	−26.5	127	55	−20.9	162	97	−25.4	122	139	−20.6	−25
14	−26.4	83	56	−23.1	64	98	−30.0	−113	140	−31.7	−15
15	−27.7	147	57	−26.4	−6	99	−28.6	−59	141	−34.8	9
16	−21.8	72	58	−28.2	−64	100	−23.6	−175	142	−33.0	19
17	−26.9	−50	59	−22.0	−17	101	−19.6	−138	143	−24.3	70
18	−26.2	−177	60	−23.1	16	102	−20.9	−112	144	−27.5	176
19	−25.1	13	61	−23.3	126	103	−22.3	−54	145	−28.0	178
20	−15.6	−30	62	−24.9	88	104	−19.8	30	146	−31.8	−135
21	−17.8	−16	63	−22.9	176	105	−20.2	82	147	−39.0	48
22	−26.1	−69	64	−24.0	128	106	−33.4	55	148	−32.9	106
23	−21.0	−108	65	−23.4	93	107	−28.9	−135	149	−30.9	61
24	−24.1	−154	66	−29.4	41	108	−31.9	−36	150	−30.7	88
25	−21.9	−123	67	−25.9	17	109	−32.7	−29	151	−33.3	−171
26	−22.0	−61	68	−25.4	97	110	−28.4	87	152	−40.6	−101
27	−18.9	−18	69	−30.3	−138	111	−25.3	110	153	−26.8	32
28	−22.2	−62	70	−22.5	171	112	−23.3	143	154	−29.5	−159
29	−19.4	−145	71	−26.1	−26	113	−25.0	158	155	−26.0	−144
30	−21.5	−116	72	−23.5	24	114	−33.1	−159	156	−29.2	−73
31	−19.2	−103	73	−25.3	32	115	−42.6	31	157	−31.6	−75
32	−21.2	−131	74	−26.0	110	116	−26.4	−43	158	−29.8	−12
33	−32.9	33	75	−20.3	139	117	−29.5	−3	159	−41.9	−21
34	−22.9	−16	76	−24.3	−132	118	−29.8	34	160	−27.6	158
35	−19.7	−71	77	−26.1	104	119	−23.5	34	161	−28.6	−68
36	−26.4	−154	78	−26.0	63	120	−24.8	−8	162	−33.2	−55
37	−32.9	−150	79	−20.9	106	121	−26.5	−82	163	−26.3	−34
38	−25.3	−95	80	−19.0	154	122	−20.5	−80	164	−25.3	−66
39	−22.2	−30	81	−32.2	−138	123	−21.3	−145	165	−29.6	149
40	−23.8	30	82	−23.6	−8	124	−20.5	155	166	−27.2	67
41	−22.0	52	83	−38.9	−20	125	−39.2	103	167	−43.1	−170
42	−27.3	32	84	−24.5	60	126	−29.4	−126	168	−35.0	41

Table 21. Concluded

Element	Amplitude, dB	Phase, deg	Element	Amplitude, dB	Phase, deg	Element	Amplitude, dB	Phase, deg	Element	Amplitude, dB	Phase, deg
169	−26.5	−26	181	−40.2	−150	193	−33.9	84	205	−26.8	24
170	−29.2	143	182	−34.0	−6	194	−33.9	−163	206	−30.6	−50
171	−25.4	144	183	−29.2	89	195	−35.1	171	207	−26.9	173
172	−24.6	157	184	−24.0	151	196	−33.3	−113	208	−34.4	98
173	−30.0	104	185	−24.8	101	197	−27.7	12	209	−23.9	−54
174	−29.6	74	186	−31.1	−70	198	−29.5	38	210	−25.4	117
175	−30.7	48	187	−19.2	−35	199	−35.3	−96	211	−28.4	76
176	−34.7	−62	188	−25.4	−33	200	−31.7	42	212	−28.5	−65
177	−32.7	−149	189	−50.5	−57	201	−25.1	104	213	−27.1	−154
178	−39.0	−158	190	−31.1	−105	202	−39.3	−89	214	−28.2	142
179	−48.8	−64	191	−25.1	66	203	−36.5	122	215	−31.6	113
180	−37.6	131	192	−27.2	67	204	−29.7	30	216	−30.3	−70
									217	−30.2	177

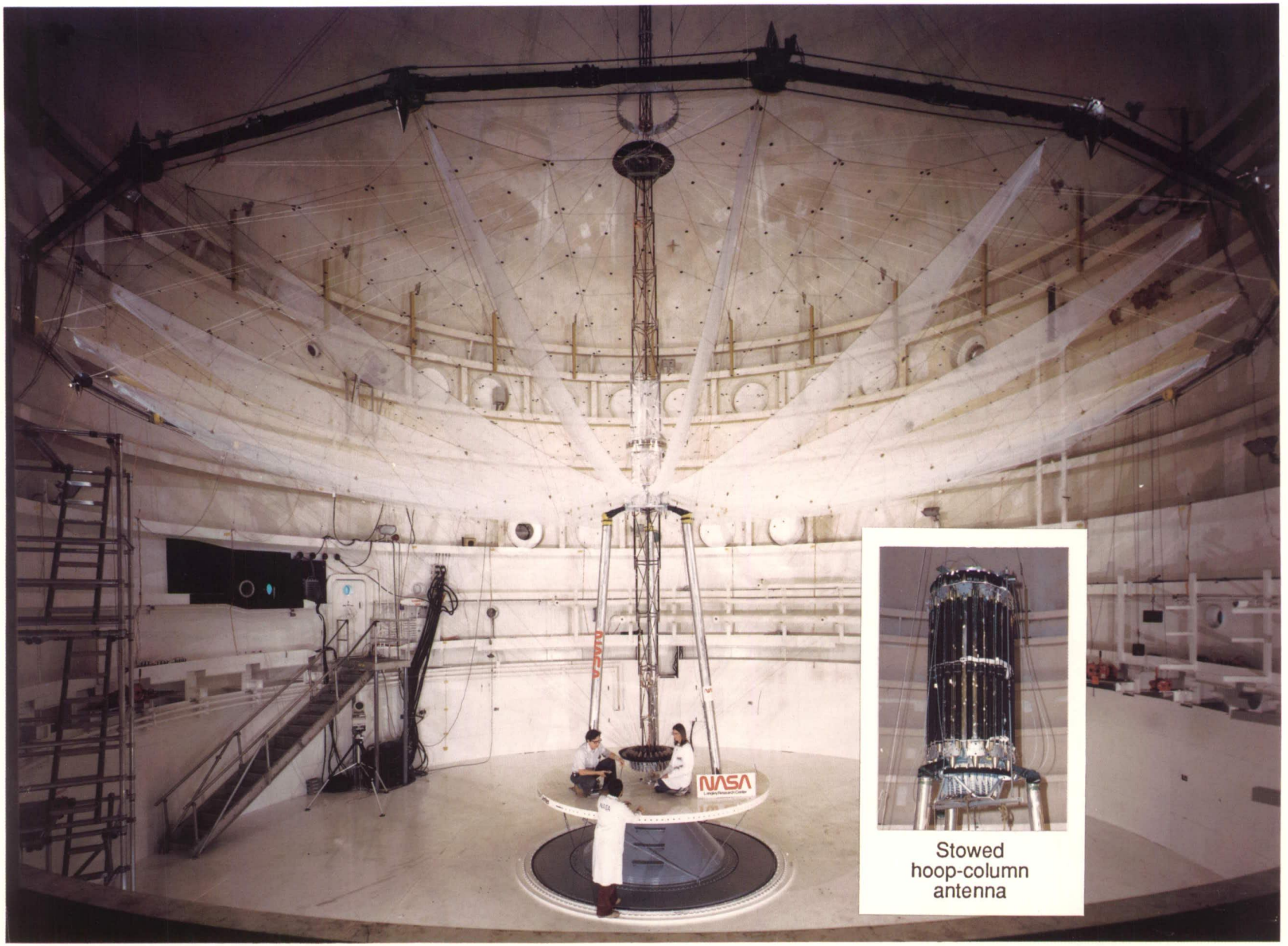

Figure 1. Hoop-column antenna deployed in 16-meter thermal-vacuum cylinder.

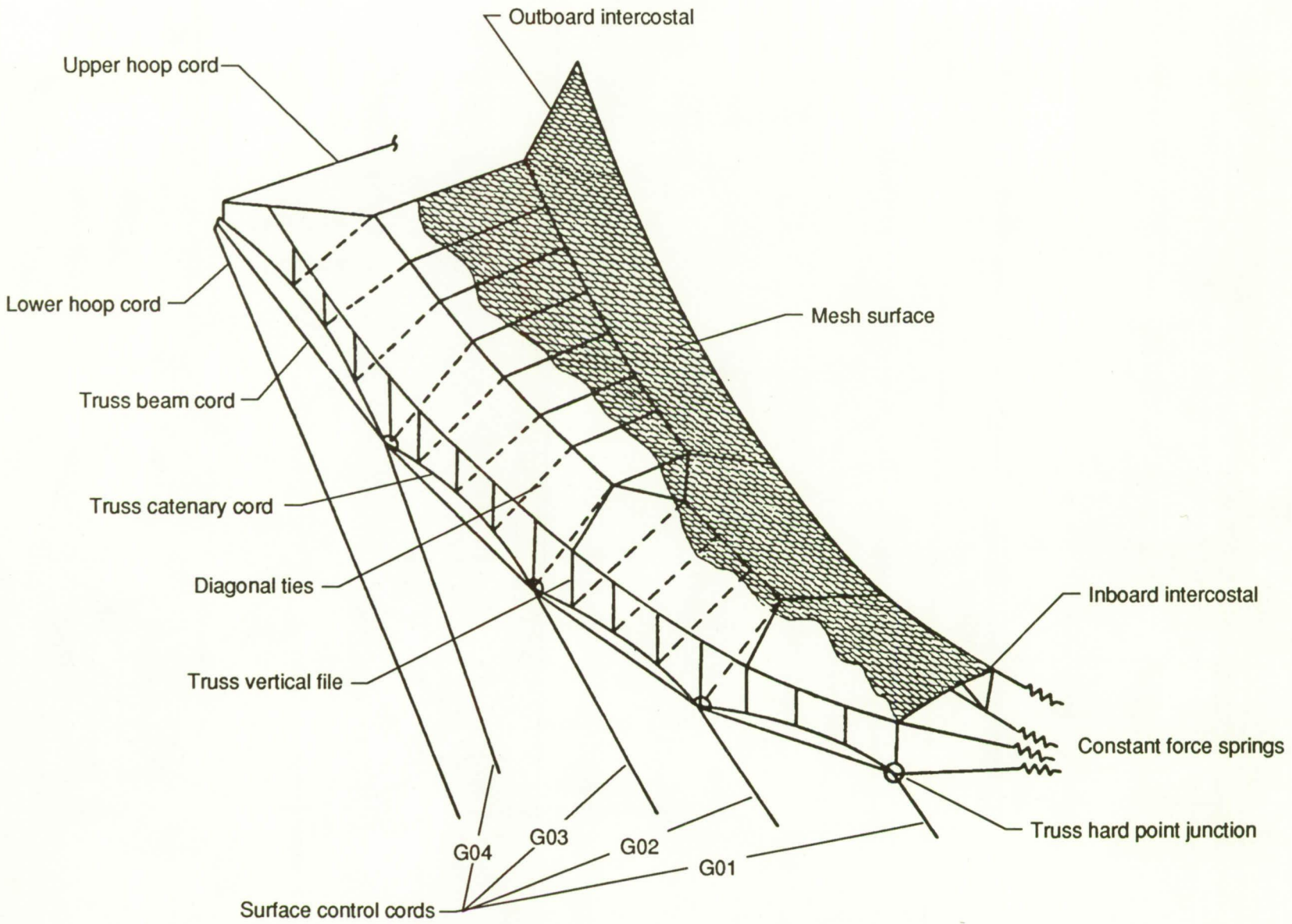

Figure 2. Mesh and cord structure of antenna reflector surface.

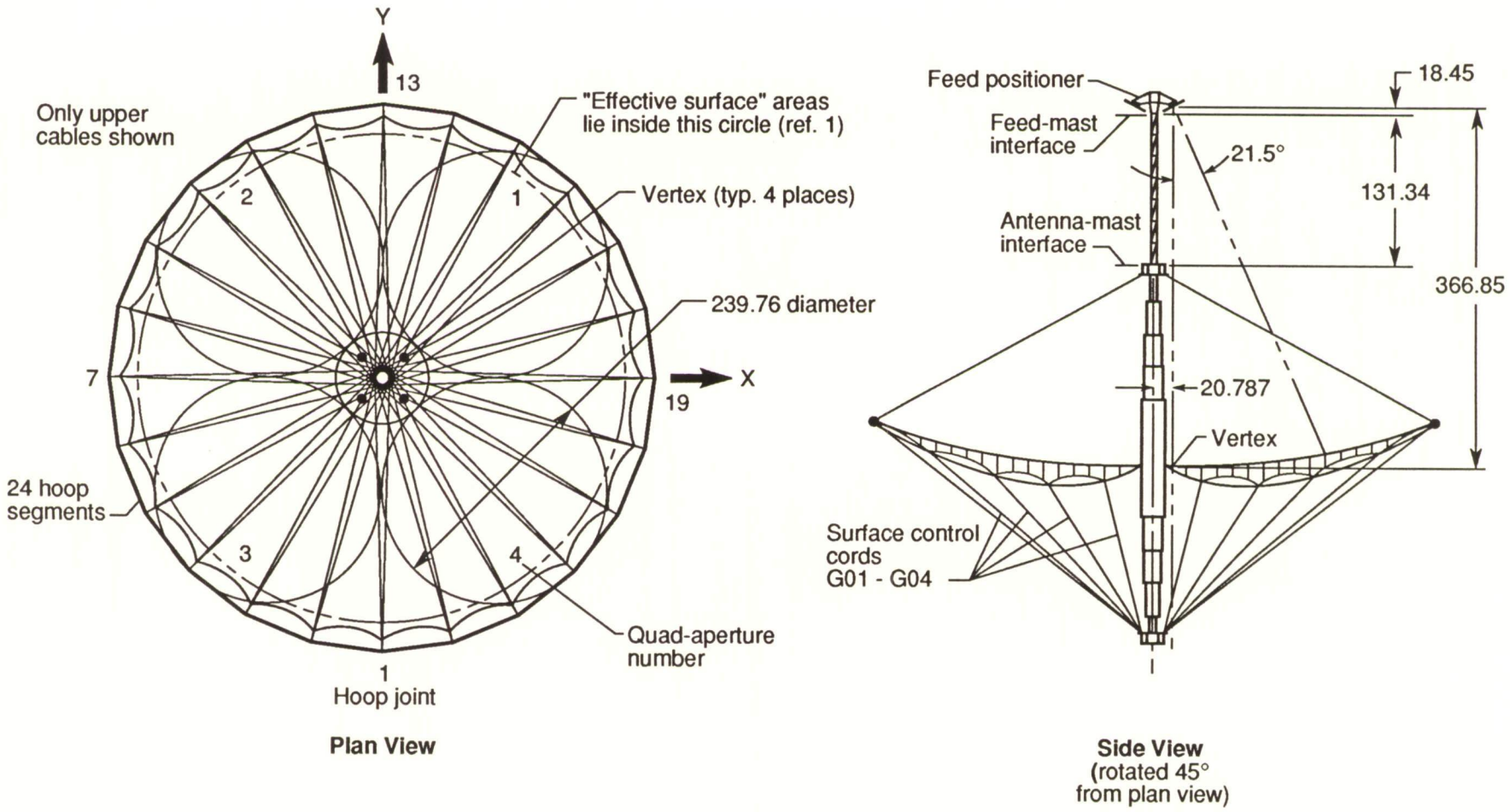

Figure 3. Design details of 15-meter hoop-column antenna. Linear dimensions are in inches.

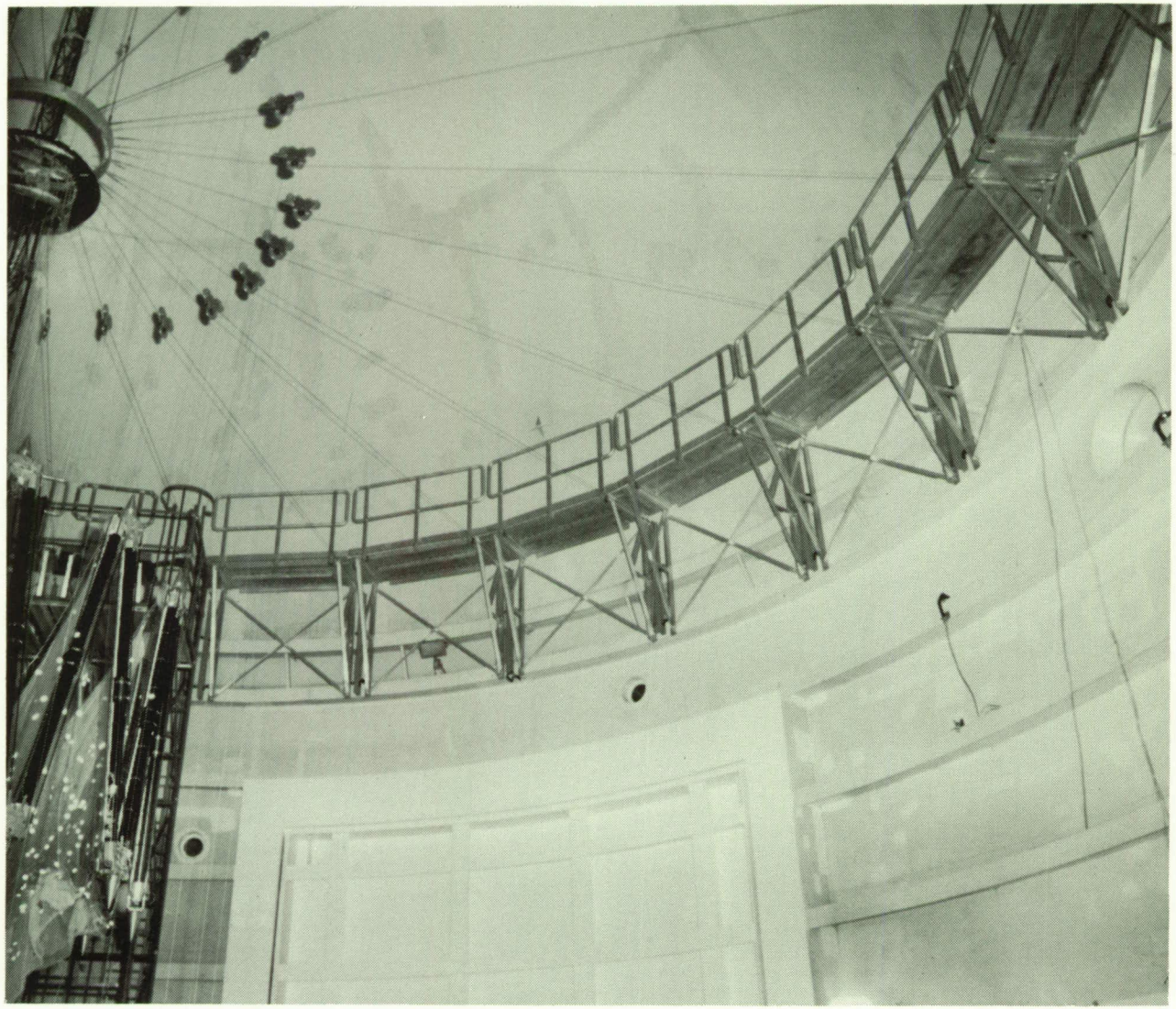

L-87-9268

Figure 4. View of 16-meter thermal-vacuum cylinder showing metric camera walkway, counterbalance radial cables, and cylinder access door.

L-89-8645

Figure 5. Manual adjustment of reflector surface control cords.

ORIGINAL PAGE
COLOR PHOTOGRAPH

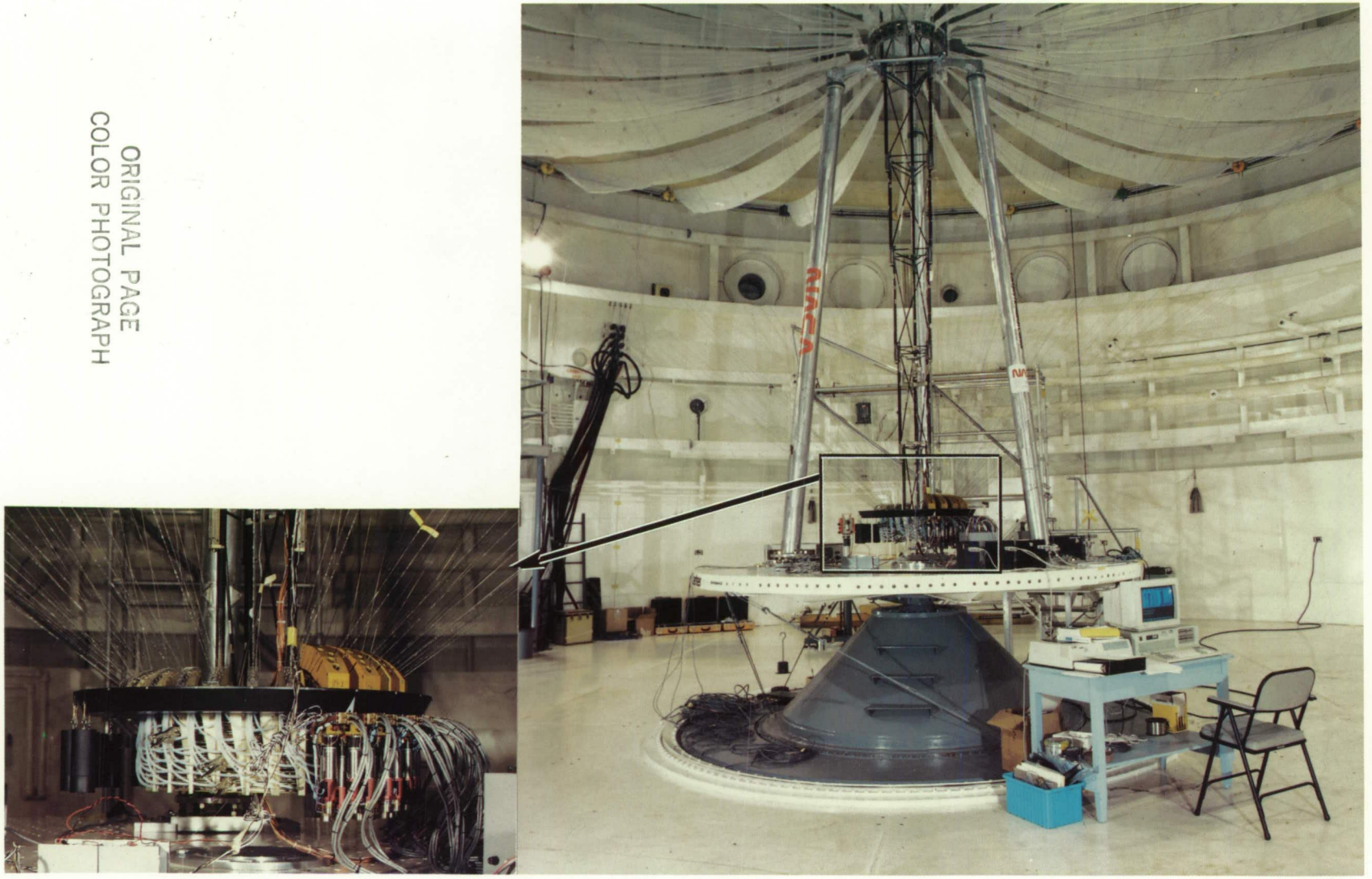

Figure 6. 15-meter antenna modified to add computer-controlled adjustment system.

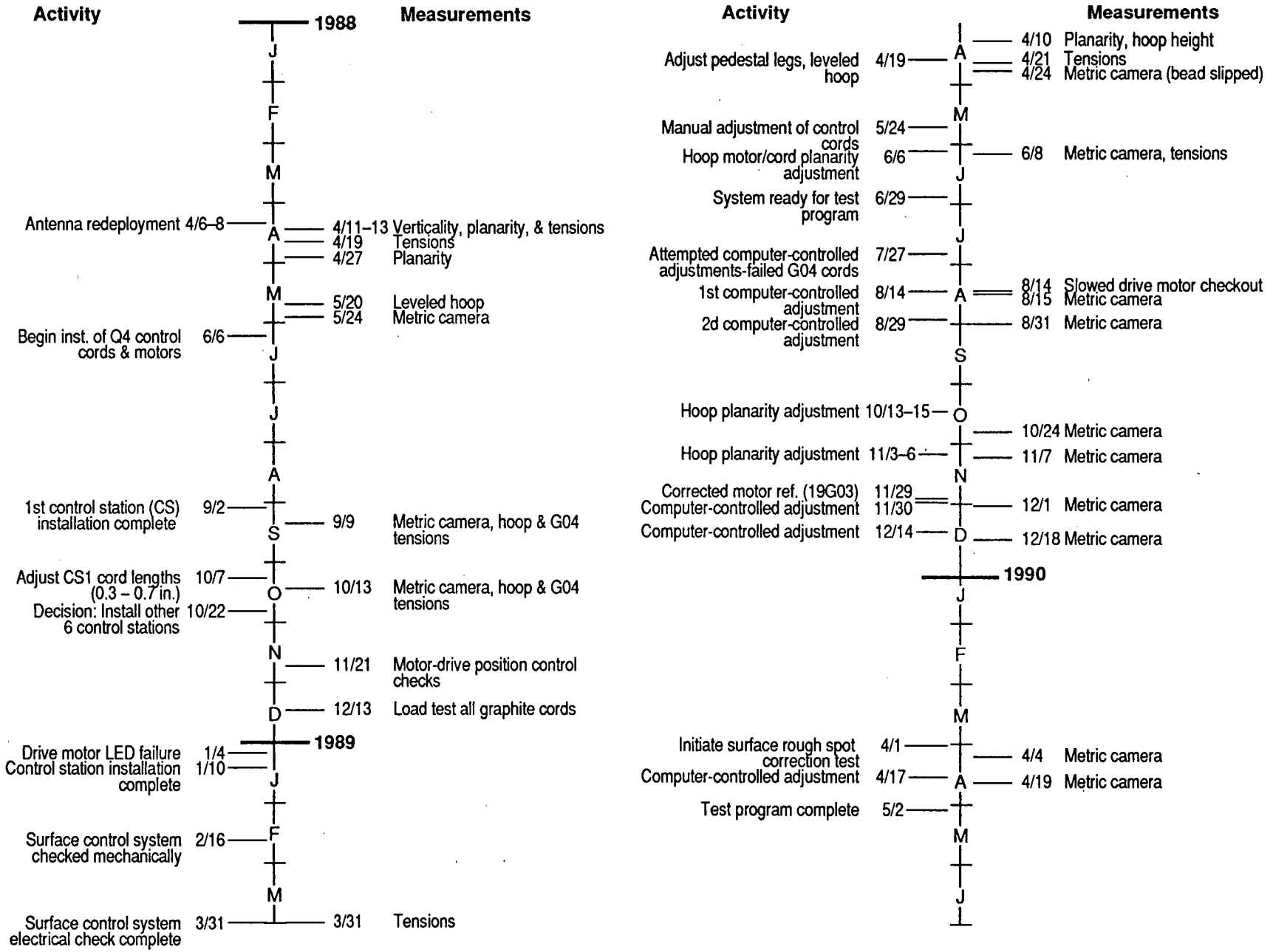

Figure 7. Timeline for computer-controlled motor system installation and test program.

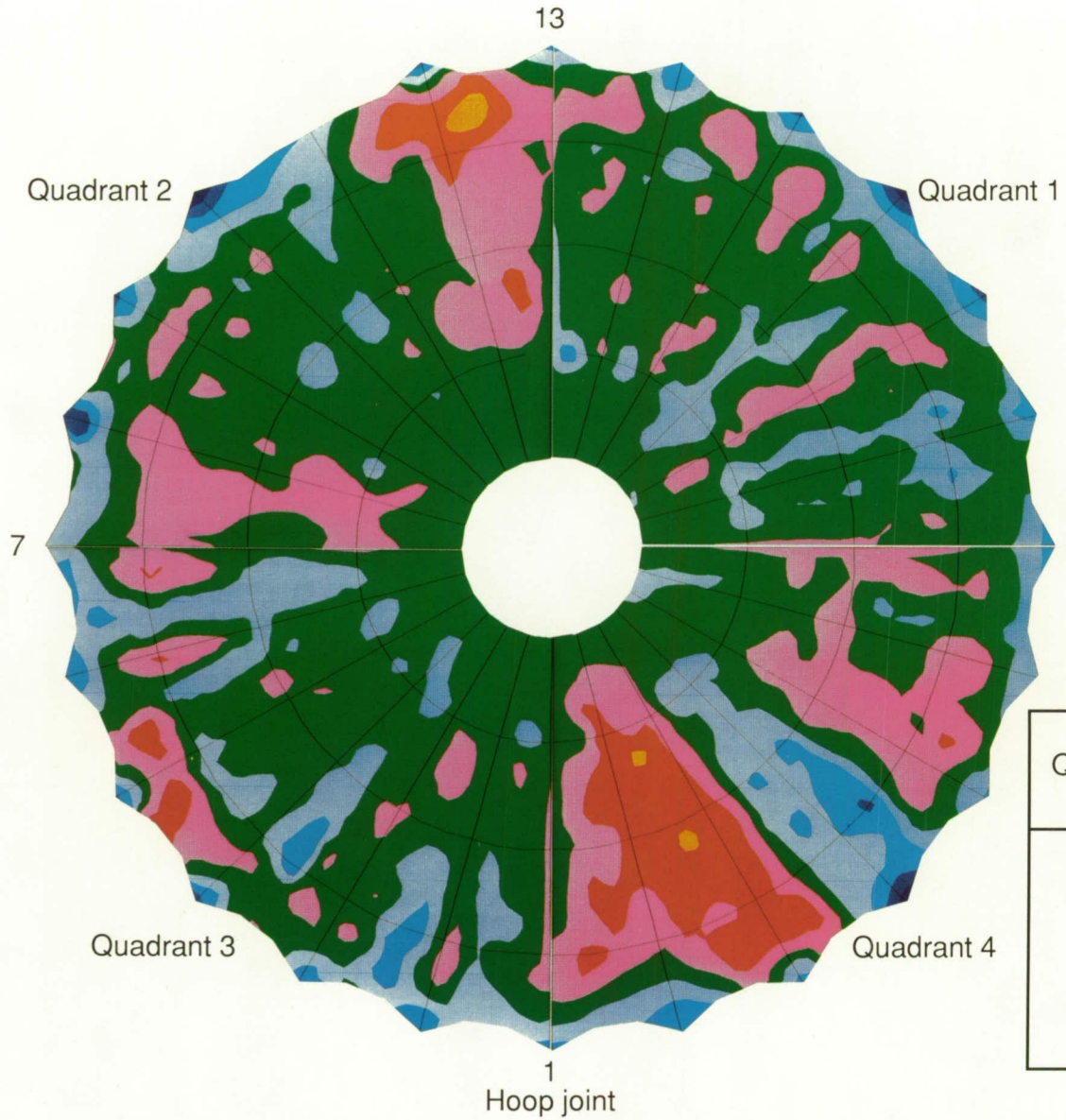

Quadrant	Surface rms error, in.	
	Effective area	Complete
1	0.076	0.106
2	0.090	0.129
3	0.098	0.117
4	0.147	0.164

Figure 8. Reflector surface roughness prior to computer-controlled adjustment. Surface measurement of 8/8/89.

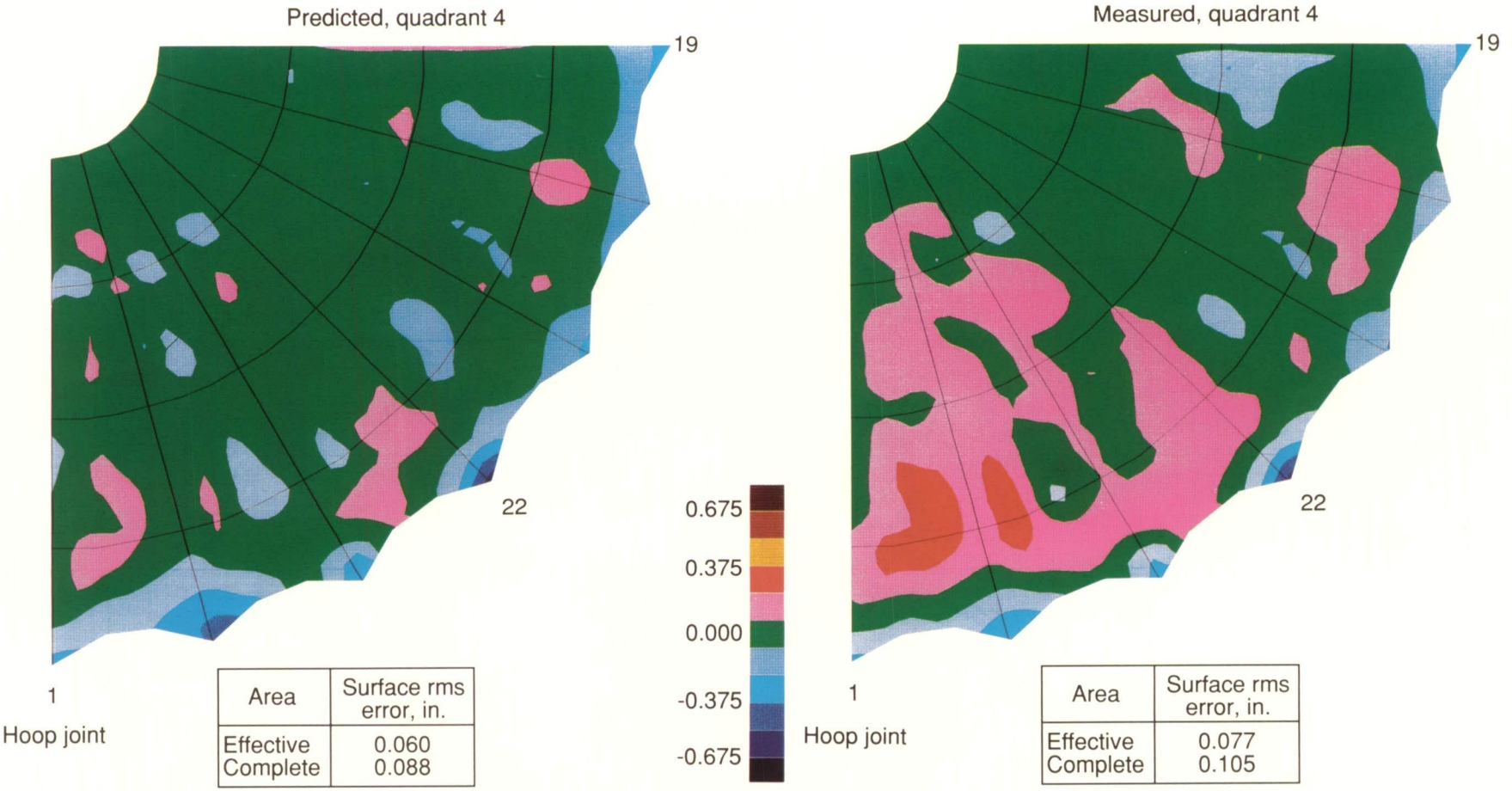

Area	Surface rms error, in.
Effective	0.060
Complete	0.088

Area	Surface rms error, in.
Effective	0.077
Complete	0.105

Hoop joint	Control cord adjustment, in., for –			
	G01	G02	G03	G04
19	0.013	-0.003	-0.048	-0.027
20	0.107	0.024	0.000	0.005
21	0.088	0.015	-0.050	-0.050
22	-0.010	-0.001	0.059	0.095
23	0.060	-0.031	-0.086	-0.094
24	0.050	-0.122	-0.127	-0.030
1	0.026	-0.019	-0.014	-0.022

Figure 9. Predicted and actual surface roughness for first computer-controlled adjustment on 8/14/89.

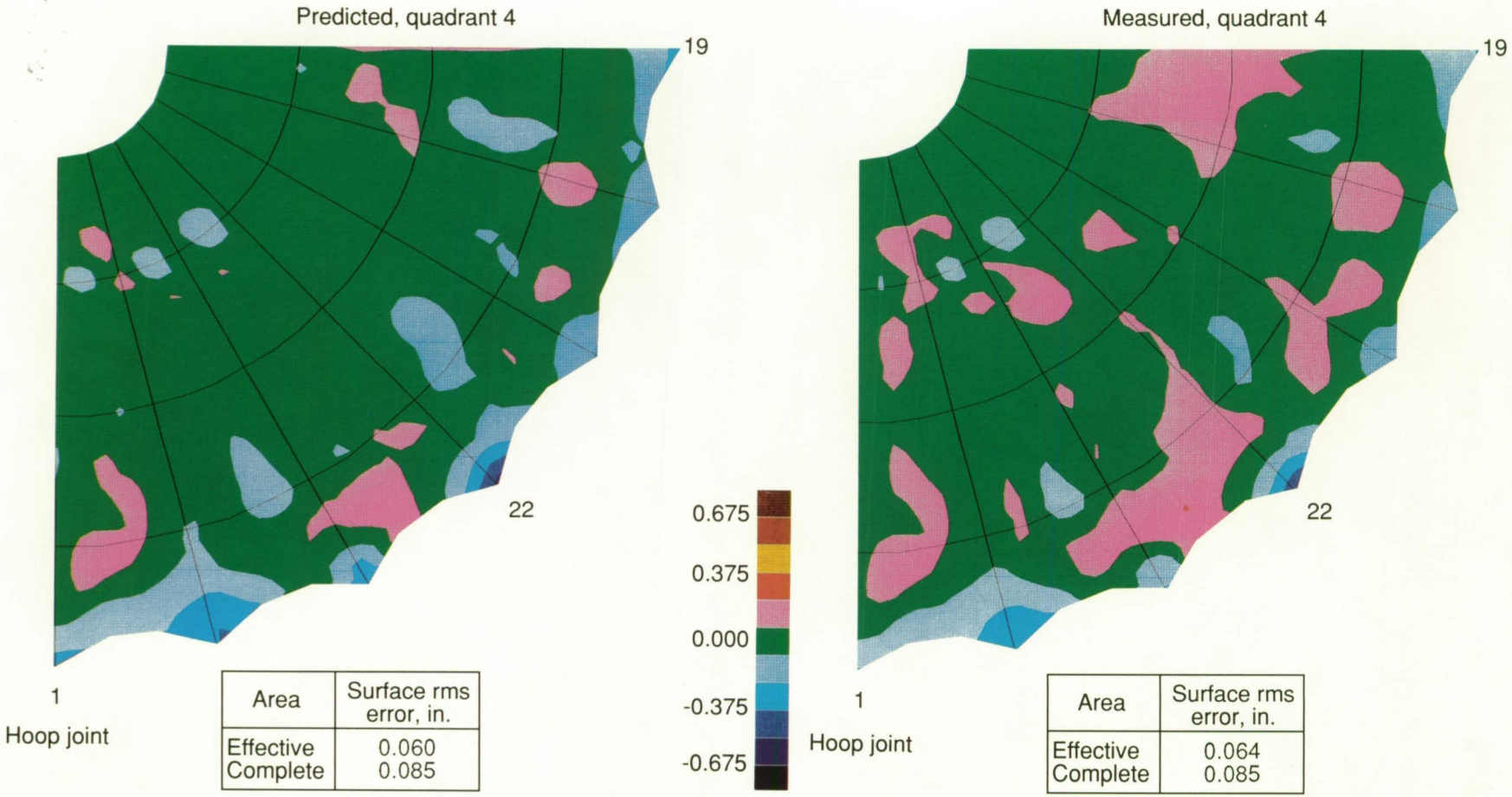

Area	Surface rms error, in.
Effective	0.060
Complete	0.085

Area	Surface rms error, in.
Effective	0.064
Complete	0.085

Hoop joint	Control cord adjustment, in., for –			
	G01	G02	G03	G04
19	0.014	-0.031	0.096	0.008
20	-0.009	0.014	0.005	-0.021
21	0.017	-0.034	0.003	0.000
22	-0.007	0.007	0.006	-0.029
23	0.002	-0.029	-0.027	-0.018
24	0.005	-0.003	-0.008	-0.060
1	0.013	0.001	-0.003	-0.019

Figure 10. Predicted and actual surface roughness for second computer-controlled adjustment on 8/29/89.

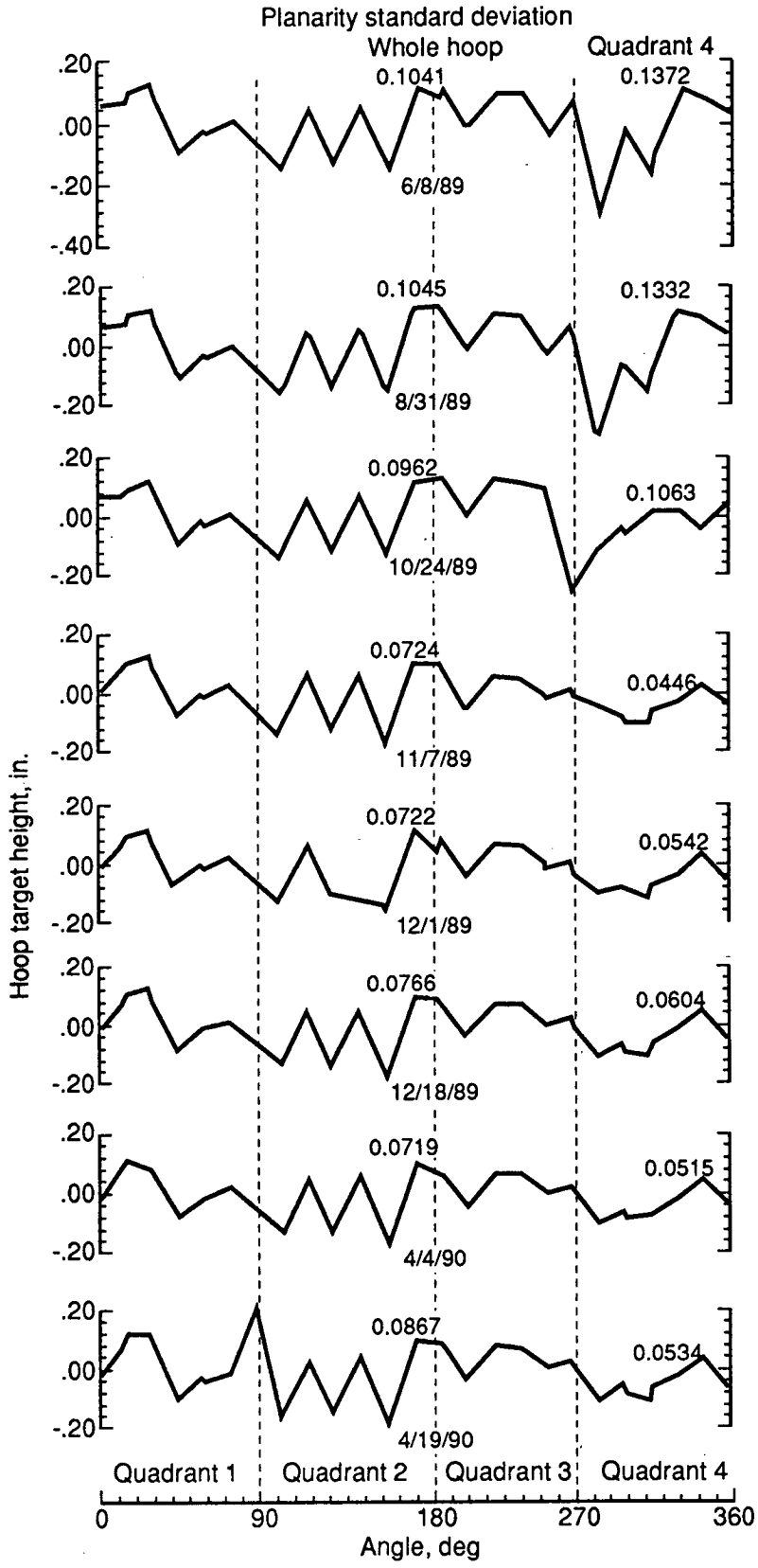

Figure 11. Hoop planarity history.

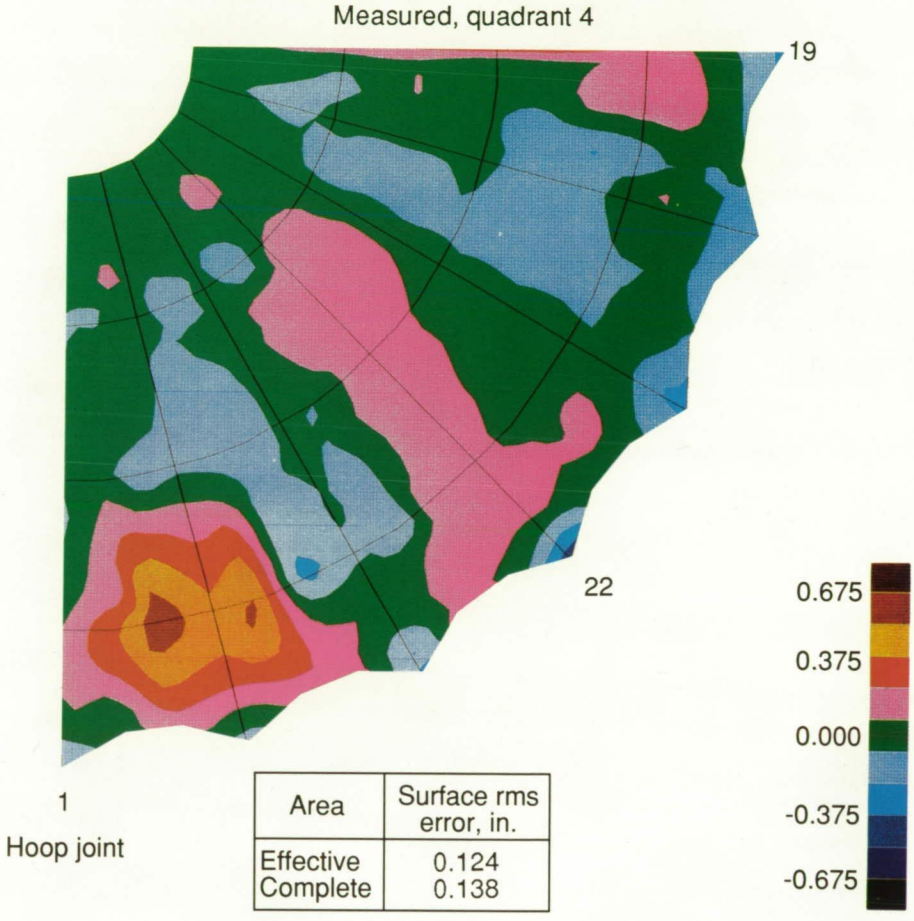

Figure 12. Reflector surface roughness after hoop planarity adjustment. Surface measurement of 11/7/89.

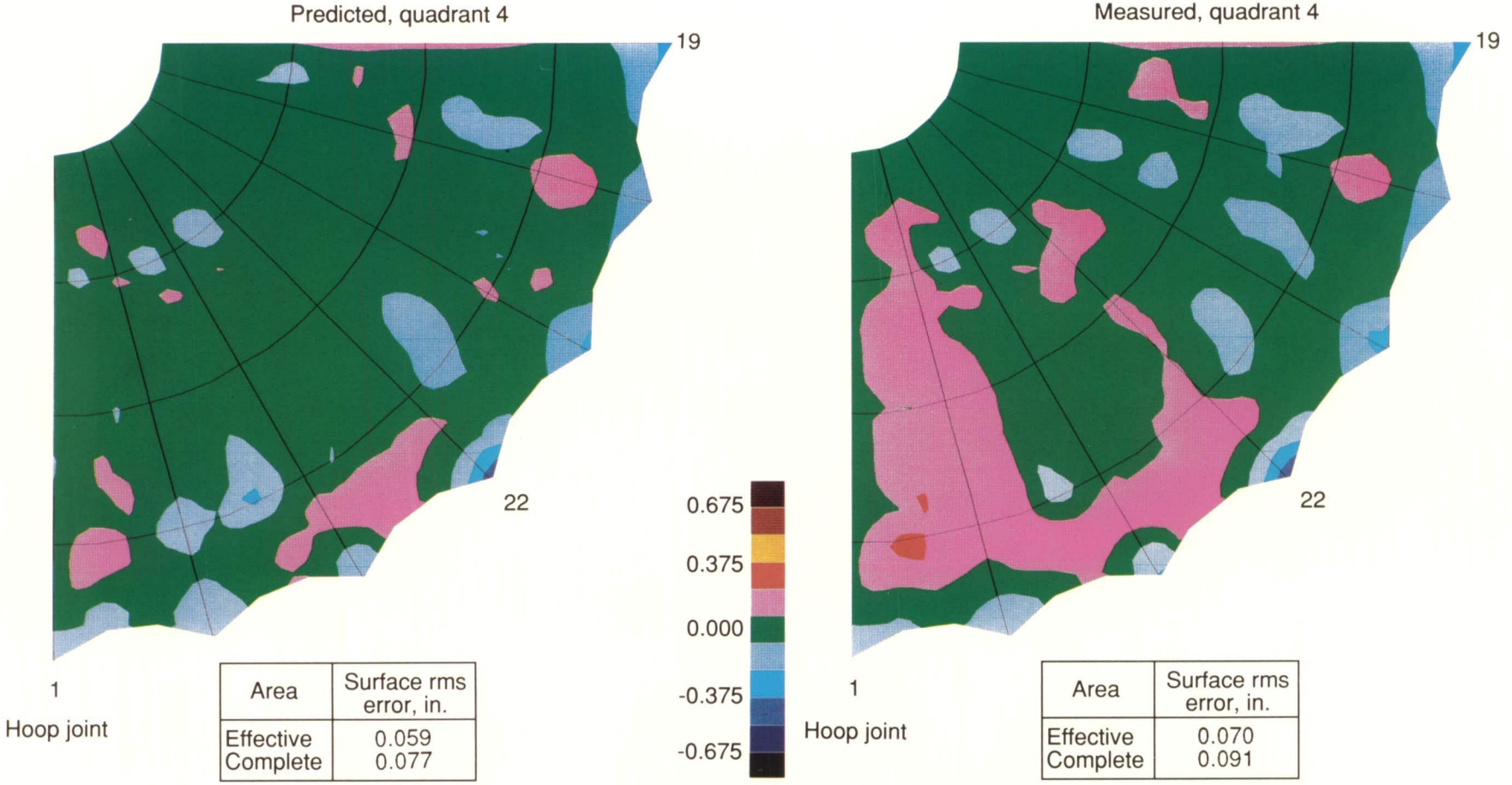

Area	Surface rms error, in.
Effective	0.059
Complete	0.077

Area	Surface rms error, in.
Effective	0.070
Complete	0.091

Hoop joint	Control cord adjustment, in., for –			
	G01	G02	G03	G04
19	-0.035	0.006	0.033	-0.046
20	0.020	0.044	0.040	0.036
21	0.018	-0.026	0.013	0.007
22	-0.015	-0.017	-0.048	-0.045
23	0.011	-0.003	0.013	0.032
24	0.054	0.122	0.198	-0.138
1	-0.003	0.029	0.033	-0.024

Figure 13. Predicted and actual surface roughness for third computer-controlled adjustment on 11/30/89.

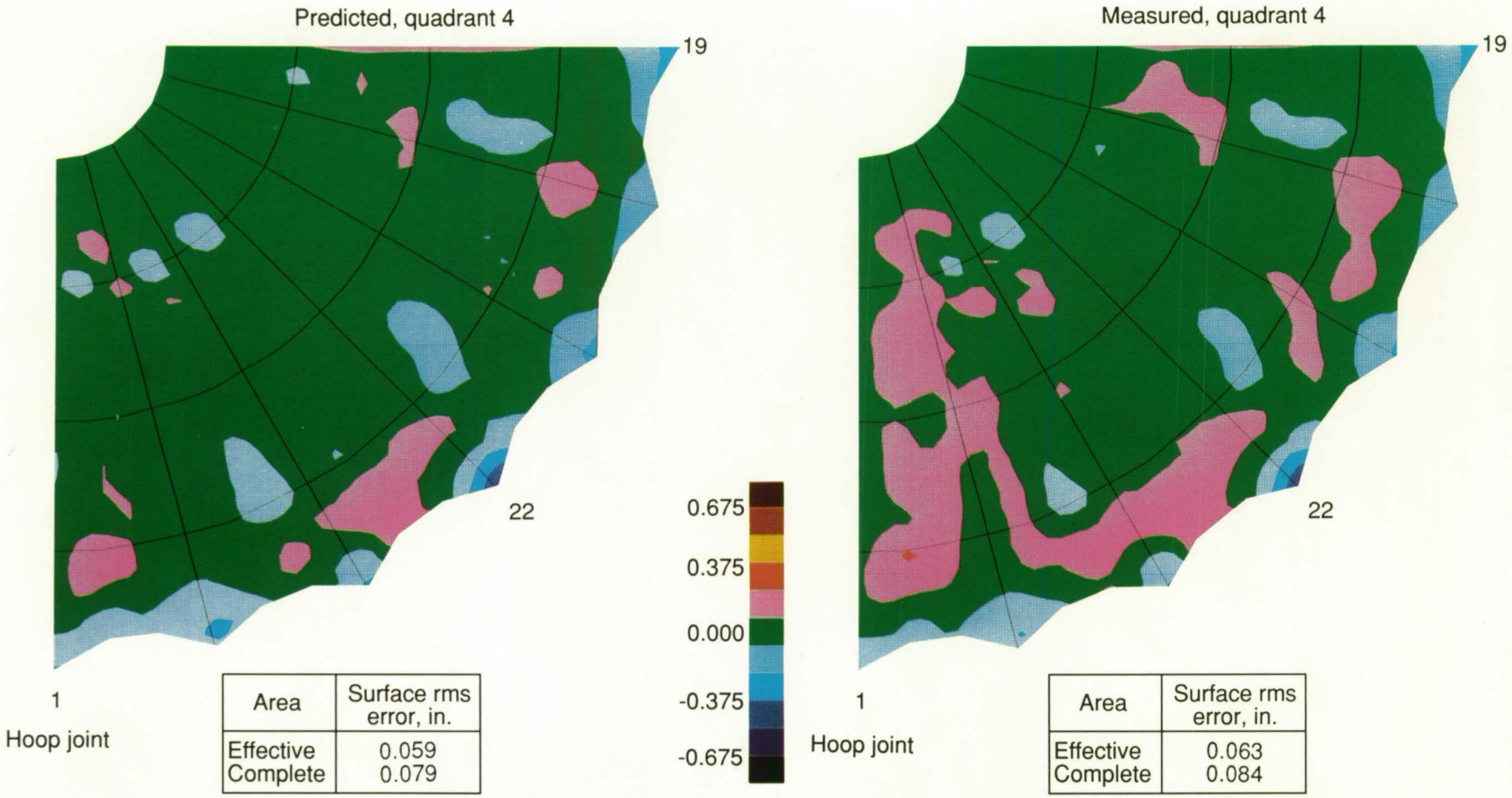

Area	Surface rms error, in.
Effective	0.059
Complete	0.079

Area	Surface rms error, in.
Effective	0.063
Complete	0.084

Hoop joint	Control cord adjustment, in., for –			
	G01	G02	G03	G04
19	0.016	-0.021	-0.003	-0.004
20	0.007	0.015	0.017	0.005
21	0.014	-0.008	0.007	0.010
22	0.004	-0.018	-0.017	-0.017
23	0.012	0.005	0.003	-0.009
24	-0.004	-0.027	-0.035	-0.045
1	0.008	-0.012	-0.006	-0.003

Figure 14. Predicted and actual surface roughness for fourth computer-controlled adjustment on 12/14/89.

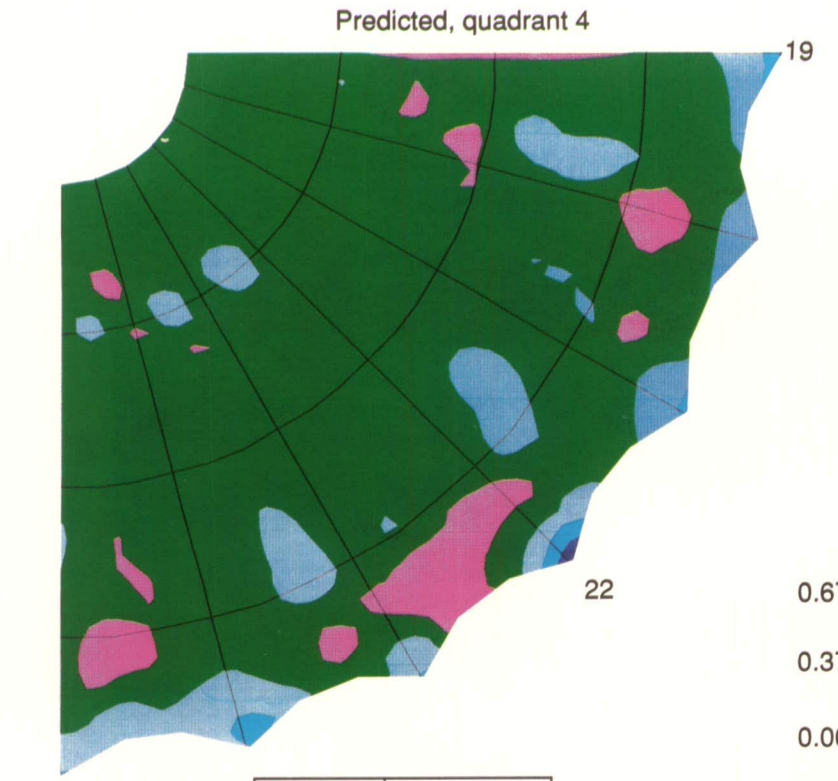

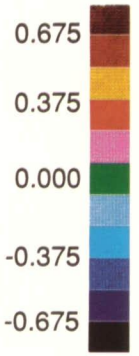

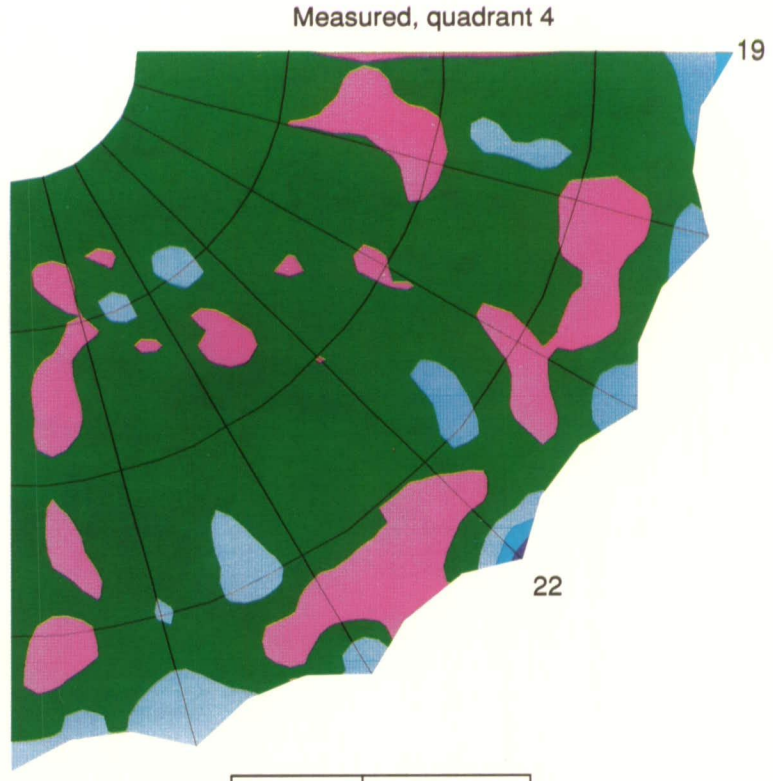

Area	Surface rms error, in.
Effective	0.058
Complete	0.079

Hoop joint	Control cord adjustment, in., for –			
	G01	G02	G03	G04
19	0.003	-0.018	-0.004	0.001
20	-0.003	-0.002	0.000	-0.002
21	-0.006	-0.003	-0.002	-0.009
22	0.000	-0.012	-0.006	-0.004
23	-0.010	-0.009	-0.011	-0.011
24	-0.008	-0.035	-0.028	-0.017
1	-0.010	-0.005	-0.007	-0.010

Figure 15. Control cord adjustments and predicted surface roughness if surface had been adjusted after 12/18/89 measurement.

Area	Surface rms error, in.
Effective	0.062
Complete	0.079

Figure 16. Reflector surface roughness after 3 months of inactivity on 4/4/90.

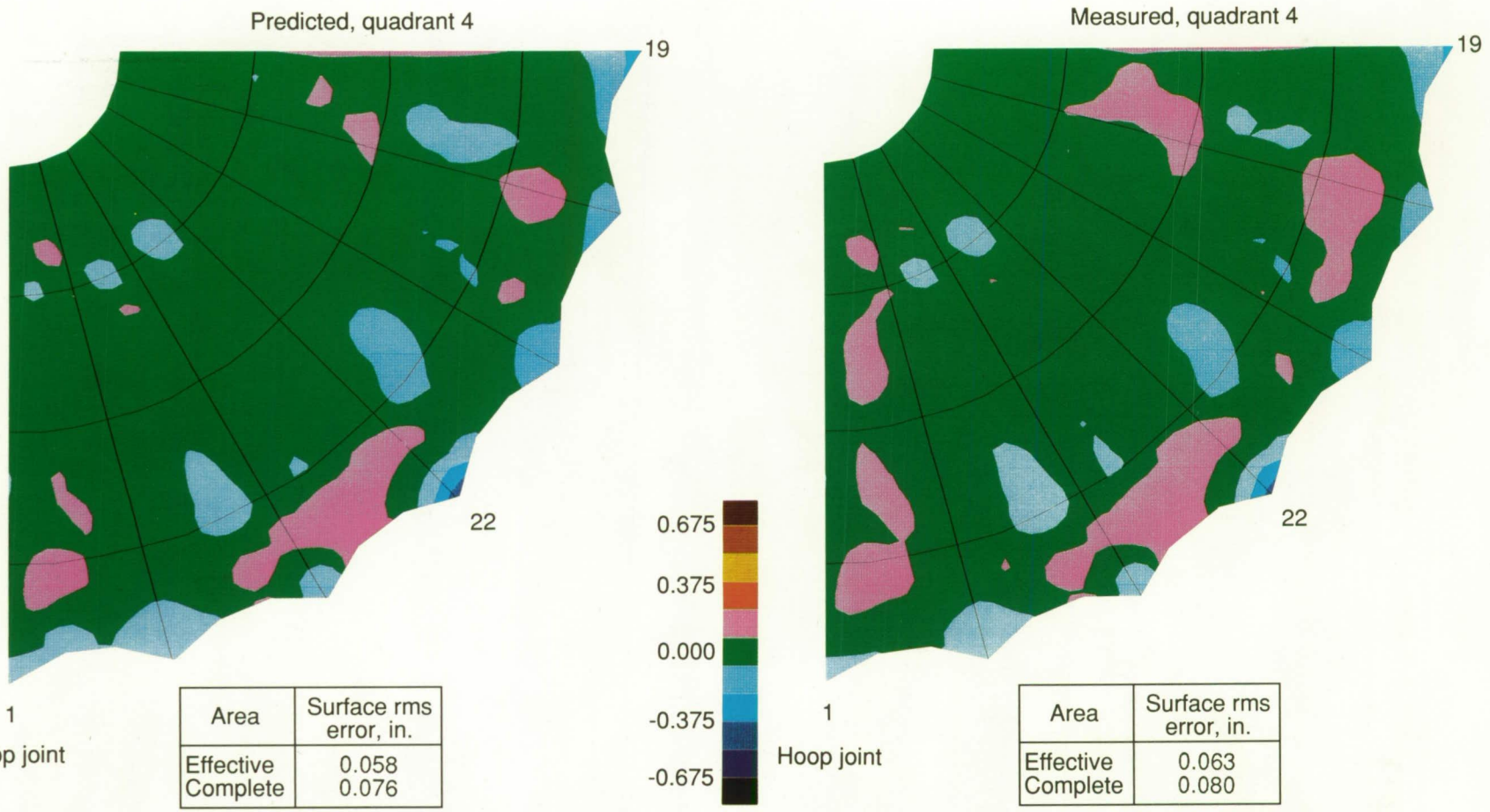

Area	Surface rms error, in.
Effective	0.058
Complete	0.076

Area	Surface rms error, in.
Effective	0.063
Complete	0.080

Hoop joint	Control cord adjustment, in., for –			
	G01	G02	G03	G04
19	-0.002	-0.021	-0.009	-0.003
20	-0.010	-0.002	-0.005	-0.006
21	-0.013	-0.006	-0.008	-0.013
22	-0.010	-0.016	-0.008	-0.006
23	-0.017	-0.003	-0.004	-0.007
24	-0.007	-0.028	-0.008	0.007
1	-0.017	0.002	-0.004	-0.005

Figure 17. Predicted and actual surface roughness for final computer-controlled adjustment on 4/17/90.

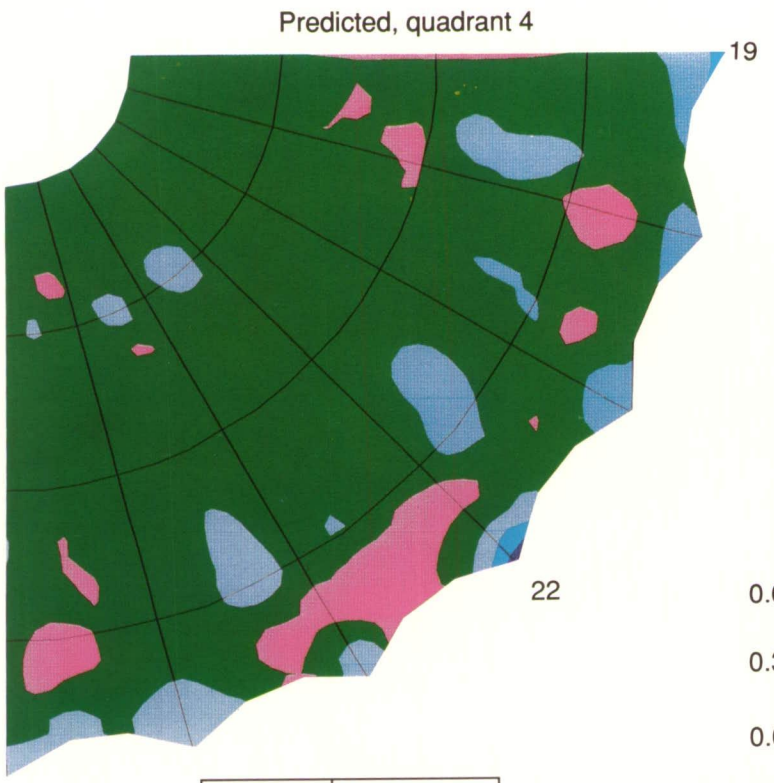

Area	Surface rms error, in.
Effective Complete	0.058 0.075

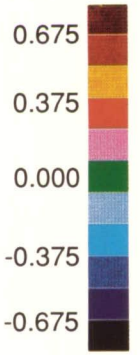

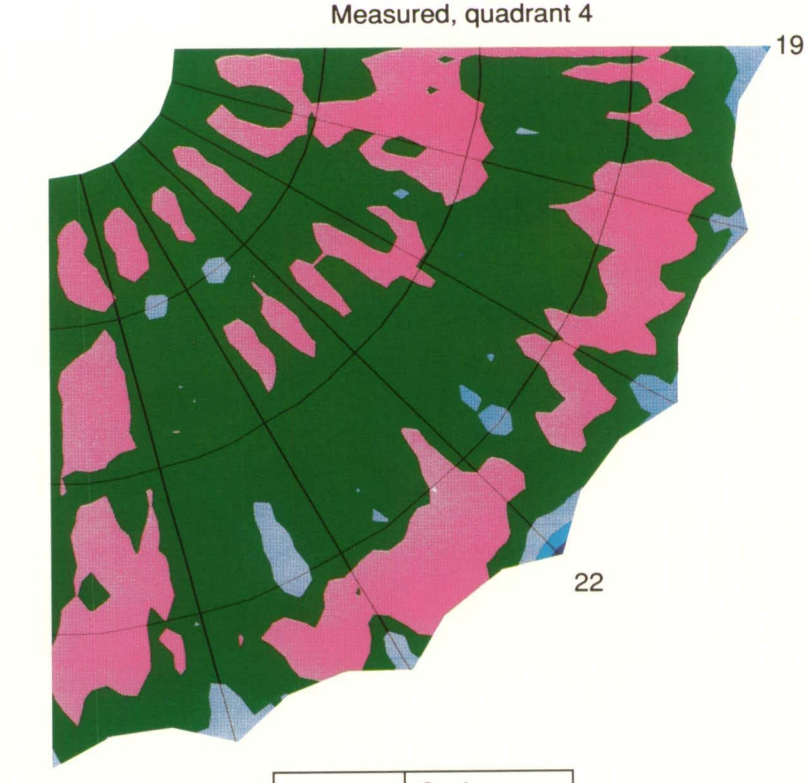

Area	Surface rms error, in.
Effective Complete	0.065 0.079

Hoop joint	Control cord adjustment, in., for –			
	G01	G02	G03	G04
19	-0.002	-0.012	0.002	-0.007
20	-0.009	-0.002	-0.002	-0.009
21	-0.008	-0.008	0.002	-0.002
22	-0.003	-0.002	-0.001	-0.004
23	-0.006	-0.003	0.005	0.002
24	-0.004	-0.006	0.000	-0.003
1	-0.004	-0.005	0.001	-0.007

Figure 18. Control cord adjustments and predicted surface roughness if surface had been adjusted after 4/19/90 measurement.

Figure 19. Actual surface roughness for 4/19/90 metric camera data, which include Pillows I targets.

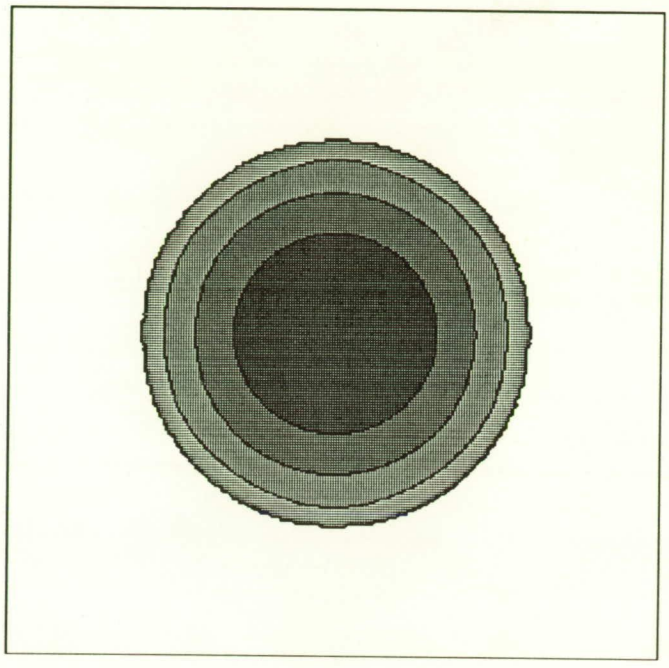

(a) Circular equivalent aperture.

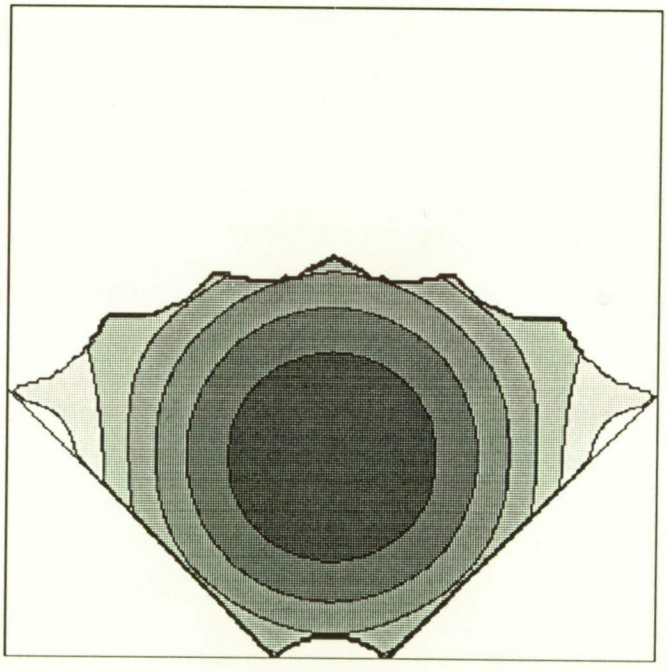

(b) Scalloped pie aperture.

Figure 20. Aperture field distribution in 5-dB increments for paraboloidal reflector with 7-element array feed.

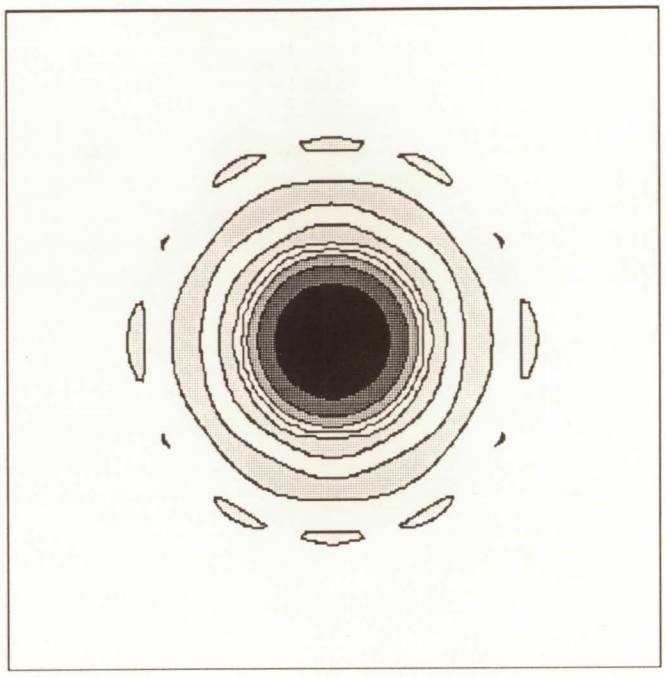

(a) Circular equivalent aperture.

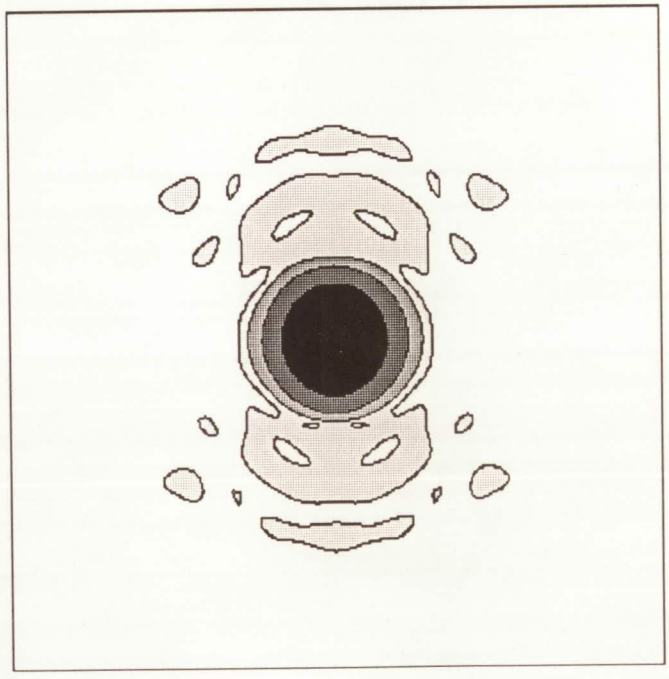

(b) Scalloped pie aperture.

Figure 21. Radiation pattern contours in 10-dB increments for paraboloidal reflector with 7-element array feed.

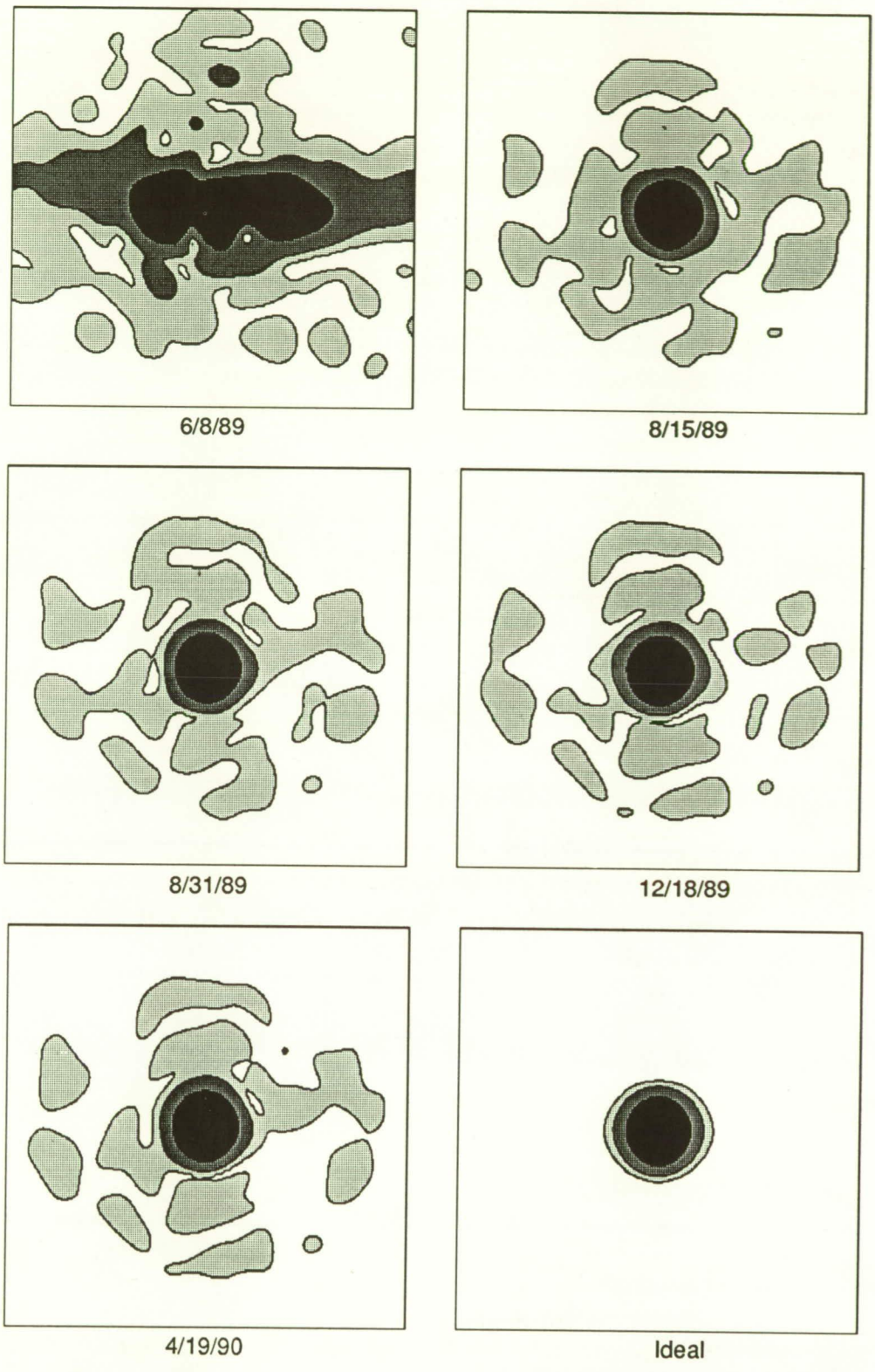

Figure 22. Radiation pattern contours in 10-dB increments over ±3° angular region at 6 GHz for distorted reflector with 7-element array feed.

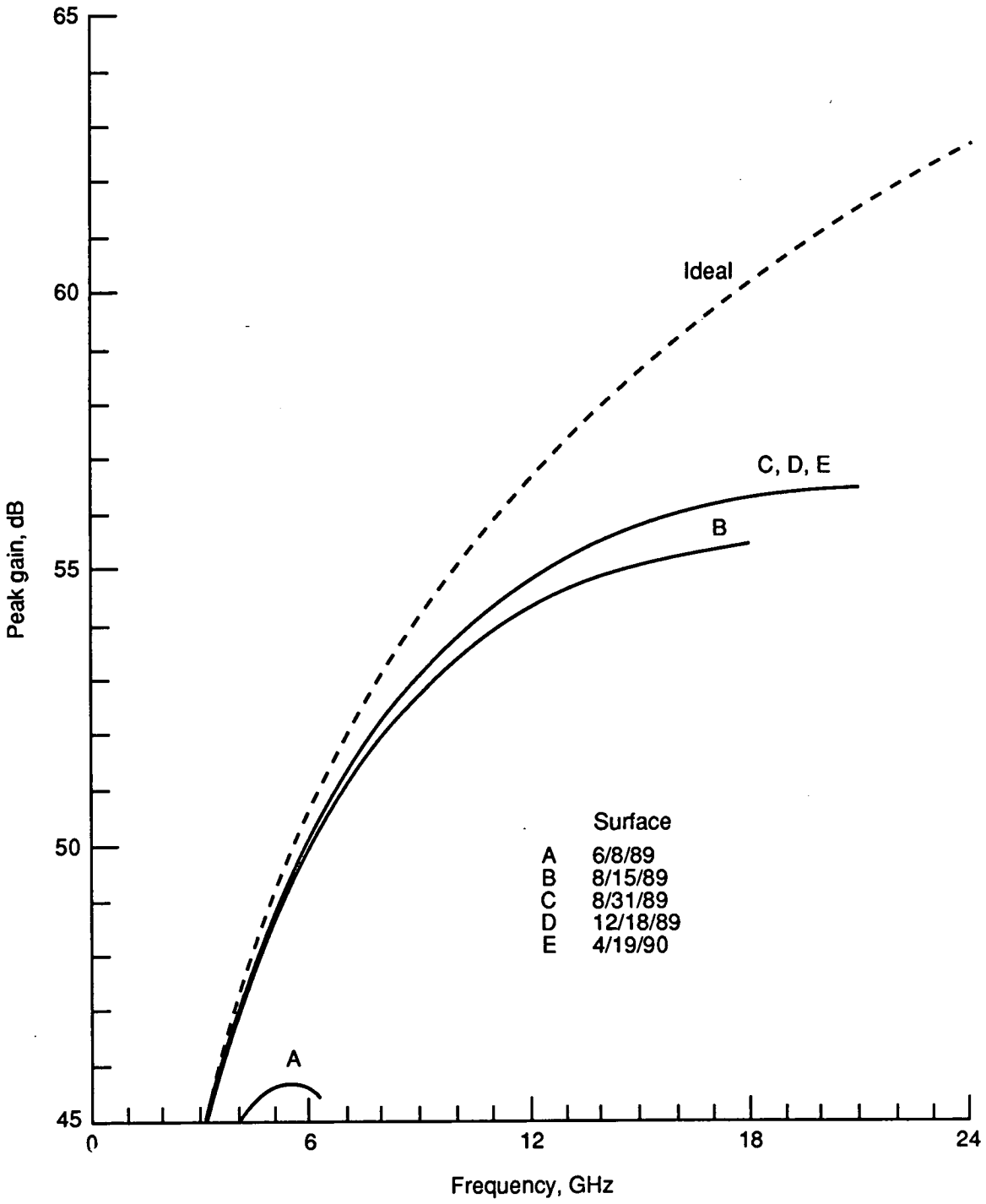

Figure 23. Antenna gain at peak of main beam for distorted reflector with 7-element array feed.

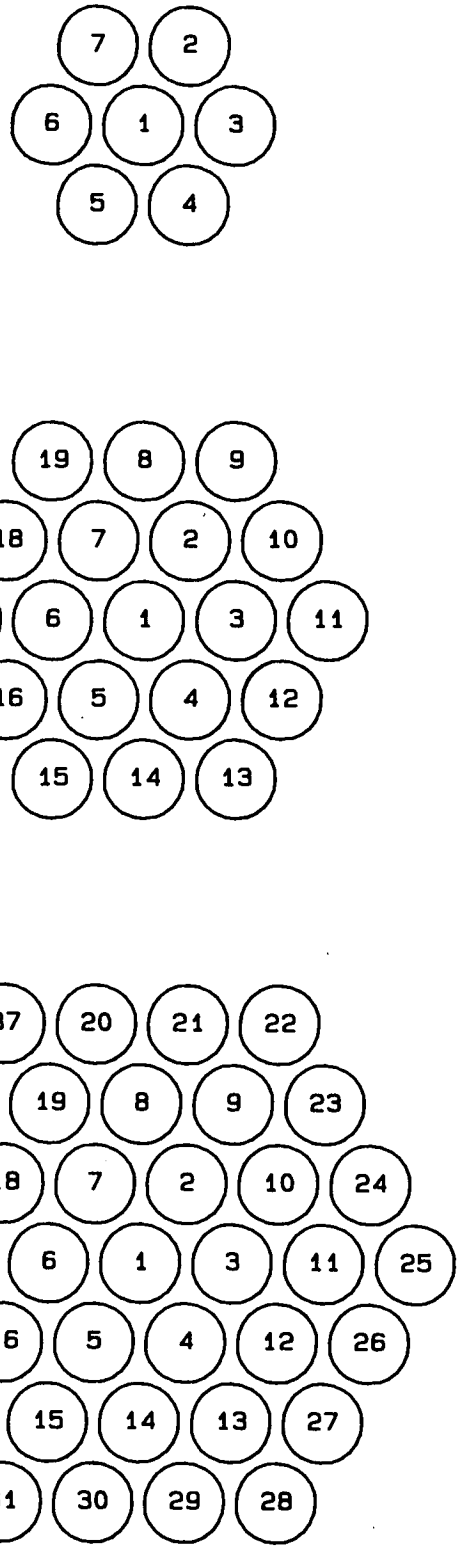

Figure 24. Array-feed configurations for 7, 19, and 37 elements.

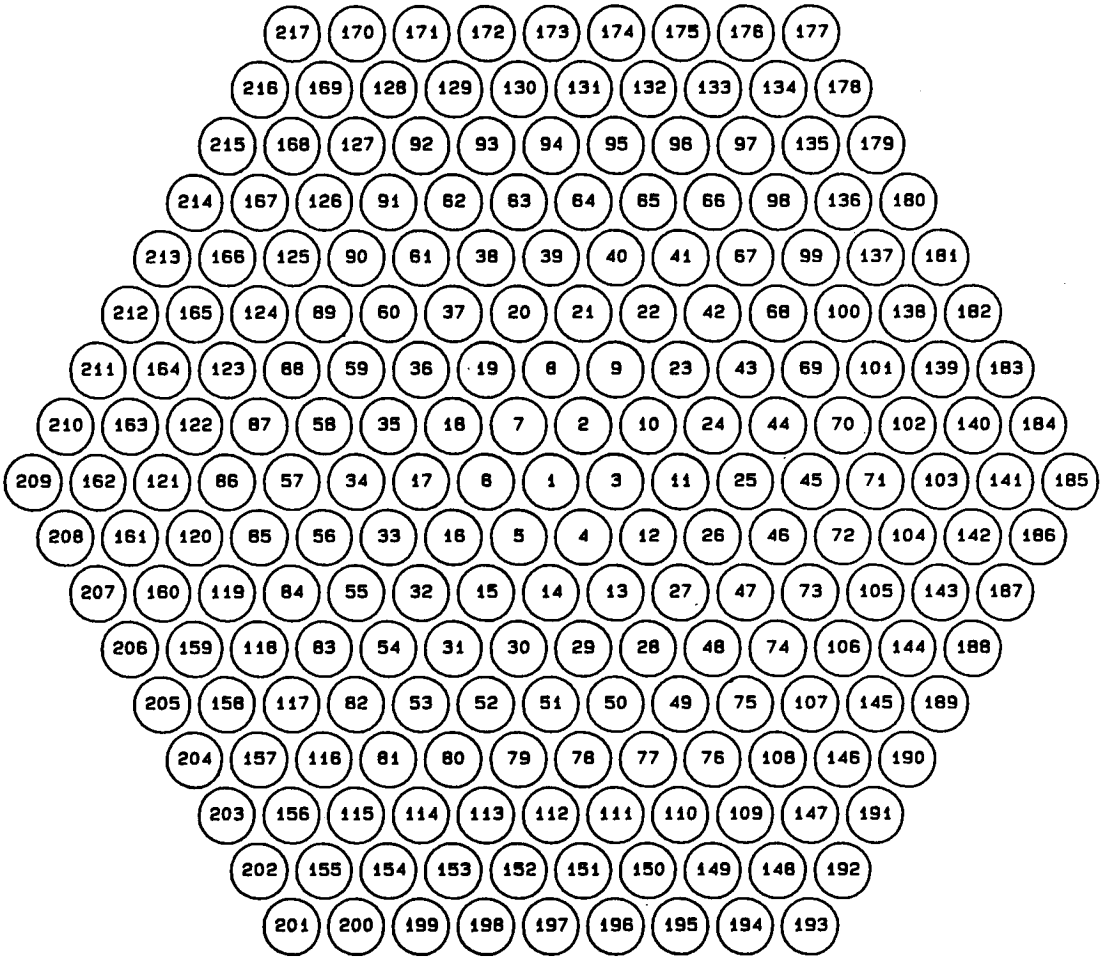

Figure 25. Array-feed configurations for 217 elements.

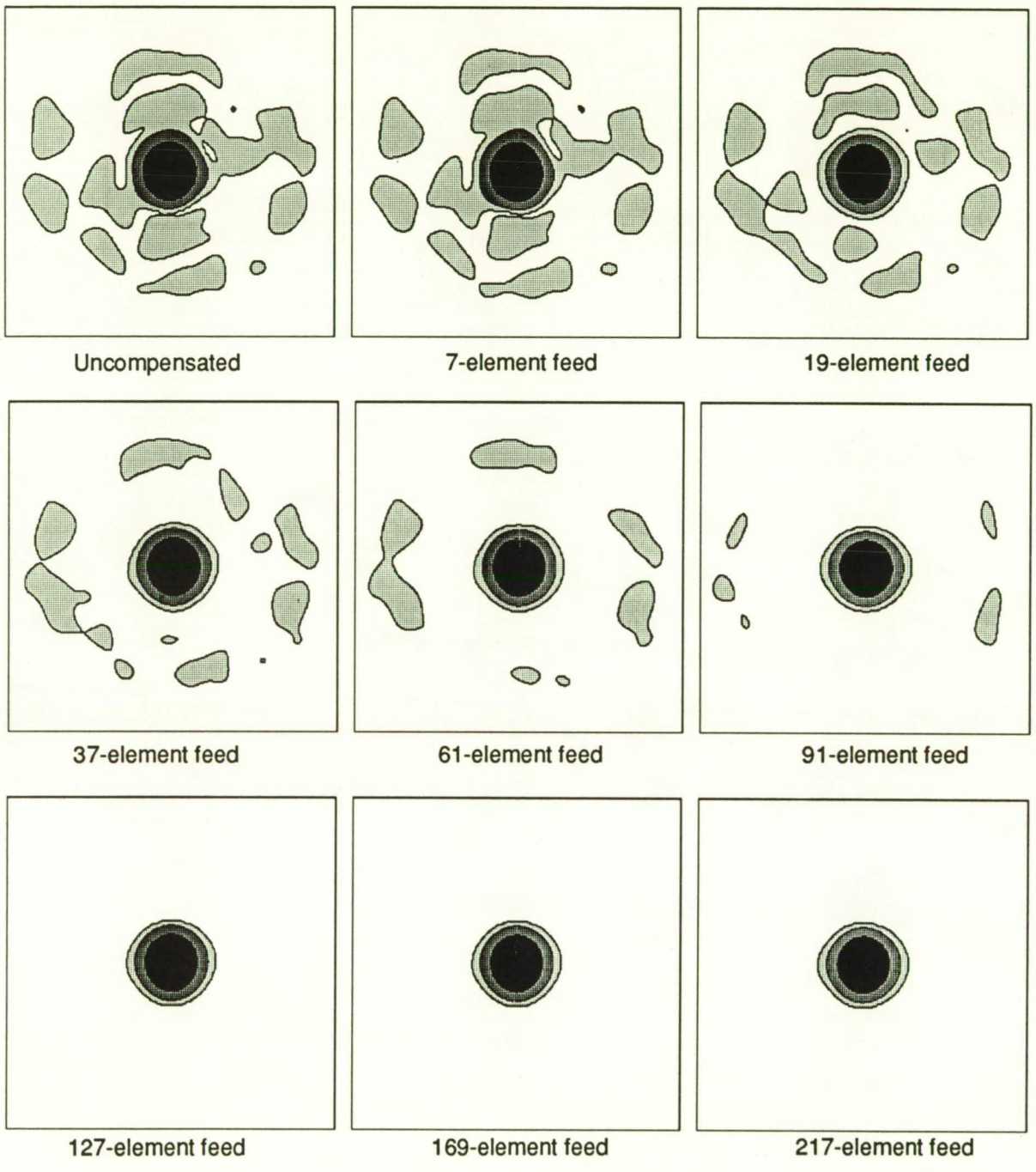

Figure 26. Radiation pattern contours in 10-dB increments over ±3° angular region at 6 GHz for 4/19/90 distorted reflector with array-feed compensation.

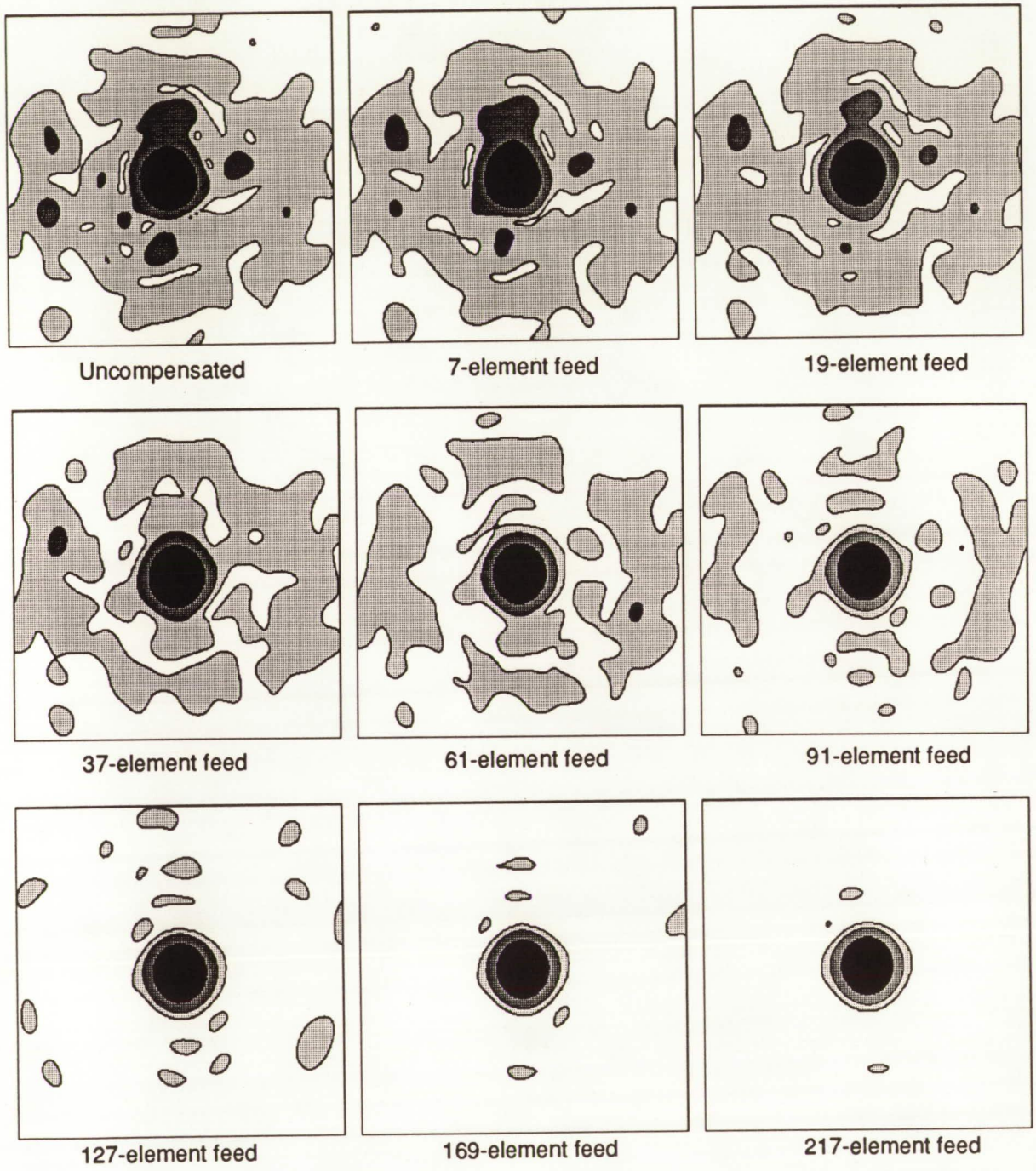

Figure 27. Radiation pattern contours in 10-dB increments over $\pm 1.5^\circ$ angular region at 12 GHz for 4/19/90 distorted reflector with array-feed compensation.

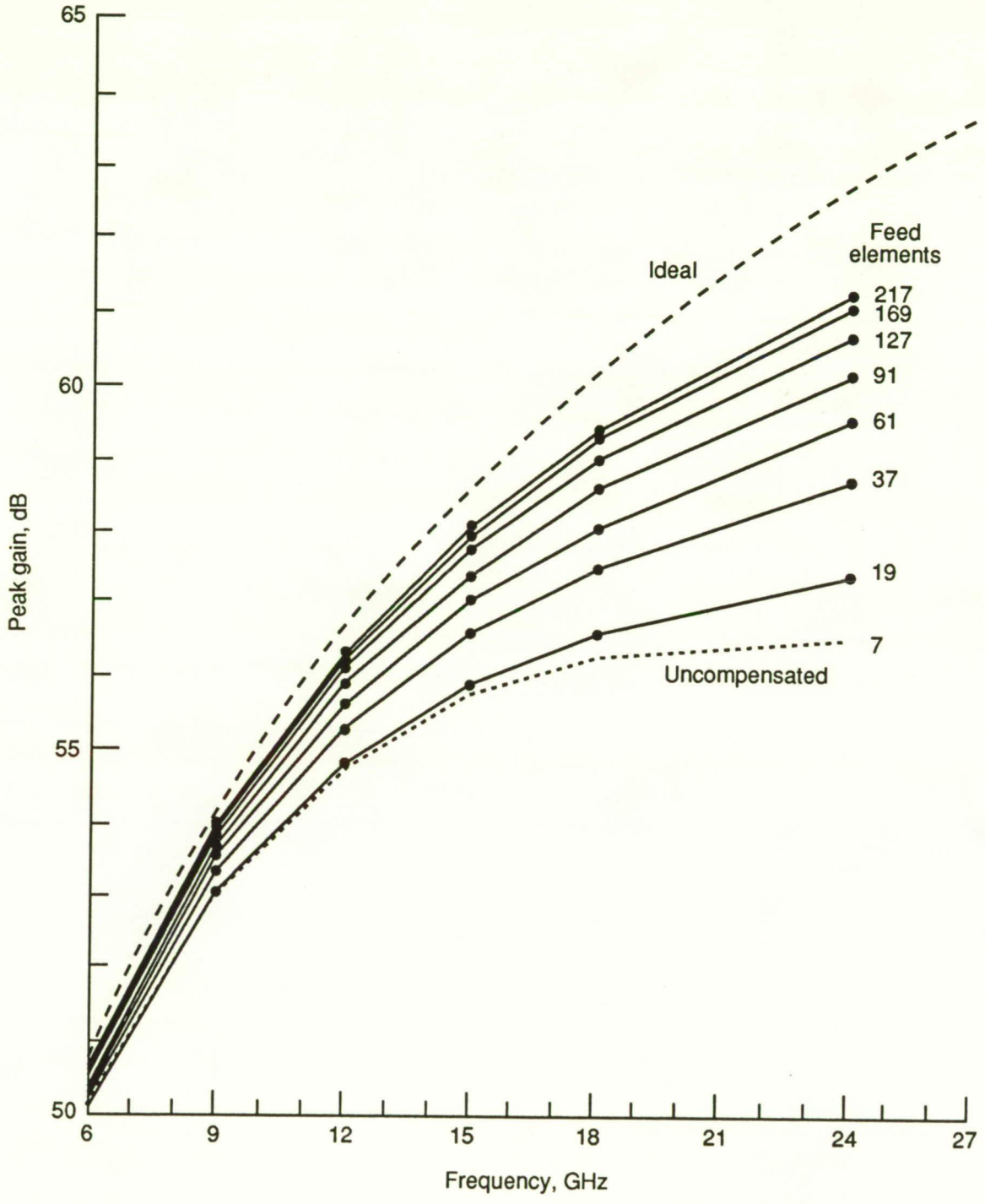

Figure 28. Antenna gain at peak of main beam for 4/19/90 distorted reflector with array-feed compensation.

Figure 29. Radiation pattern contours in 10-dB increments over ±4° angular region at 12 GHz for 4/19/90 pillowed reflector with 7-element array feed.

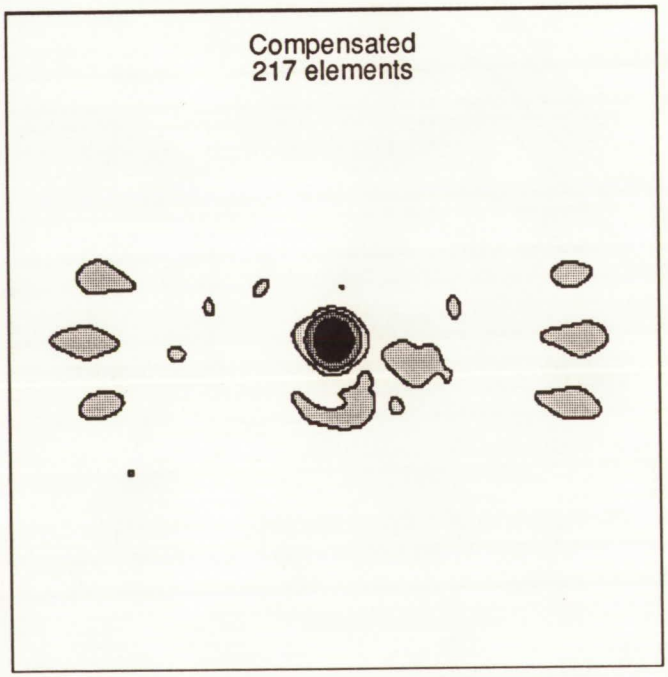

Figure 30. Radiation pattern contours in 10-dB increments over ±4° angular region at 12 GHz for 4/19/90 pillowed reflector with 217-element array feed.

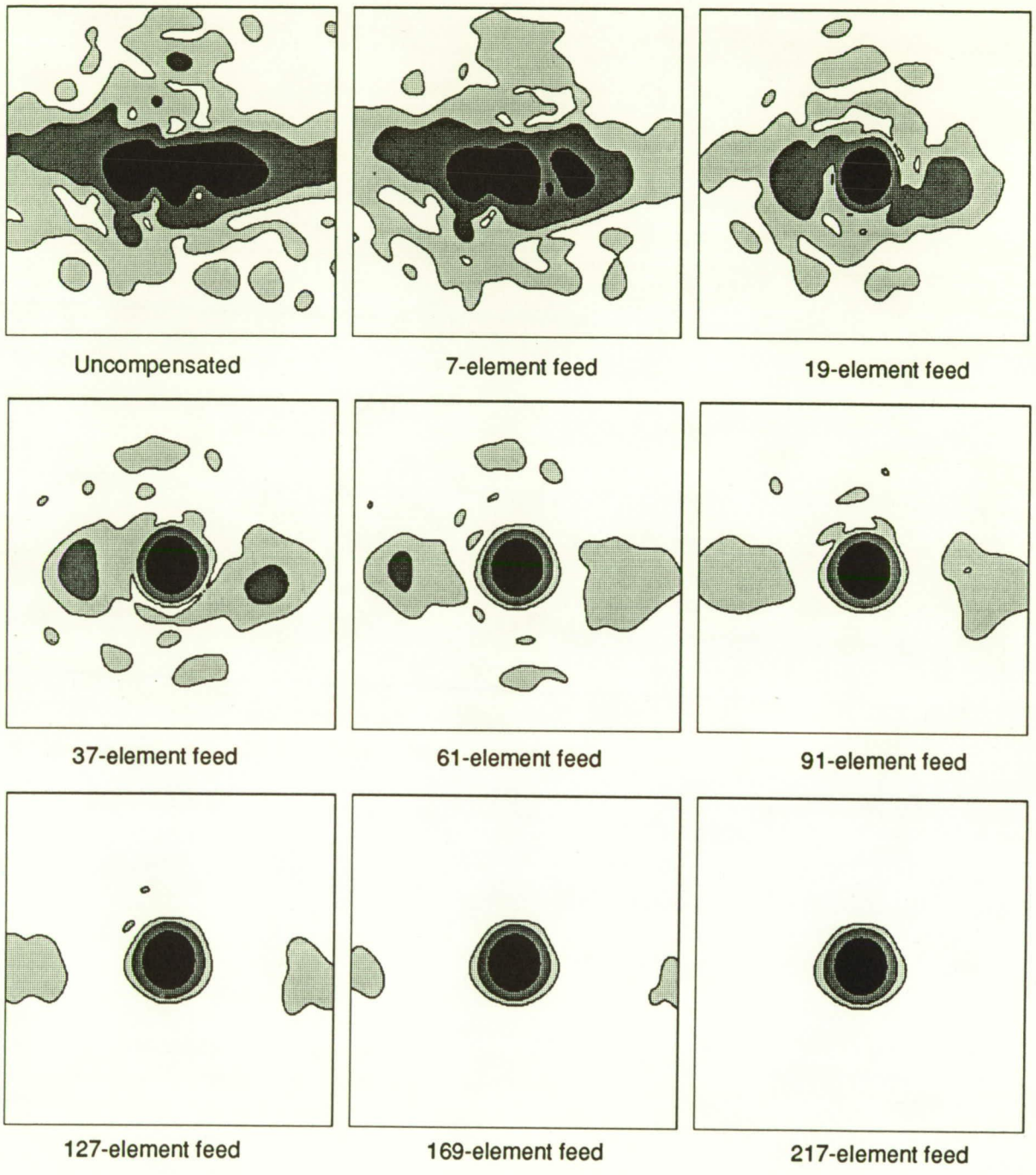

Figure 31. Radiation pattern contours in 10-dB increments over ±3° angular region at 6 GHz for 6/8/89 distorted reflector with array-feed compensation.

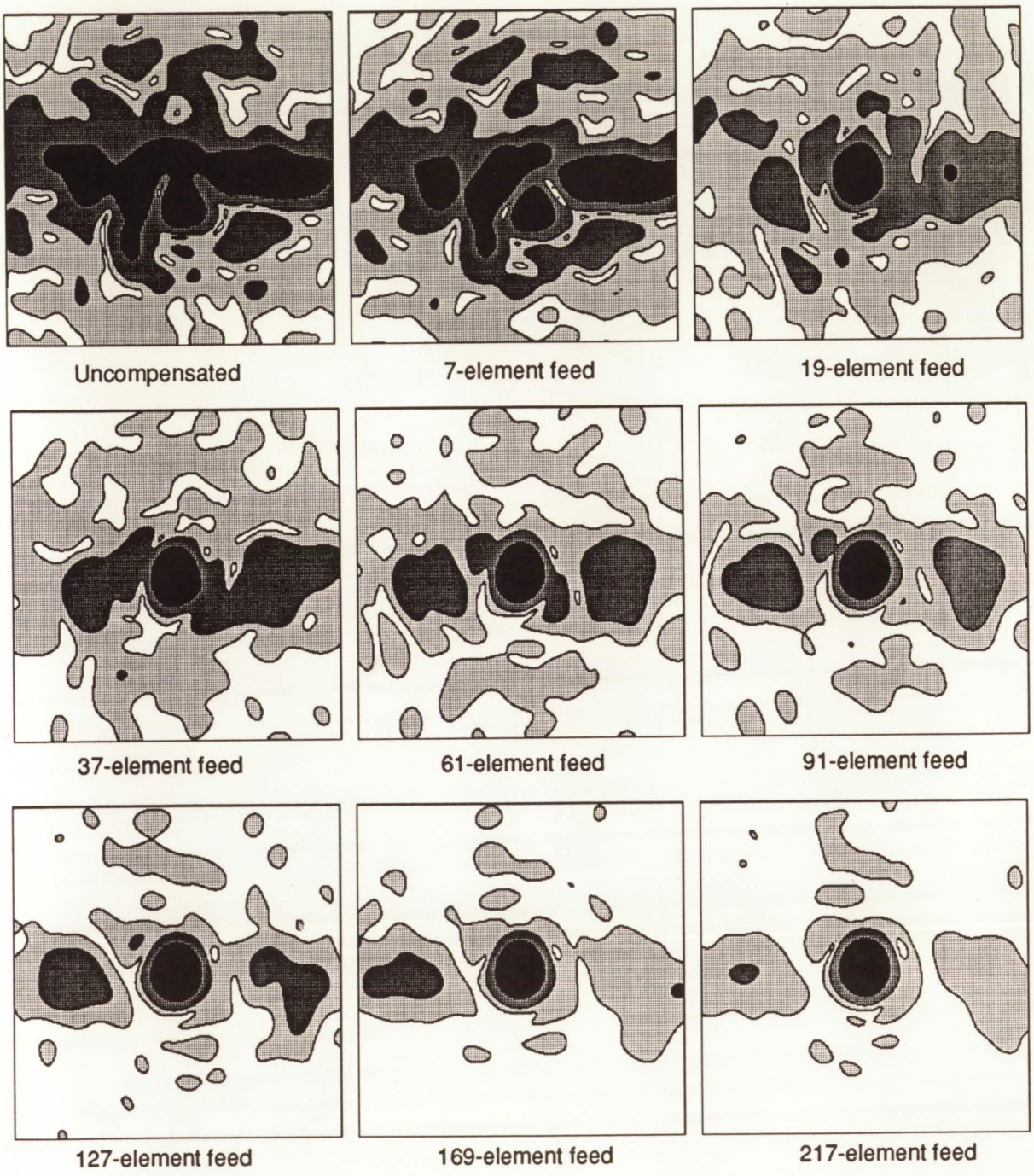

Figure 32. Radiation pattern contours in 10-dB increments over ±1.5° angular region at 12 GHz for 6/8/89 distorted reflector with array-feed compensation.

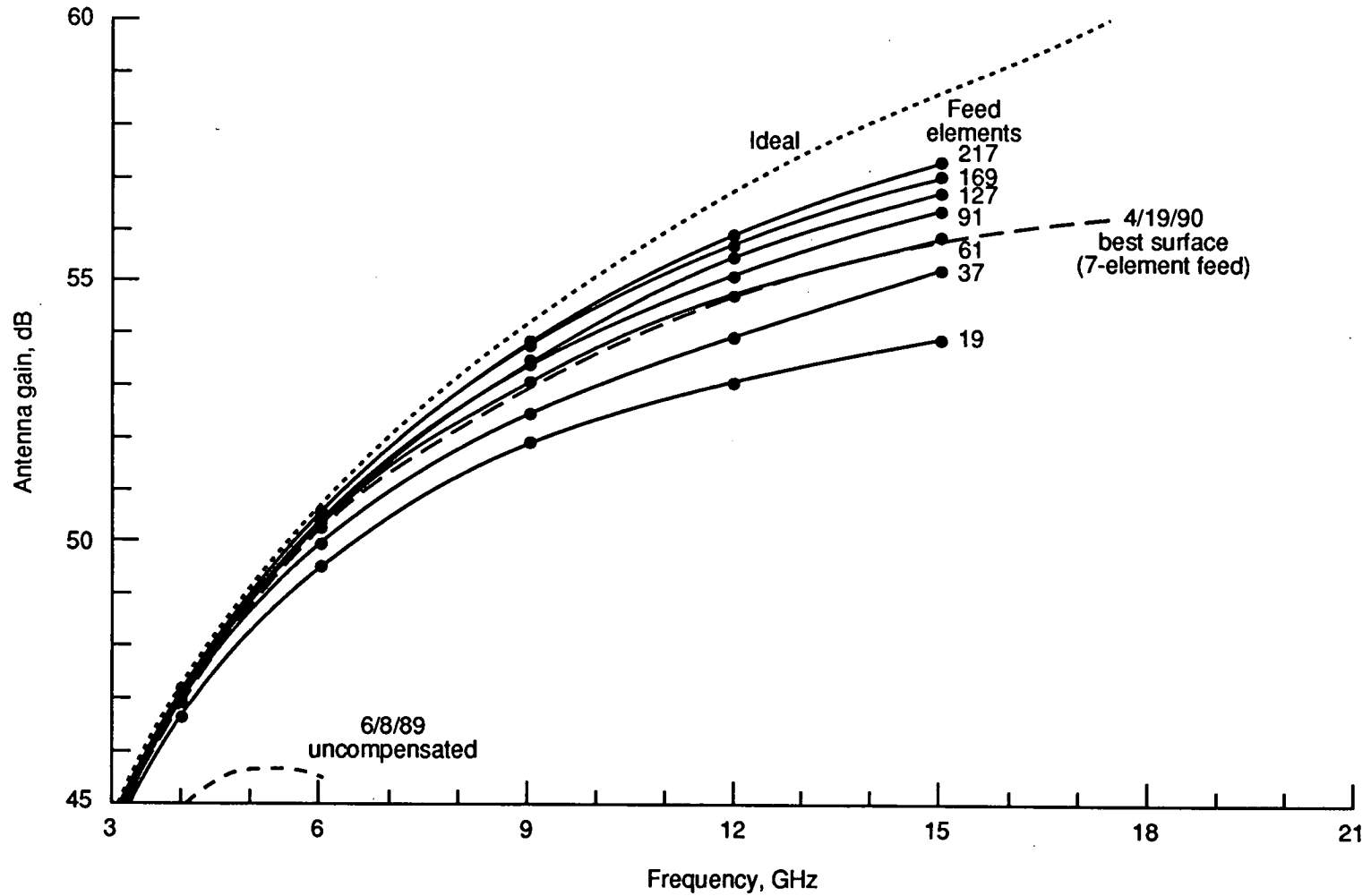

Figure 33. Antenna gain at peak of main beam for 6/8/89 distorted reflector with array-feed compensation.

REPORT DOCUMENTATION PAGE

Form Approved
OMB No. 0704-0188

1. AGENCY USE ONLY *(Leave blank)*	2. REPORT DATE	3. REPORT TYPE AND DATES COVERED
	October 1992	Technical Paper

4. TITLE AND SUBTITLE
Deployable Reflector Antenna Performance Optimization Using Automated Surface Correction and Array-Feed Compensation

5. FUNDING NUMBERS
WU 590-14-41-03

6. AUTHOR(S)
Lyle C. Schroeder, M. C. Bailey, and John L. Mitchell

7. PERFORMING ORGANIZATION NAME(S) AND ADDRESS(ES)
NASA Langley Research Center
Hampton, VA 23681-0001

8. PERFORMING ORGANIZATION REPORT NUMBER
L-17065

9. SPONSORING/MONITORING AGENCY NAME(S) AND ADDRESS(ES)
National Aeronautics and Space Administration
Washington, DC 20546-0001

10. SPONSORING/MONITORING AGENCY REPORT NUMBER
NASA TP-3228

11. SUPPLEMENTARY NOTES
Schroeder and Bailey: Langley Research Center, Hampton, VA; Mitchell: Lockheed Engineering & Sciences Co., Hampton, VA.

12a. DISTRIBUTION/AVAILABILITY STATEMENT
Unclassified–Unlimited

Subject Category 15

12b. DISTRIBUTION CODE

13. ABSTRACT *(Maximum 200 words)*

Methods for increasing the electromagnetic (EM) performance of reflectors with rough surfaces were tested and evaluated. First one quadrant of the 15-meter hoop-column antenna was retrofitted with computer-driven and controlled motors to allow automated adjustment of the reflector surface. The surface errors, measured with metric photogrammetry, were used in a previously verified computer code to calculate control motor adjustments. With this system, a rough antenna surface (rms of $\approx$0.180 inch) was corrected in two iterations to approximately the structural surface smoothness limit of 0.060 inch rms. The antenna pattern and gain improved significantly as a result of these surface adjustments. The EM performance was evaluated with a computer program for distorted reflector antennas which had been previously verified with experimental data. Next, the effects of the surface distortions were compensated for in computer simulations by superimposing excitation from an array feed to maximize antenna performance relative to an undistorted reflector. Results showed that a 61-element array could produce EM performance improvements equal to surface adjustments. When both mechanical surface adjustment and feed compensation techniques were applied, the equivalent operating frequency increased from approximately 6 to 18 GHz.

14. SUBJECT TERMS	15. NUMBER OF PAGES
Large space deployable antenna; Surface adjustment; Array-feed antenna compensation	68
	16. PRICE CODE A04

17. SECURITY CLASSIFICATION OF REPORT	18. SECURITY CLASSIFICATION OF THIS PAGE	19. SECURITY CLASSIFICATION OF ABSTRACT	20. LIMITATION OF ABSTRACT
Unclassified	Unclassified		

NSN 7540-01-280-5500

Standard Form 298(Rev. 2-89)
Prescribed by ANSI Std. Z39-18
298-102

NASA-Langley, 1992